Durham E-Theses

Investigations of ion-atom collisions

Catlow, G. W.

How to cite:

Catlow, G. W. (1969) *Investigations of ion-atom collisions*, Durham theses, Durham University. Available at Durham E-Theses Online: http://etheses.dur.ac.uk/8625/

INVESTIGATIONS OF ION-ATOM COLLISIONS

by

G. W. Catlow

Submitted in partial fulfillment of

the requirements for the degree of

Doctor of Philosophy

Department of Mathematics

Durham University

England

1969

ABSTRACT

This work is concerned with elastic and inelastic scattering of ions and atoms.

Semi-classical and quantal phase shift treatments are applied to the system of lithium ions in helium. A SCF-MO calculation of the interaction potential for the ground state of the system is reported and the results compared with other quantal calculations and with semi-emperical cross-sections. The cross-section for scattering through an angle greater than a given angle, the total elastic cross-section, the diffusion cross-section and the mobility are obtained and compared with experiment. The presence of orbiting is seen in the total cross-sections. It is predicted that the SCF-MO potential supports seven bound vibrational states.

A classical binary encounter impulse approximation is applied to ionization of atoms. The velocity distribution of the bound atomic electrons is given by Hartree Fock wave function. Inner and outer shell ionizations cross-sections of atomic helium, lithium, oxygen, nitrogen and neon by electron and proton impact are calculated. The results are compared with other classical and quantal calculations, and where possible with experiment.

Finally the excitation of atomic hydrogen by proton impact is considered within the framework of the impact parameter model. The closure approximation, which implicitly takes account of all rearrangement channels, is used to obtain excitation cross-sections into the 2s-state. The calculation is performed retaining only two states explicitly and the results are compared with those predicted by other quantal treatments. No experimental results are available for comparison.

ACKNOWLEDGEMENTS

TABLE OF CONTENTS

TABLE OF CONTENTS (Continued)

LIST OF TABLES

LIST OF FIGURES

CHAPTER I

MODELS OF HEAVY PARTICLE COLLISIONS

1.   Introduction

The theory of ion-atom collisions can be considerably
simplified by adopting models and using approximations that
take advantage of the comparatively large masses involved in
the collision. The present work investigates both elastic
and inelastic collisions for some ion-atom systems using
classical, semi-classical and quantal treatments.

In general, for elastic collisions, the nuclei can
be considered as moving in some averaged field due to the
interaction of all particles (nuclei & electrons) in the
system in a way in which, in the absence of excitations,
allows their motion to be considered independently of the
electrons.   Such a separation of nuclear and electron motion
was first demonstrated by Born and Oppenheimer (1932). The
collision can then be represented by a potential scattering
model.

A classical potential scattering analysis is appli-
cable if the de Broglie wave length associated with the
collision is small compared with atomic dimensions, which is
the case for heavy particle collisions above thermal energies.
However it is well known that the classical analysis fails

for total elastic cross-sections for the realistic infinite
potentials that will be considered in this present work, but
it may be valid for differential elastic cross-sections,
$I(\theta)$, over a wide range of angles say $\theta > \theta_c > 0$. An estimate
of this critical angle θ_c below which the classical analysis
fails can be obtained form the uncertainty principle, and
for protons above thermal energies is of the order of 0.1°
(Mott and Massey 1965). At thermal energies, semi-classical
(see section 2) and quantal treatments are required.

Classical models of inelastic scattering would be
expected to be adequate if the dominant contribution to the
cross-sections came from angles greater than θ_c. For example
if energy transfers greater than ΔE are required for ioniza-
tion, there is a corresponding angle $\theta_o(E)$ such that for
$\theta < \theta_o$ the energy transferred is insufficient to cause the
transition. Then for energies such that $\theta_o(E) > \theta_c$, it can be
expected that classical models could adequately describe
ionization. The major argument against the application of a
classical theory is that the theory is unable to describe
distant collisions correctly. This is reflected in the high
energy region of the cross-sections where the distant colli-
sions make a significant contribution. For example the be-
haviour of the classical ionization cross-section at high
energies is E^{-1} in disagreement with the correct quantal
result of $E^{-1}\ln E$.

Ion-atom collisions with energies in the kilovolt

region, can be described in the impact parameter model. In this model the nuclei are treated as classical particles describing rectilinear trajectories with constant velocity and the electrons are treated quantum mechanically as they move in the time dependant fields of the "infinitely massive" nuclei. Mittleman (1961) has shown these assumptions not to be unjustified in this energy region.

The following sections of this chapter will be devoted to elastic ion-atom scattering, classical theory of inelastic collisions and impact parameter treatments of heavy particles respectively. In view of the range of topics included, a comprehensive review of the theory and previous work in these fields will not be attempted (see Coleman & McDowell, 1969) but the discussion will be such as to introduce the particular theoretical models that will appear in Chapters II, III, IV.

2. Elastic Ion-Atom Collisions

In the absence of inelasticity, the Born-Oppenheimer separation allows ion-atom collisions to be treated in a central potential model. The exact quantum treatment for spherically symmetric potentials using the Faxen-Holtzmark method of partial waves is well known (Mott & Massey 1965) and the results will only be stated here. The differential cross-section $I(\theta)$ is given in terms of an elastic scattering amplitude, $f(\theta)$

$$f(\theta) = \frac{1}{2ik} \sum_{\ell=0}^{\infty} (2\ell+1) \left[2e^{2i\eta_\ell}-1\right] P_\ell(\cos\theta) \qquad (1.1)$$

such that

$$I(\theta) = |f(\theta)|^2 . \qquad (1.2)$$

Here $P_\ell(x)$ is the Legendre polynomial of order ℓ and η_ℓ is the ℓ-order phase shift defined by the requirement that the asymptotic form of the regular solution of the radial equation.

$$\left[\frac{d^2}{dr^2}+k^2-2\mu V(r)-\frac{\ell(\ell+1)}{r^2}\right]u_\ell(r) = 0 \qquad (1.3)$$

should be

$$u_\ell(r) \underset{r\to\infty}{\sim} \sin(kr-\tfrac{1}{2}\ell\pi+\eta_\ell) \qquad (1.4)$$

where in the usual notation, k is the momentum of the collision, μ is the reduced mass, V(r) is the interaction potential and ℓ is the angular momentum quantum number. Hence the phase shift η_ℓ refers to the displacement of the solution of the radial equation at large distances relative to that of the corresponding ℓth order spherical Bessel function, $j_\ell(kr)$. (krj_ℓ is a solution of (1.3) for V(r) = 0). Thus, given any realistic potential function, one solves (by numerical methods) the equation for successive values of ℓ evaluating a sufficient number of phase shifts to obtain convergence (to some specified limit of accuracy) in the sum over ℓ in eqn. (1.1).

However a complete quantal phase shift analysis can be probibitively time consuming when large numbers of phase shifts are required. Ford and Wheeler (1959), and more recently

Munn, Mason and Smith (1964) and Bernstein (1966), have examined the effect of "semi-classical" approximations in the derivation of the phase shifts on the behaviour of the phase shifts and on the scattering observables.

The two main deviations from the quantal analysis which are made to obtain the semi-classical approximation are:

(i) The exact phase shifts are replaced by JWKB phase shifts (see Coleman and McDowell 1969). The approximate solution of Jeffreys to eqn. (1.3) from which the JWKB phases are determined, is valid when the potential does not vary appreciably in a distance comparable with the wave length 1/k. of the collision. The JWKB phase shift can be written as

$$\eta_\ell^{JWKB} = \lim_{r \to \infty} \left[\int_{r_m}^{r} (k^2 - 2\mu V(r) - (\ell+1/2)^2/r^2)^{1/2} dr \right.$$

$$\left. - \int_{(\ell+1/2)/k}^{r} (k^2 - (\ell+1/2)^2/r^2)^{1/2} dr \right] \quad (1.5)$$

where r_m is the classical turning point.

When ℓ is sufficiently large (eg. $\ell \sim kR$ where R is some "range" parameter of the potential), Massey and Mohr (1934) showed that (1.5) could be simplied by expanding the first integrand to yield the so called Jeffreys-Born phase shift.

$$\eta_\ell^{JB} = - \int_{\frac{\ell+1/2}{k}}^{\infty} \frac{\mu V(r) \, dr}{(k^2 - (\ell+1/2)^2/r^2)^{1/2}} \quad (1.6)$$

(ii)   The summations of the phase shifts to produce cross-sections are approximated by integrals.

The validity of the first approximation has been examined by Munn et al (1964) for a L-J (12,6) potential. The approximation is essentially valid for "large" k and they show there is always a region of ℓ and k for which the approximation is poor, and this region is dependant on the potential parameters and the reduced mass of the collision. The success or prior calculations using JWKB phase shifts and semiclassical analysis (Bernstein (1960), Marchi and Mueller (1962, 1963)) was due to avoidence, for the most part, of these regions.

Massey and Mohr (1934) obtained an approximate expression (in closed form) for the total elastic cross-section by considering two regions of angular momentum. The first where the phase shifts are large and essentially random and the randon phase approximation is applicable, and the second where they are small and non-random but for which the cross-section summation (Chapter II, eqn. (2.6)) can be replaced by an integral over the JB eqn. (1.6), approximation to the phase shift. These approximations produce the Massey-Mohr cross-section. Landau and Lifshitz (1959) obtained a more accurate formula by replacing the whole sum by an integral over the JB phase shifts. (Schiff (1956) obtained an identical expression using an independent treatment and the cross-section in the analysis will be called the SLL approximation).

Undulatory deviations from the Massey-Mohr cross-

section caused by regions of stationary phase corresponding to
glory scattering, were predicted by Bernstein (1961) and have
since been observed experimentally (Rothe et al, 1962).
Bernstein (1962, 1963) then semi-classically related the num-
ber of oscillations to the number of bound states (vibrational-
rotational) that the potential can support. Because the semi-
classical analysis fails for thermal energies the relationship
is not rigorous and can only be stated as "The observation
of m maxima in the elastic cross-section implies the existance
of at least m vibrational bound states." (Bernstein, 1966)

Rainbow scattering also causes structure in the
cross-section and if an estimate of the number of vibrational
bound states is to be deduced from the behaviour of the total
cross-section using the Bernstein relationship, then this
structure must be identified and subtracted out before hand.
(Munn et al, 1964)

It is known that a semi-classical analysis includ-
ing approximations (i) and (ii), reduces transport cross-
sections to the results obtained by exact classical methods,
which are in error for low energies where orbiting and res-
onance effects occur. It is thus necessary to revert to the
exact quantal analysis for such results (Dickenson 1968a, b).

When averaging over transport cross-sections to
obtain mobilities much of the structure in the quantal cross-
section is lost and semi-classical analysis predicts mobili-
ties which are in reasonable accord with experiment for a

wide temperature range (Dalgano et al (1958), Dalgano (1958)).

Experimental results of differentially scattering can be used to predict interaction potentials using inversion techniques (Hoyt (1939), Firsov (1953)). However the resultant potentials are only available for a restricted range of internuclear separation and completely unsuitable for collisions in the thermal energy range. Recently with the development of fast digital computers, accurate a priori quantal calculations of the potentials have become possible and are comprehensively reviewed by Krauss (1967).

3. Classical Models of Inelastic Scattering

The classical binary encounter impulse approximation has been used to describe ionization, excitation and charge-transfer in electron-atom and ion-atom collisions but the following discussion will be in the main concerned with ionization. The basic assumptions of the theory are:

(i)   The projectile describes a classical orbit.

(ii)   The mutual interaction between the atomic electron and nucleus are disregarded during the collision. This is known as the impulse approximation.

(iii)   The interaction of the target electrons with the projectile are treated independently. This is the binary encounter approximation.

(iv)   The projectile is regarded as a structureless particle.

(v)   The interactions of the projectile with the target particles are Coulombic.

The cross-section for any process will be obtained from the formulae

$$Q = N \int d(\Delta E) \frac{d\sigma}{d(\Delta E)} \qquad (1.7)$$

where $d\sigma/d(\Delta E)$ is the differential cross-section for a given energy transfer, N is the effective number of electrons in the target and the integral is taken over those values of the energy transfer which contribute to the process under consideration. In the case of excitation and charge transfer a difficulty arises. Only one value of ΔE is relevant, namely the value which corresponds to the difference between the initial and final binding energies (given by quantal treatments of the electronic states or the use of empirical evidence), and the integral (1.7) vanishes. It is necessary to assume that a specific excitation or charge-transfer process will occur if the energy transfer, ΔE, satisfies

$$E_1 < \Delta E < E_2$$

for suitable E_1 and E_2. Similarly we assume ionization will occur if the energy transfer exceeds the binding energy of the atomic electron.

The atomic electrons in this model are assumed to be independant scattering centres. This assumption is justified when the effective interaction between the projectile and target takes place in a region small compared with atomic dimensions. If this is the case, the energy transfer to the target electron is far greater than the binding energy, and the model should therefore be more accurate when applied to ionization processes than for excitation and charge transfer.

Also for ionization there is no ambiguity in choosing the classical band of energies to represent the final state whereas for excitation and charge-transfer this is not the case.

In the following analysis let m_1 and m_2 be the masses of a target electron and incident projectile with charge z. (designated by 1 and 2 respectively) and let $\underline{v}_1$ and $\underline{v}_2$ be their initial velocities in the laboratory frame. Then the energy transfer cross-section is

$$\frac{d\sigma(\underline{v}_1,\underline{v}_2)}{d(\Delta E)} = \frac{2\pi V_g^2 z^2}{V^2|\Delta E|^3} \left(1-\cos^2\psi + \frac{\Delta E}{\mu V V_g}\cos\psi\right) \qquad (1.8)$$

where ΔE is the energy transfer, μ is the reduced mass, $\underline{V}_g$ is the constant velocity of the centre of mass, $\underline{V}$ is the initial relative velocity and ψ is the angle between $\underline{V}_g$ and $\underline{V}$. (For a detailed derivation of this, and following equations, see Coleman & McDowell 1969). The range of ΔE is restricted by the inequality.

$$-1 \leqslant \cos\psi - \frac{\Delta E}{\mu V V_g} \leqslant 1 \qquad (1.9)$$

and this ensures that $d\sigma/d(\Delta E)$ is a positive quantity.

Thomson (1912) considered the simple case where the atomic electron is at rest (ie. $\underline{v}_1=0$). The ionization cross-section at impact energy E_2 is given by

$$Q_T(E_2) = \int_I^E \frac{d\sigma(0,\underline{v}_2)}{d(\Delta E)} d(\Delta E) \qquad (1.10)$$

where I is the binding energy of the atomic electron and E is

the maximum value of ΔE such that the inequality (1.9) is satisfied. It is convenient to use atomic units, then $m_1 = 1$ and

$$Q_T(E_2) = \frac{z^2 m_2}{E_2 I}\left[1 - \frac{I}{E_2}\frac{(m_2+1)^2}{4m_2}\right](\pi a_0^2). \qquad (1.11)$$

In the high energy limit the Thomson ionization cross-section is proportional to E_2^{-1} which is in disagreement with both quantal treatments and experiment which both behave as $E_2^{-1}\ln E_2$.

In order to investigate the cross-section near threshold, let

$$E_2 = I + \varepsilon \qquad \varepsilon \ll I$$

and a linear dependence on the excess energy near threshold immediately follows for electron impact ($m_2=1$). This is in agreement with the quantal result of Rudge and Seaton (1965) for electron impact ionization of atomic hydrogen. For heavy particle impact the model fails completely near threshold because of the unrealistic assumption to consider the atomic electron fixed ($v_1=0$) in comparison with the heavy particle at these energies. For example in the case of proton impact ionization of hydrogen, the Thomson cross-section vanishes below 6.25 k.e.V.

The derivation of eqn. (1.8) is completely symmetric with respect to the two particles. When we consider the scattering of a beam of particles with initial velocity v_2, the relevant differential cross-section is related to that in (1.8) by a invariant reaction rate and is given by

$$\frac{d\sigma_2(\underline{v}_1\underline{v}_2)}{d(\Delta E)} = \frac{V}{v_2} \frac{d\sigma(\underline{v}_1,\underline{v}_2)}{d(\Delta E)} \tag{1.12}$$

For $v_1 = 0$, the cross-sections become identical.

For an isotropic distribution of $\underline{v}_1$, eqn.(1.12) may be averaged over angles,

$$\frac{d\sigma_2(v_1,v_2)}{d(\Delta E)} = \frac{1}{4\pi v_2} \int_C \frac{V \, d\sigma(\underline{v}_1,\underline{v}_2)}{d(\Delta E)} \, d\Omega \tag{1.13}$$

where C denotes the solid angle (for given E_1, E_2, and E) in which the inequality (1.9) is satisfied. The ionization cross-section is then given by

$$Q(E_1 E_2) = \int_I^{E_2} \frac{d\sigma_2(v_1,v_2)}{d(\Delta E)} \, d(\Delta E) \tag{1.14}$$

Stabler (1964) performed both these integrations for election impact ionization (ie. $m_1=m_2=1$) and obtained cross-sections in closed form.

$$Q(E_1,E_2) = \frac{2}{3E_2 I^2} \frac{(E_2-I)^{3/2}}{E_1^{1/2}} (\pi a_0^2) \quad E_2 \geqslant E_1 + I$$

$$\tag{1.15}$$

$$= \frac{1}{3E_2} \left[\frac{2E_1+3I}{I^2} - \frac{3}{E_2-E_1} \right] (\pi a_0^2) \quad E_2 \leqslant E_1 + I$$

As early as 1927, Thomas (1927a, b) and Williams (1927) had independently refined the theory of Thomson by considering the atomic electrons to have a spherically

symmetric velocity distribution. They derived expressions for $d\sigma_2(v_1 v_2)/d(\Delta E)$ by performing the integration in (1.13) but only obtained results for restricted energy ranges and hence were unable to derive the ionization cross-sections (1.15). More recently Gryzinski (1959) derived classical relations for coulombic collisions of two moving particles and laid the foundations for Stabler(1964) to derive the ionization cross-sections for the "equal mass" case obtaining agreement with the Thomas-Williams energy transfer cross-section in the process.

McDowell (1966) and Vriens (1967) have pursued the theory for unequal masses. McDowell, for proton impact ionization of hydrogen evaluated eqn. (1.13) in closed form and then numerically integrated (1.14) to obtain the ionization cross-section. Vriens introduced the momentum transfer as a variable in the analysis and obtained ion-impact ionization cross-sections to first order in $1/m_2$ in closed form in a simple way.

$$Q(E_1,E_2) = \frac{2z^2}{v_2^2}\left[\frac{1}{I}+\frac{v_1^2}{3I^2} - \frac{1}{2(v_2^2-v_1^2)}\right] (\pi a_o^2) \quad I \leqslant 2v_2(v_2-v_1)$$

$$= \frac{z^2}{v_2^2}\left[\frac{1}{2v_1(v_2+v_1)}+ \frac{1}{I} +\frac{1}{3v_1 I^2}\left(2v_2^3+v_1^3-(2I+v_1^2)^{3/2}\right)\right]$$

$$(\pi a_o^2) \quad 2v_2(v_2-v_1) \leqslant I \leqslant 2v_2(v_2+v_1) \qquad (1.16)$$

$$= 0, \text{ otherwise.}$$

Gerjuoy (1966) derived energy transfer cross-sections for unequal masses, and in the relevant energy regions they were identical to the much earlier formulae of Williams (1927). Garcia, Gerjuoy and Welker (1968) using these cross-sections performed the integration (1.14) analytically and obtained exact classical ionization cross-sections for ion-impact with bound electrons at fixed non zero velocity.

The cross-section (1.14) is given for fixed values of E_1 & E_2 and it should therefore be averaged over the velocity distribution, $f(v_1)$, of the bound electrons to give an ionization cross-section

$$Q(E_2) = \int_0^\infty Q(E_1 = \tfrac{1}{2}v_1^2, E_2) \, f(v_1) dv_1 \qquad (1.17)$$

where, of course,

$$\int_0^\infty f(v_1) dv_1 = 1. \qquad (1.18)$$

McDowell (1966) calculated $Q(E_2)$ for electron and proton impact ionization of hydrogen using the classical microcanonical velocity distribution for the atomic electrons (Mapleton 1966) which is identical to the quantal result. Because of the lack of knowledge of velocity distributions in other systems, it is usual to assume

$$f(v_1) = \delta(v_1 - (2I)^{1/2}) \qquad (1.19)$$

Prasad and Prasad (1963) with this assumption used the early Gryzinski theory to calculate ionization cross-sections for several atoms and diatomic molecules. Bauer and Bartky (1965) further extended the theory to excitation and ionization of molecules. Proton impact ionization cross-sections for noble gases have been performed by Garcia et al (1968).

In general the results are in excellant agreement, considering the simplicity of the model, with quantal calculations and experiment, differing at most by a factor of two up to large impact energies. The failure of the classical model to take account of distant collisions causes the high energy limit of the ionization cross-section to behave as E^{-2} in disagreement with both the experimental and quantal result of E^{-1} $\ln E$.

The above models with minor refinements have been applied by numerous workers to other processes such as excitation (Kingston 1964a,b, 1966a,b) and charge transfer (Thomas 1927, Bates & Mapleton 1967, amongst others) without the same measure of success in reproducing experimental and quantal results.

Finally, Percival and his collaborators (Abrines & Percival 1964, 1966a, b) have considered classical models of proton impact ionization of atomic hydrogen in which the target gas is represented by a classical microcononical ensemble of two body (e+p) systems which are allowed to interact classically with the incident proton. The Newtonian equations

of motion of the three particles are then solved numerically for a wide range of impact parameters, incident energies and a suitable distribution of two body systems. The resultant trajectories are examined to see whether as t → ∞, they represent a bound orbit of the initial target pair, electron transfer to the incident proton or three free particles (ionization).

4.   Impact Parameter Methods

For not too low impact velocities, the theory of collisions between atomic systems can be considerably simplified by considering it within the frame-work of the impact parameter model.   In this model the motion of the heavy nuclei are not only treated classically, but in most cases the motion is assumed to be rectilinear and can be uniquely distinguished by an impact parameter ρ and a velocity $\underline{v}$.   The electrons are treated quantum mechanically in the time dependant field of the nuclei.

The following discussion will be confined to proton-hydrogen collisions as this avoids unnecessary algebraic complexity in the analysis without undue loss in generality. Electron transitions of the type

$$H^+ + H(n,\ell) \rightarrow H^+ + H(n',\ell') \qquad (1.20)$$
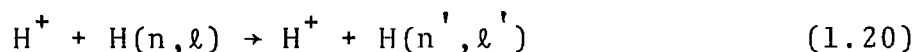
(direct excitation) and

$$H^+ + H(n,\ell) \rightarrow H(n',\ell') + H^+ \qquad (1.21)$$
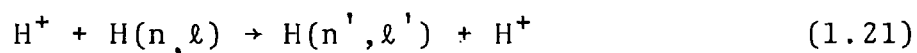
(rearrangement) will be considered.

In the impact parameter model, the target nucleus, A, is assumed to be at rest and the proton, B, moves in a straight line with velocity $\underline{v}$. Let $\underline{R}$ be the position vector of B relative to A then

$$\underline{R} = \underline{\rho} + \underline{v}t$$

where the time, t, is choosen so that A and B have a minimum separation ρ at t=0. Denote the centre of mass by 0 then let the position vectors of the electron, e, relative to A, B and 0 be $\underline{x}$, $\underline{s}$ and $\underline{r}$ respectively.

The time dependant Schrodinger equation (in atomic units) for the complete electronic wave function $\Psi(r,t)$ is

$$(T_A + V_B)\Psi = 0 \qquad (1.22)$$

where

$$T_A = \frac{1}{2}\nabla_r^2 + \frac{1}{x} + i\frac{\partial}{\partial t} \qquad V_B = \frac{1}{s} \qquad (1.23)$$

Let $\phi_i(r)$ denote the hydrogenic eigenfunction with eigen-energy ε_n which satisfies

$$(\frac{1}{2}\nabla^2 + \frac{1}{r} + \varepsilon_n) \phi_n(r) = 0 \qquad (1.24)$$

To allow for the translation motion of the protons, Bates and McCarroll (1958) introduced travelling orbitals

$$\phi_n^A(\underline{x}) = \phi_n(x) \exp\left[-i(\frac{1}{2}\underline{v}\cdot\underline{r} + \frac{1}{8}v^2 t + \varepsilon_n t)\right] \qquad (1.25)$$

and it is readily shown that

$$T_A \phi_n^A = 0 \qquad (1.26)$$

The boundary conditions (as $t \to -\infty$) of the required solution of (1.22) must describe an electron bound to the proton A in a state p, say. In early impact parameter treatments (c.f. Bates 1958), it was assumed that a sufficient boundary condition was given by ignoring the term V_B in (1.20) for large t, and hence the boundary condition was

$$\Psi \underset{t \to \infty}{\sim} \Phi_p^A (x).$$

Cheshire (1964) showed that the Coulomb potential V_B has a residual effect at large t and the boundary condition should be multiplied by a phase factor and is given by

$$\Psi \underset{t \to -\infty}{\sim} \Phi_p^A(\underline{x}) \, \exp\left[-\frac{i}{v}\ln(vR-v^2 t)\right] \tag{1.27}$$

For excitation transitions it is convenient to consider a formal expansion of

$$\Psi = \Phi^A \, A \tag{1.28}$$

where Φ^A is a row matrix with elements Φ_n^A and A is a column matrix with elements $a_n(t)$ with boundary conditions.

$$a_n(t) \underset{t \to -\infty}{\sim} \delta_{np} \, \exp\left[-\frac{i}{v}\ln(vR-v^2 t)\right] \tag{1.29}$$

The scalar product in (1.28) implies summation over all bound states and integration over the continuum. The probability of excitation to a bound state q, also on A, is given by

$$P_A(p,q) = \lim_{t \to \infty} \left| a_q(t) \right|^2 \tag{1.30}$$

The Schrodinger equation may also be written

$$(T_B + V_A) \; \Psi = 0 \tag{1.31}$$

where

$$T_B = \tfrac{1}{2}\nabla_r^2 + \frac{1}{s} + i\frac{\partial}{\partial t} \qquad V_A = \frac{1}{x} \tag{1.32}$$

and travelling orbitals centred on the proton B are given by

$$\Phi_m^B = \phi_m(s) \; \exp\left[i(\underline{v}\cdot\underline{r}\,\tfrac{1}{2} - \frac{v^2 t}{8} - \epsilon_n t)\right] \tag{1.33}$$

When considering rearrangement collisions, it is convenient to expand Ψ, in parallel with (1.28), as

$$\Psi = \Phi^B \; B \tag{1.34}$$

and the probability that the electron is finally bound to proton B in state q is given by

$$P_B(p,q) = \lim_{t\to\infty} \left| b_q(t) \right|^2 \tag{1.35}$$

The major difficulty of such an expansion (1.34), is that the boundary condition of the solution Ψ as $t\to-\infty$ describing a bound state of A, cannot be represented by a linear combination of functions Φ^B centred on proton B. It is thus necessary to also include an expansion of the form (1.28) in the analysis of charge transfer collisions.

Finally, cross-sections for transitions (1.20) and (1.21) are obtained by integrating the relevant probabilities over all impact parameters.

$$Q_{A,B}(p,q) = \int d\underline{\rho} \; P_{A,B}(p,q). \tag{1.36}$$

It has long been realized (Frame (1931)) that the cross-sections given by (1.36) are equivalent to the exact (non-relativistic) quantum theory result provided that the impact energy is much larger than the energy transfer involved in the collision. Following Moiseiwitch (1966) and Crothers and Holt (1966), McCarroll and Salin (1966) proved this result with the added restrictions equivalent to ensuring that the deBroglie wavelength of the relative motion is small compared with atomic dimensions so that the orbit of the heavy particle may be described in an unambiguous way.

More recently, McCarroll and Salin (1968) have considered the impact parameter formulation in terms of a purely quantal formalism in the limit as the masses of the atomic nuclei become infinite and have succeeded in obtaining expressions for differential scattering cross-sections in terms of amplitudes obtained from the impact parameter calculation.

A few previous applications of the impact parameter model will now be considered. Projecting the Schrodinger equation (1.22), on the complete set of states Φ^A results in a equivalent set of equations

$$(\Phi^A | T_A | \Psi) = -(\Phi^A | V_B | \Psi) \qquad (1.38a)$$

Similarly for equation (1.31) and Φ^B,

$$(\Phi^B | T_B | \Psi) = -(\Phi^B | V_A | \Psi) \qquad (1.38b)$$

where
$$(\Phi_n^{A,B} | Z | \Psi) = \int d\underline{r} \; \Phi_n^{A,B*} Z \Psi \qquad (1.39)$$

Using the expansion (1.28) of Ψ and equation (1.26), (1.38a) reduces to

$$\frac{dA}{dt} = i(\Phi^A|V_B|\Phi^A)A \tag{1.40}$$

This is an infinite set of coupled differential equations for the variables $a_n(t)$ and is exact up to this point within the framework of the impact parameter model. In practice these equations are reduced by neglecting all terms containing states other than the few bound states considered to be most dominant in the collision (e.g. initial, final and an intermediate state). One would hope that as more intermediate states are included the final transition amplitude would converge to the correct results.

If only the diagonal elements in (1.40) are retained then

$$a_n = \delta_{np} \exp \left[i \int^t \left[\Phi_n^A|V_B|\Phi_n^A\right] dt' \right] \tag{1.41}$$

The distortion approximation of Bates (1959) for excitation into state q, is obtained from (1.40) by retaining only terms containing states p and q

$$\dot{a}_q = i\left(\Phi_q^A|V_B|\Phi_q^A\right)a_q + i\left(\Phi_q^A|V_B|\Phi_p^A\right)a_p \tag{1.42}$$

and substituting from (1.41) for a_p. This procedure can be extended by retaining more states and solving the coupled equations numerically (Lovell & McElroy, 1965) but the usefulness of (1.40) is extremely limited as it contains no coupling to

the important rearrangement states on proton B, and so the hope of converging on the correct solution by the addition of more states, can never be realized.

As an alternative to (1.40), we can consider the equations

$$\frac{dA}{dt} = i(\Phi^A | V_B | \Phi^B) B \tag{1.43a}$$

$$\frac{dB}{dt} = i(\Phi^B | V_A | \Phi^A) A \tag{1.43b}$$

obtained from (1.38a, b) using expansions (1.35) and (1.28) respectively. Rearrangement amplitudes can be obtained using (1.43b) once the matrix A is known. The Brinkman-Kramers approximation is obtained by substituting $a_n = \delta_{np}$, but as Cheshire (1965) pointed out, this is in consistant with the boundary conditions (1.29). The modified Brinkman-Kramers approximation is obtained using

$$a_n = \delta_{np} \exp\left[-\frac{i}{v} \ln(vR - v^2 t)\right] \tag{1.44}$$

in the right hand side of (1.43b).

It is easily shown that the only effect of the addition of an arbitary function, W(R), of the internuclear distance to the Hamiltonian of the Schrodinger equation (1.31), is to change the exact solution Ψ by a phase factor and hence will leave the calculated cross-sections unchanged. Bates and Dalgano (1952), and Jackson and Schiff (1953) performed rearrangement calculations including the nuclear-nuclear interaction term in the matrix elements and hence

solved

$$(T_B + V_A^1) \ \Psi = 0 \tag{1.45}$$

where

$$V_A^1 = \frac{1}{x} + \frac{1}{R} \tag{1.46}$$

and with the boundary condition given by

$$\Psi \underset{t \to -\infty}{\sim} \Phi_p^A \ (\underline{x}) \tag{1.47}$$

The exact solution Ψ, is identical to that obtained from (1.31) (1.32) and (1.27). This is not true when Ψ is represented by truncated expansions of atomic orbitals and the cross-sections of Bates & Dalgano differed from the Brinkman-Kramers approximation. We now have the unsatisfactory situation where the cross-sections are not independant of the nuclear-nuclear interaction potential.

To rectify this, Bates (1958) proposed an over complete expansion

$$\Psi = \Phi^A A + \Phi^B B$$

The advantage of this two centre expansion is that is make explicit allowance for each reaction path and circumvents the defect of the single centre expansion where rearrangement states are contained in the continuum. Substituting (1.49) in (1.38a, b) gives

$$\frac{dA}{dt} + (\Phi^A|\Phi^B)\frac{dB}{dt} = i(\Phi^A|V_B|\Phi^A)A + i(\Phi^A|V_A|\Phi^B)B \tag{1.50}$$

$$\frac{dB}{dt} + (\Phi^B|\Phi^A)\frac{dA}{dt} = i(\Phi^B|V_A|\Phi^B)B + i(\Phi^B|V_B|\Phi^A)A \tag{1.51}$$

and these equations, when truncated, give cross-sections that
are uneffected by the addition of W(R) to the Hamiltonian.
Equations (1.50) and (1.51) have provided the basis for sev-
eral calculations on proton-hydrogen collisions. McCarroll
(1961) calculated resonance charge transfer between the 1s
states and included only one orbital on each nuclei. Lovell
and McElroy (1965) extended the calculations to excitation
and capture into the 2s-states. They used various combina-
tions of 1s and 2s orbitals, with a total maximum of three,
to investigate rates of convergence of the cross-sections.
However the most extensive calculation of this type so far
is that by Wilets and Gallaher (1966) who include all n = 1
and n = 2 states of A and B and check convergence by extend-
ing the calculation to 3s and 3p states for some selected
impact parameters and energies. The change in the cross-
sections with the addition of the n=3 states is small and
although the solution would have appeared to have converged,
no account has yet been taken of continuum states.

In an attempt to include effects due to continuum
states, Gallaher and Wilets (1968) expanded the electronic
wave function in terms of Sturmian functions. These functions
form an infinite discrete and complete basis set without a
continuum and the transition amplitudes are obtained by pro-
jection onto the hydrogenic states.

A completely different approach was proposed by
Cheshire (1965). Using equations (1.43), he eliminated the B

coefficients by using closure, and then the calculation of the Λ amplitudes from the resulting second order equation would take implicit account of the complete set of rearrangement states. This closure approximation is discussed further in Chapter IV.

REFERENCES

Abrines, R., and Percival, I.C., 1964, Phys. Letters, 13, 216-7.

Abrines, R., and Percival, I.C., 1966a, Proc. Phys. Soc., 88, 861-72.

Abrines, R., and Percival, I.C., 1966b, Proc. Phys. Soc., 88, 873-84.

Bates, D.R., 1958, Proc. Roy. Soc., A 245, 299-301.

Bates, D.R., 1959, Proc. Phys. Soc., 72, 227-32.

Bates, D.R., and Dalgano, A., 1952, Proc. Phys. Soc., A 65, 919-25.

Bates, D.R., and Mapleton, R.A., 1967, Proc. Phys. Soc. 90, 909-12.

Bates, D.R., and McCarroll, R., 1958, Proc. Roy. Soc., A 245, 175-83.

Bauer, E., and Bartley, C.D., 1965, J. Chem. Phys., 43, 2466-76.

Bernstein, R.B., 1960, J. Chem. Phys., 33, 795-804.

Bernstein, R.B., 1961, J. Chem. Phys., 34, 361-5.

Bernstein, R.B., 1962, J. Chem. Phys., 37, 1880-1.

Bernstein, R.B., 1963, J. Chem. Phys., 38, 2599-2609.

Bernstein, R.B., 1966, Adv. Chem. Phys., 10, 75-134.

Born, M., and Oppenheimer, J.R., 1932, Ann. d. Physik, 84, 457.

Cheshire, I.M., 1964, Proc. Phys. Soc., 84, 89-98.

Cheshire, I.M., 1965, Phys. Rev., 138, A992-8.

Coleman, J.P., and McDowell, M.R.C., 1969, Introduction to the theory of Ion-Atom Collisions (Amsterdam: North Holland).

Crothers, D.S.F., and Holt, A.R., 1966, Proc. Phys. Soc., 88, 75-81.

Dalgano, A., 1958, Phil. Trans. Roy Soc. A., 250, 426-439.

Dalgano, A., McDowell, M.R.C., and Williams, A., 1958, Phil. Trans. Roy. Soc. A., 250, 426-439.

Dickenson, A.S., 1968a, J. Phys. B. (Proc. Phys. Soc.), [2], 1, 387-394.

Dickenson, A.S., 1968b, J. Phys. B. (Proc. Phys. Soc.), [2], 1, 395-401.

Firsov, O.B., 1953, Zh. Eksperim. i Teor. Fiz (USSR), 24, 279-83.

Ford, K.W., and Wheeler, J.A., 1959, Ann. Phys. N.Y., 7, 25-86.

Frame, J.W., 1931, Proc. Camb. Phil. Soc., 27, 511-7.

Gallaher, D.F., and Wilets, L., 1968, Phys. Rev., 169, 139-49.

Garcia, J.D., Gerjuoy, E., and Welker, J.E., 1968, Phys. Rev., 165, 66-71.

Gerjuoy, E., 1966, Phys. Rev., 148, 54-59.

Gryzinski, M., 1959, Phys. Rev., 115, 374-83.

Hoyt, F.C., 1939, Phys. Rev., 55, 664-5.

Jackson, J.D., and Schiff, H., 1953, Phys. Rev., 89, 359-65.

Kingston, A.E., 1964a, Phys. Rev., 135, A1529-36.

Kingston, A.E., 1964b, Phys. Rev., 135, A1537-9.

Kingston, A.E., 1966a, Proc. Phys. Soc., 87, 193-200.

Kingston, A.E., 1966b, Proc. Phys. Soc., 89, 177-8.

Krauss, M., 1967, Compendium of ab initio Calculations of Mole. Energies and Properties. (N.B.S., Washington).

Landau, L.D., and Lifshitz, E.M., 1959, Quantum Mechanics, (Pergamon Press: London).

Lovell, S.E., and McElroy, M.B., 1965, Proc. Roy. Soc. A.,
    283, 100-14.

Mapleton, R.A., 1966, Proc. Phys. Soc., 87, 219-22.

Marchi, R.P., and Mueller, C.R., 1962, J. Chem. Phys.,
    36, 1100-1.

Marchi, R.P., and Mueller, C.R., 1963, J. Chem. Phys.,
    38, 740-4.

Massey, H.S.W., and Mohr, C.B.O., 1934, Proc. Roy. Soc.,
    A144, 188-205.

McCarroll, R., 1962, Proc. Roy. Soc. A284, 547-57.

McCarroll, R., and Salin, A., 1966, C.R. Acad. Sci. Paris,
    263B, 329-32.

McCarroll, R., and Salin, A., 1968, J. Phys. B. (Proc.
    Phys. Soc.), [2], 1, 163-71.

Mittleman, M.H., 1962, Phys. Rev., 122, 499-506.

Moiseiwitch, B.L., 1966, Proc. Phys. Soc., 87, 885-8.

Mott, N.F., and Massey, H.S.W., 1965, The Theory of Atomic
    Collisions, (Cambridge Univ. Press).

Munn, R.J., Mason, E.A., and Smith, F.J., 1964, J. Chem.
    Phys., 41, 3978-88.

Prasad, S.S., and Prasad, K., 1963, Proc. Phys. Soc., 82,
    655-8.

Rothe, E.W., Rol, P.K., Trujillo, S.M., and Neynaber, R.H.,
    1962, Phys. Rev.,128, 659-62.

Rudge, M.R., and Seaton, M.J., 1965, Proc. Roy. Soc., A
    283, 262-90.

Schiff, L.I., 1956, Phys. Rev., 103, 443-53.

Stabler, R.C., 1964, Phys. Rev., 133, A1268-73.

Thomas, L.H., 1927a, Proc. Camb. Phil. Soc., 23, 713-16.

Thomas, L.H., 1927b, Proc. Camb. Phil. Soc., 23, 829-31.

Thomson, J.J., 1912, Phil. Mag., 23, 449-57.

Vriens, L., 1967, Proc. Phys. Soc., 90, 935-44.

Wilets, L., and Gallaher, D.F., 1966, Phys. Rev., 147, 13-20.

Williams, E.J.; 1927, Nature (London), 119, 489-90.

CHAPTER II

ELASTIC SCATTERING OF LITHIUM ION IN HELIUM

1. Introduction

The system Li^+, He is sufficiently simple as to pro-
vide a testing ground for theoretical models of elastic ion-
atom scattering. Data of Aberth and Lorents (1965) show that
the inelastic component of the cross-section is less than 1%
of the elastic component at an angle of 10° for an incident
energy of 600 e.V. Therefore the system provides a ready
comparison between theory and experiment without having to take
inelastic effects into account.

The scattering predicted by some of the semi-empir-
ical potentials (derived from experimental data) has been
analyzed by Weber and Berstein (1965) using a JWKB approxi-
mation for the phase shifts. The purpose of this present
work is to extend this analysis to more recent semi-empirical
potentials and more importantly, to the more accurate a
priori potentials now available. In the regions where the
JWKB is inaccurate, exact quantal phase shifts are obtained.
Experimental measurements of differential scattering through
angles greater than a given angle, $S(\Theta)$, (Zehr and Berry,
1967), differential cross-sections, $I(\Theta)$, (Aberth & Lorents,
1969) and the temperate variation of the mobility K (Hosel-
itz, 1941), are available for comparison. Atomic units are

used throughout except where otherwise stated.

2. The Radial Equation and Solutions

In the absence of inelastic processes the scattering of Li^{+} by He may be described by the appropriate solution of the differential equation

$$\left[\frac{d^2}{dr^2}+k^2-2\mu V(r)-\frac{\ell(\ell+1)}{r^2}\right]u_\ell(r) = 0 \tag{2.1}$$

satisfying

$$u_\ell(o) = 0 \quad , \quad u_\ell(r) \underset{r\to\infty}{\sim} k^{-1/2} \sin(kr-\tfrac{1}{2}\ell\pi+\eta_\ell) \tag{2.2}$$

where η_ℓ is the phase shift, ℓ is the angular momentum quantum number, k is the relative momentum of the collision, μ is the reduced mass of the system and V(r) is the interaction potential.

This equation can be solved numerically and the phase shift can be determined at large r. Extraction of the phase shift from the solution at a finite value of r, r_1 say, incurs an error since the effect of the non-vanishing potential for $r>r_1$ has not been accounted for. At large r the potential is slowly varying and a JWKB analysis has been used by Seaton and Peach (1962) and by Burgess (1963) to determine, to first and second order respectively, a correction factor to the solution at $r=r_1$ due to the long range tail of the potential, $r>r_1$. For large r, the interaction potential is

effectively the polarization potential of He written

$$V_{pol}(r) = -\frac{\alpha}{2r^4} \quad \text{a.u.} \tag{2.3}$$

where $\alpha = 1.384\ a_o^3$, is the polarization of helium (see section 4).

If we write

$$u_\ell(r) \underset{r\to\infty}{\sim} \sin(\phi(r) + \eta_\ell),$$

the second order approximation (including terms up to r^{-3}) of $\phi(r)$ for a potential (2.3) as derived by Burgess is

$$\phi(r) = (k^2 r^2 - c)^{1/2} - \frac{1}{2}\ell\pi + \Theta - \frac{1}{8(k^2 r^2 - c)^{1/2}} - \frac{5c}{24(k^2 r^2 - c)^{3/2}}$$

with $c = \ell(\ell+1)$ and

$$\tag{2.4}$$

where

$$\Theta = \frac{(c+1/8)}{c^{1/2}}\text{arc sin}\frac{c^{1/2}}{kr} + \frac{\alpha\mu(k^2 r^2 - c)^{1/2}}{8cr^2}$$

$$-\frac{\alpha\mu k^2}{8c^{3/2}}\text{arc sin}\frac{c^{1/2}}{kr} \qquad c > o$$

$$= \frac{1}{8kr} - \frac{\mu\alpha}{12kr^3} \qquad c = 0$$

The phase shift can now be determined to a high degree of accuracy without the necessity of continuing the step by step integration of the radial equation to the much larger distances required if only the first order asymptotic forms of the solution are used.

At sufficiently large energies (Munn, Mason and Smith, 1964), the JWKB approximation is valid and can be used to determine the phase shifts (eqn. (1.5)). These phase

shifts themselves can be replaced for large ℓ by the Jefferys-Born phase shift (eqn. (1.6)). At these large distances ($r \sim \ell/k$) the potential is given by (2.3) and the J-B phase shift is readily obtained in closed form

$$\eta_\ell^{JB} = \frac{\alpha \mu k^2}{2(\ell+1/2)^3} \frac{\pi}{4} \quad \text{(radians)} \qquad (2.5)$$

3. Theoretical Prescription of Scattering Cross-Sections

The derivation of cross-sections in terms of infinite sums of phase-shifts is well known (Mott & Massey 1965) and the cross-sections required in the following analysis will be only stated here for the purpose of completeness.

The total elastic scattering cross-section is given by,

$$Q_{el}(k^2) = \frac{4\pi}{k^2} \sum_{\ell=0}^{\infty} (2\ell+1)\sin^2\eta_\ell \qquad (a_o^2) \quad (2.6)$$

while the diffusion cross-section is

$$Q_d(k^2) = \frac{4\pi}{k^2} \sum_{\ell=0}^{\infty} (\ell+1)\sin^2(\eta_\ell - \eta_{\ell+1})(a_o^2). \quad (2.7)$$

The differential scattering cross-section at angle Θ is

$$I(\Theta) = \frac{1}{4k^2}(A^2+B^2) \qquad (a_o^2) \quad (2.8)$$

where

$$A = \sum_\ell (2\ell+1)(\cos 2\eta_\ell - 1)P_\ell(\cos\Theta)$$

$$B = \sum_\ell (2\ell+1)\sin 2\eta_\ell P_\ell(\cos\Theta) .$$

By integration, the cross-section $S(\Theta)$ for scattering outside a cone of semi-angle Θ about the forward direction

$$S(\Theta) = 2\pi \int_{-1}^{\cos\Theta} I(\Theta) \, d(\cos\Theta) \quad (a_o^2). \quad (2.9)$$

The above infinite sums in practice have to be truncated and the number of phase-shifts giving an appreciable contribution is determined by the range, R, of the interaction and the momentum, $k=\mu v$. As will be seen in the next section, the range of the interaction potentials is of the order of $10a_o$.

Now $\ell_{max} \sim Rk$, which means at the highest collision energy considered, $E \sim 250$ eV ($k=3\times10^2$ a.u.), approximately 3×10^3 phases shifts are required. However for extremely low energies of interest in mobility calculations, fewer than 10^2 phase shifts contribute to the cross-sections.

Finally the mobility, K, is determined from the diffusion cross-section Q_d,

$$K = \frac{eD}{k_B T} \quad (cm^2 \, volt^{-1} \, sec^{-1}) \quad (2.10)$$

where T is the absolute temperature, k_B is the Boltzmann's constant, e is the ionic charge and D, the diffusion coefficient, is given by

$$D = \frac{3\pi^{1/2}}{16n} \left[\frac{2k_B T}{\mu}\right] \frac{1}{P} \quad (2.11)$$

with

$$P = \int_0^\infty \exp(-x^2)x^5 \, Q_d(x)dx \quad , \quad x^2 = \frac{\mu v^2}{2k_B T} \qquad (2.12)$$

to first order (Dalgano et al, 1958) where n is the number density of the gas. We ignore the second order correction factors of the Chapman-Enskog theory (Dickenson 1968). The reduced mobility K' is that obtained with $n = 2.98 \times 10^{19}$ cm^{-3}.

4. Li^+ -He Interaction Potentials

Several groups of workers have attempted to deduce an interaction potential for the ground state of LiHe$^+$ from one or other set of experimental measurements. Potentials derived from mobility data may be represented by that of Dalgano et al (1958),

$$V_1(r) = 37.10e^{-2.75r} - 0.695r^{-4} \quad , \text{ for all } r. \qquad (2.13)$$

Zehr and Berry (1967) used a classical model (Hoyt, 1939) to invert their data on S(θ) to obtain

$$V_2(r) = 13.60e^{-2.70r}, \qquad 0.1 < r < 1.4a_o \qquad (2.14)$$

while Olson et al (1969) have deduced a potential

$$V_3(r) = 10.92e^{-2.28r} + 37.01e^{-10.79r} \quad 0.3 < r < 1.7a_o \quad (2.15)$$

from the differential cross section measurements of Aberth and Lorents (1969) by a classical analysis with the aid of expansion formulae (F.T. Smith et al, 1966).

With the development of fast, large digital compu-
ters in the last few years, a priori calculations of the
potential have become possible. Preliminary calculations
for a restricted range of the internuclear separations
$(0.2 < r < 1.4a_0)$ have been made by Fischer (1968) and of the
long range part $(2 < r < 8a_0)$ by Schneiderman and Michels (1965).
An outline of a more extensive calculation performed in the
main by Kaufman and Sachs, and reported more fully by Catlow
et al, 1969, covering all internuclear seperations is now
reported and results presented.

The calculations were of the Hartree-Fock-Roothaan
type (Roothaan 1951) where the wave function for a closed
shell species is a single determinant of the one-electron
molecular orbitals (MO's) built up from the atomic orbitals
centered on the atoms. The actual computations were carried
out with the MOSES program (Sachs and Geller 1967) utilizing
Gaussian basis functions centered on both atoms. Gaussian-
type orbitals have the same structural form as Slater-type
orbitals except the exponential, $e^{-\zeta r}$, in the latter is re-
placed by a Gaussian $e^{-\alpha r^2}$. There is no denying that the
Gaussian-type orbitals are far inferior basis functions to
the STO's in representing atomic orbitals but their advan-
tage lies in the contrasting simplicity of the evaluation of
molecular integrals over Gaussian functions.

In Table 2.1 are listed the Gaussian exponents used
in the present calculations. As a check on the necessity of

TABLE 2.1

Gaussian Exponents

	He	Li
s_1	0.1080	0.02854
s_2	0.2409	0.0772
s_3	0.5526	0.2634
s_4	1.3524	0.7179
s_5	3.5223	1.9060
s_6	9.7891	5.4033
s_7	30.1799	16.7798
s_8	108.7723	60.0718
s_9	488.8941	267.0960
s_{10}	3293.6930	1782.9000
p_1	0.0035	0.0140
p_2	0.0085	0.0340
p_3	0.0217	0.0870
p_4	0.0525	0.2100
p_5	0.2000	0.8000
p_6	0.8250	3,3000

including p orbitals in the basis set to allow for polariz-
ation, E_{HF} of LiHe$^+$ was calculated using only the 10^S expon-
ents on each atom.

In spite of the fact that E_{HF}(LiHe$^+$) $(10^S; 10^S)$
(=10.09832145 a.u.) at r=3.75a_o, was for ordinary purposes
quite close to the E_{HF}(LiHe$^+$) $(10^S6^P; 10^S6^P)$ (=10.10022048
a.u.) at the same r, it failed completely when calculating
the polarization potential, the discrepancy of 0.00290598
a.u. being actually larger than the entire calculated attrac-
tive polarization potential of -0.002363 a.u.

The calculated quantity is the energy $E_{mol}(r)$ of
the ground state of the LiHe$^+$ molecule. It is related to
the scattering potential V(r) by

$$V(r) = E_{mol}(r) - E_o(Li^+) - E_o(He) \text{ a.u.} \qquad (2.16)$$

where E_o(A) is the ground state energy of atom (or ion)A.
We take the Hartree-Fock values of E_o(Li$^+$), E_o(He) generated
with the same basis set, so much of the small error due to
omission of the correlation energy in the MO-SCF procedure
is subtracted out. The program becomes impractically time
consuming for r<0.1a_o and an extrapolation to the spectro-
scopic value of the united atom energy is made. As Fischer
(1968) has already pointed out the $(1\sigma)^2 (2\sigma)^2$ ground state
configuration of LiHe$^+$ goes over in the united atom limit to
the $(1s)^2 (2s)^2$ ground state of B$^+$.

At moderate values of r, (5<r<8a_o) the calculated

potential $V(r)$ is closely fitted by the polarization potential (2.3) which is then used for $r > 8a_o$.

The potential of Fischer (1968) is also calculated in the MO-SCF model with Gaussian basis sets and is indistinguishable from the present calculations in his range of values. The potential given by Schniederman & Michels (1965) is not as close a fit to (2.3) for $r > 5a_o$ as the present results.

An independant calculation of the interaction potential by Junker & Browne (1969), denoted by $V_4(r)$ here, is in progress and preliminary results are available for comparison. Table 2.2 shows that Junker's total separted atom energy is closer to the spectroscopic value than the present work but that the latter agrees well with SCF values of Roothaan et al.

TABLE 2.2

Separated Atom Energies

$$E = E_0(Li^+) + E_0(He)$$

Browne[a]	This work	Best SCF[b]	Experiment[c]
-10.17198	-10.09786	-10.0981	-10.1809

(a)   Junker and Browne (1969)

(b)   Roothaan et al (1960)

(c)   Moore (1949)

In comparing the two sets of values of $V(r)$, (Table 2.3) it is seen that Junker and Browne's potential is shallower than

TABLE 2.3

Comparison of the SCF-MO and the Junker-Browne
potentials in a.u.

r(a.u.)	SCF-MO $V(r)$	Junker-Browne $V_4(r)$
0.1	46.977379	
0.25	13.667331	13.69017
0.5	4.794386	5.05615
0.75	2.331407	2.43838
1.00	1.211805	1.28242
1.25	0.632821	0.68392
1.5	0.327374	0.36129
1.75	0.166478	0.18899
2.0	0.082306	0.09721
2.25	0.038786	0.04716
2.50	0.016708	0.02148
3.00	0.000123	0.00314
3.5	-0.002259	-0.00072
4.0	-0.002171	-0.00106
4.5	-0.001591	-0.00085
5.0	-0.001011	-0.00064
5.5	-0.000765	-0.00046
6.0	-0.000544	-0.00037
7.0	-0.000298	-0.00021
8.0	-0.000181	-0.00016

$V(r)$ at all r, and though both have a minimum near $r=3.75a_o$, the depth of the minimum of $V(r)$ (-0.002363 a.u. $\simeq -0.064$ e.V.) is considerably larger than their value (-0.0011 a.u. $\simeq 0.030$ e.V.). For $r>5a_o$, $V(r)$ is much closer to the polarization potential than is Junker and Browne's potential. However the differences between the two potentials are small.

The potentials $V_2(r)$ and $V_3(r)$ are compared with the results of the quantal calculations in the core region $0<r<2.5a_1$ in fig. 2.1. Neither of the semi-empirical potentials is sufficiently repulsive at small r ($r<1.0a_o$), though the Olson et al potential agrees well with the quantal calculations in the range $1.0<r<2.0a_o$. Neither of these potentials produce binding so no comparison is made with the quantal calculations for larger r. Olson et al point out that their absolute values are uncertain by $\pm$ 25%, so there is no disagreement in magnitude with our potential, however their slope is too shallow.

The potential $V_1(r)$ deduced from mobility data does show a minimum and has the correct long range behaviour. For $r>1a_o$ it is in excellant agreement with the potential presented here.

5. Numerical Evaluation of Phase Shifts and Phase Shift Sums

In general the phase shifts for a given potential at a centre of mass collision energy E_{cm} (momentum $k = (2E_{cm}\mu)^{1/2}$) were evaluated in the JWKB approximation (1.1) using the modified Clenshaw-Curtis quadrature method of Kennedy

FIGURE 2.1

—— S.C.F.-M.O. potential; this work.

-x-x Zehr-Berry potential.

-o-o Olson et al.

--- Junker-Browne quantal potential.
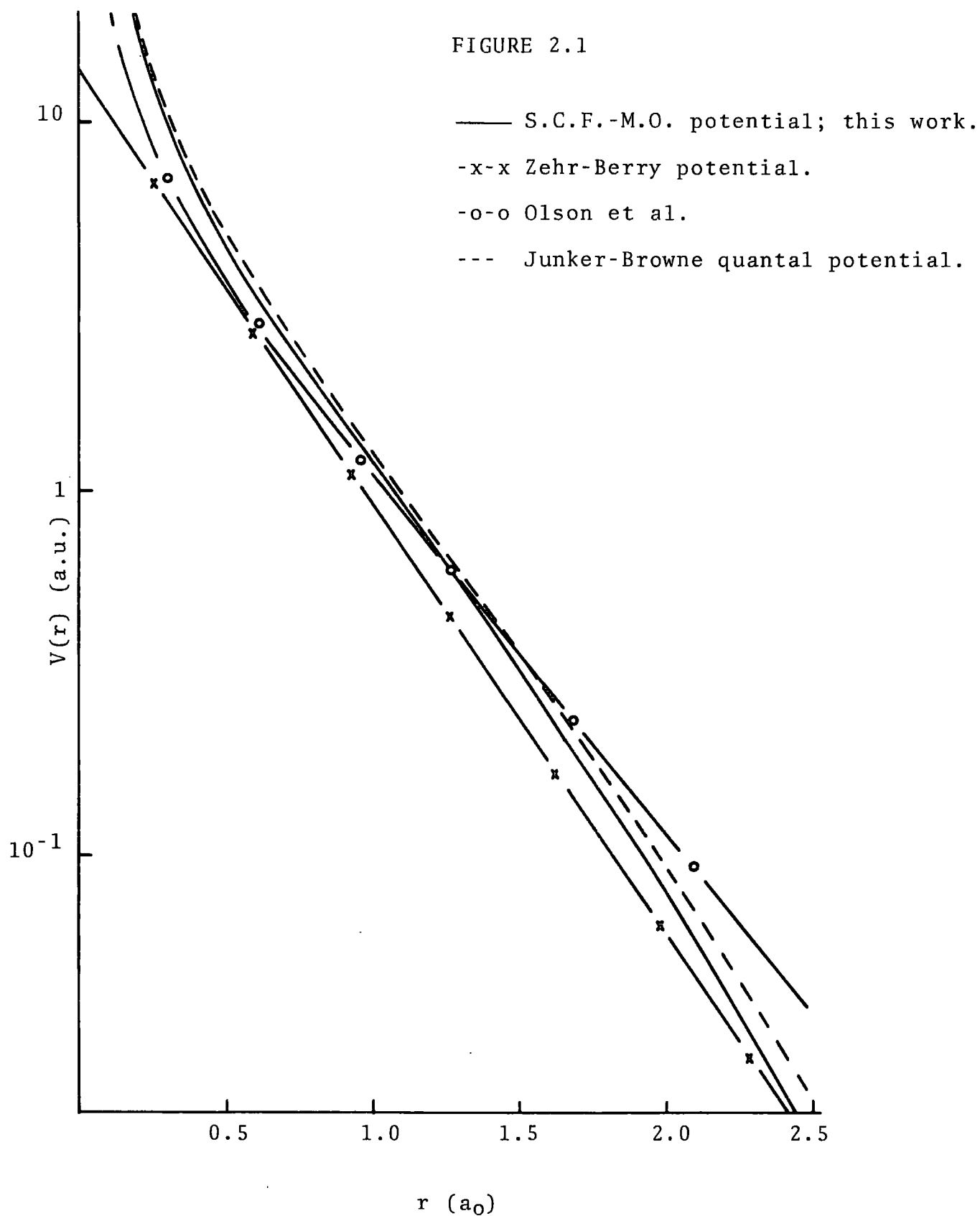
Quantal and Semi-Empirical Potentials.

and Smith (1967).

If we write

$$F(r) = \left[1 - V(r)/E_{cm} - b^2/r^2\right]^{1/2} \qquad (2.17)$$

where b is the impact parameter, the JWKB phase shift (1.1) can be approximated by

$$I_N = \frac{kr_m r_o}{2} \sum_{s=o}^{N=1} h_s^N \, F(r_m/\cos\Theta_1) \, \sin\Theta_1/\cos^2\Theta_1$$

$$+ \frac{kb\pi}{4} \sum_{s=1}^{N-1} h_s^N \left[F(b/\cos\Theta_2) - \sin\Theta_2\right] \sin\Theta_2/\cos^2\Theta_2 \qquad (2.18a)$$

if $b \geq r_m$, and

$$I_N = \frac{k(r_m+\alpha)\pi}{4} \sum_{s=1}^{N-1} h_s^N \left[F(r_3) - (1-b^2/r_3^2)^{1/2}\right] \sin\Theta_2/\cos^2\Theta_2$$

$$+ k\left[b \, \arccos \, (b/r_m) - (r_m^2 - b^2)^{1/2}\right] \qquad (2.18b)$$

if $b < r_m$. In these formulae

$$\Theta_1 = \frac{1}{2}r_o\left[1 + \cos\pi s/N\right] \, , \quad \Theta_2 = \frac{1}{4}\pi\left[1 + \cos\pi s/N\right]$$

$$r_o = \arccos \, (r_m/b), \quad r_3 = (r_m+\alpha)/\cos\Theta_2 - \alpha$$

and h_s^N are the weights given by

$$h_s^N = \frac{2(-1)^s}{N^2-1} + \frac{4}{N} \sin \frac{s\pi}{N} \sum_{r=1}^{\frac{1}{2}N} \frac{\sin \, [(2r-1)s\pi/N]}{2r-1} \qquad . \qquad (2.19)$$

The constant α is a scaling factor and was taken to be equal to a_o. Results of Kennedy and Smith for a L-J potential at three energies were reproduced to five decimal places with maximum N=64.

Hence in the present calculations, N initially took the value 16, and was increased in two steps to a maximum of 64 and the criterion for convergence was that the proportional increase in the new value of I_N was less than 10^{-4}.

Congergence was poor for k<3 a.u. (0.02 e.V.) so in this region the radial equation (2.1) was solved by Numerov's method. The solution was started at the point r=s where

$$V_{eff} \; (s,\ell) \; = \; V(s) \; + \; \frac{\ell(\ell+1)}{s^2} \; = \; 150 \quad \text{a.u.} \qquad (2.20)$$

with initial conditions

$$u_\ell(s) \; = \; 0 \; , \; u_\ell(s+h) \; = \; 10^{-30}$$

and the step length, h, equal to 5×10^{-3}.
Throughout the energy range for which Numerov's method was employed (k<3.5 a.u., see below) the solution was insensitive to the choice of the starting point criterion (2.20) or its starting values. This is illustrated in Table 2.4 where phase shifts derived with different varying initial conditions are compared. The phase shift was determined from the asymptotic form of the solution by the Burgess procedure (2.4), the criterion for convergence being that ten consecutive values of η_ℓ extracted at r+2mh (m=0,9) should agree to 2×10^{-3} radians.

TABLE 2.4

Variation of the Phase Shifts with Different
Starting Criteria at E = 0.15 e.V.

$\ell = 0$

Starting point s	Step length, h. 0.01	0.005	0.001
0.8			2.58123
0.5	2.58872	2.58328	2.58302
0.3			2.58302

$\ell = 20$

0.8			-2.30497
0.5	-2.29958	-2.30454	-2.30495
0.3			-2.30495

(Identical values are obtained if the second initial
value of the solution is taken as $u_\ell(s + h) = 1$)

At large ℓ, for all k, the JB approximation (2.5) to the phase shift is adequate and was adopted with η_ℓ^{JB} agreed with η_ℓ or η_ℓ^{JWKB} to within 0.01 radians. The phase shift sums were truncated when the phase shift became less than 0.01 radians.

The energy at which the JWKB approximation became inadequate for at least some value of ℓ was estimated from Munn, Mason and Smith's results and at different neighbouring energies results from both the JWKB procedure and the Numerov method were compared. For k>3.5 agreement was good for both phase shifts and the summed cross-sections,and this shown for the latter in Table (2.5).

TABLE 2.5

Comparison of exact and JWKB cross-sections (a_o^2)

in the region near k=3.5 for the potential V(r)

k(a.u.)	E_{cm}(ev)	$Q_{el}(k^2)$		$Q_d(k^2)$	
		Exact	JWKB	Exact	JWKB
3.5	3.576,-2	1041.9	1044.6	163.1	163.7
4.0	4.671,-2	1047.1	1049.7	130.3	126.8
4.5	5.912,-2	958.3	957.9	102.1	101.5
5.0	7.298,-2	835.4	834.9	81.97	81.52
6.0	1.051,-1	715.0	717.2	58.04	57.79

It is estimated that the quantal phase shifts are correct to 10^{-4} radians and the JWKB phase shifts to 10^{-2} radians.

Typical low energy phase shifts for $\ell<36$ are shown in fig. 2.2 and for $k<2.0$ discontinuities show the occurrence of classical orbiting and the presence of resonance bound states. These jumps in the phase shifts occur when there is a loss of a zero in the solution and this is illustrated in fig. 2.3 for $k=2.6$ a.u. The zero energy limit of the s-wave phase shift was found to be 7π and if Levinson's theorem can be applied the potential can support seven bound states.

All the above preliminary results were calculated using the SCF-MO potential, $V(r)$, which possesses both a short range repulsive part and a long range attractive part. Other potentials of this form will predict phase shifts exhibiting the same qualities as above. It is well known that the positive phase shifts arise from the attractive well of the potential whereas the repulsive region predicts negative phase shifts. Purely monotonic repulsive potentials (eg. V_2, V_3) produce no positive phase shifts and the features such as orbiting and glory scattering cannot be seen. At low energies where the positive phase shifts dominate the scattering there is a substantial disagreement in the total cross-sections and transport cross-sections predicted by the two types of potentials. This will be discussed later.

The computer code included six potentials for the Li^+-He system which were the SCF-MO potential, Junker-Browne (1969), Zehr-Berry (1967), Olson et al (1969), Dalgano et al (1958) and Weber and Bernstein's V_4 (1965). The first two

FIGURE 2.2
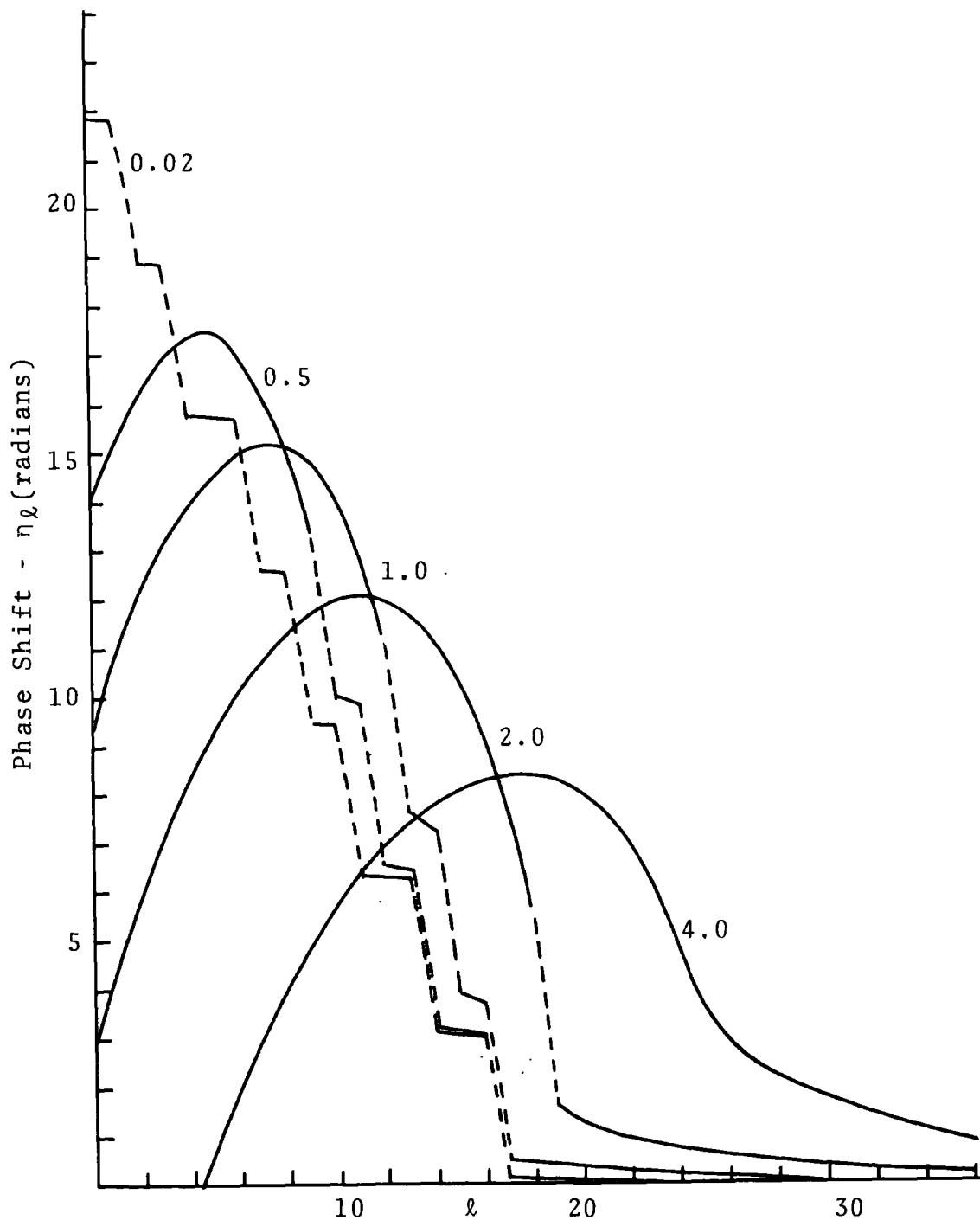
Exact Phase Shifts.

Calculated using the S.C.F.-M.O.potential. The numbers on the curve indicate the values of the momentum k (a.u.).

FIGURE 2.3

$\ell = 19$
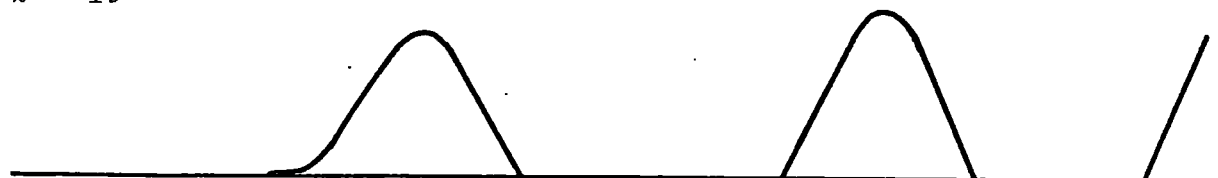
$\ell = 20$

$\ell = 23$
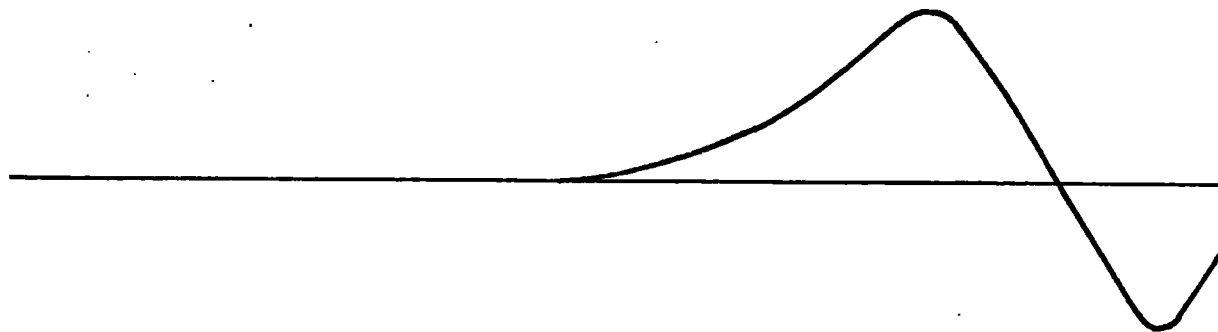
Radial Wave Function

Illustrating phenomenon of tunneling through the
centrifugal barrier for k = 2.6 a.u. (The amplitudes
are unrelated)

were non-analytic and have been given in table (2.3). The
values of the potential at intermediate points was obtained
using Aitken-Legrange interpolation routines. At small
internuclear distances r<0.2 a.u. where these routines were
inadequate, the potential was given by a crude analytic fit
to the small internuclear values and at r=0 to the ground
state of $B^+(1s^2 \, 2s^2, \, {}^1S_0)$.

$$V(r) = 14.5r - 14.26 + \frac{6}{r} \quad \text{(a.u.)} \quad 0<r<0.2a_0.$$

$$(2.21)$$

The code calculated total and diffusion cross-
sections (2.6, 2.7) and also included the option of evaluating
differential cross-sections (2.8) at specified angles.
Legendre polynomials when required were generated by the
usual recursion relation until $\ell=300$ when their asymptotic
form for large ℓ

$$P_e(\cos\theta) = \left[\frac{2}{\ell\pi\sin\theta}\right]^{1/2} \left[\left(1-\frac{1}{4\ell}\right)\cos[(\ell+1/2)\theta-\pi/4]\right.$$
$$\left. + \frac{1}{8n}\cot\theta\sin[(\ell+1/2)\theta-\pi/4]\right] \quad (2.22)$$

was used (Hobson 1931).

The code also evaluated $S(\theta)$, (2.9), from $I(\theta)$ using
a Simpson's integration. Because of the absence of structure
in the differential cross-sections ($E_{cm}>10e.V.$) only 150
Simpson intervals were required in the range $0\rightarrow180$ degrees.

The computations were performed on the N.U.M.A.C.

I.B.M. 360/67 computer of the Universities of Newcastle and Durham. The time required for one phase shift, varied but an estimated average value is of the order of 400 JWKB phase-shifts and 60 quantal phase-shifts per minute. The interpolation routines for the non-analytic potentials were found to be time consuming and total run times for these potentials could be increased by as much as a factor of three. Although in this present work the speed of the computer allowed the non-analytic potential to be used throughout the energy range, it was found that except in the low energy region where the shape of the potential is important, these potentials could be adequately represented by good analytic fits.

6. Results

The computer codes were checked by reproducing (i) the JWKB phase shifts of Kennedy and Smith (1967), and (ii) the differential cross sections of Weber and Bernstein (1965) for their potential $V_4(r)$ shown in their figures 6 and 7.

Differential cross-sections $I(\Theta)$ were computed for potentials V, V_2, V_3 and V_4 at three centre of mass energies corresponding to the measurements of Aberth and Lorents (1969) and also at two lower energies. Results are shown in figs. 2.4 a,b,c.

Excellent agreement is obtained with the classical results of Olson et al (1967) for the potentials V_2 & V_3 (not shown). The agreement with the experimental results as in the

FIGURE 2.4a.

Centre of mass angles θ (degrees)
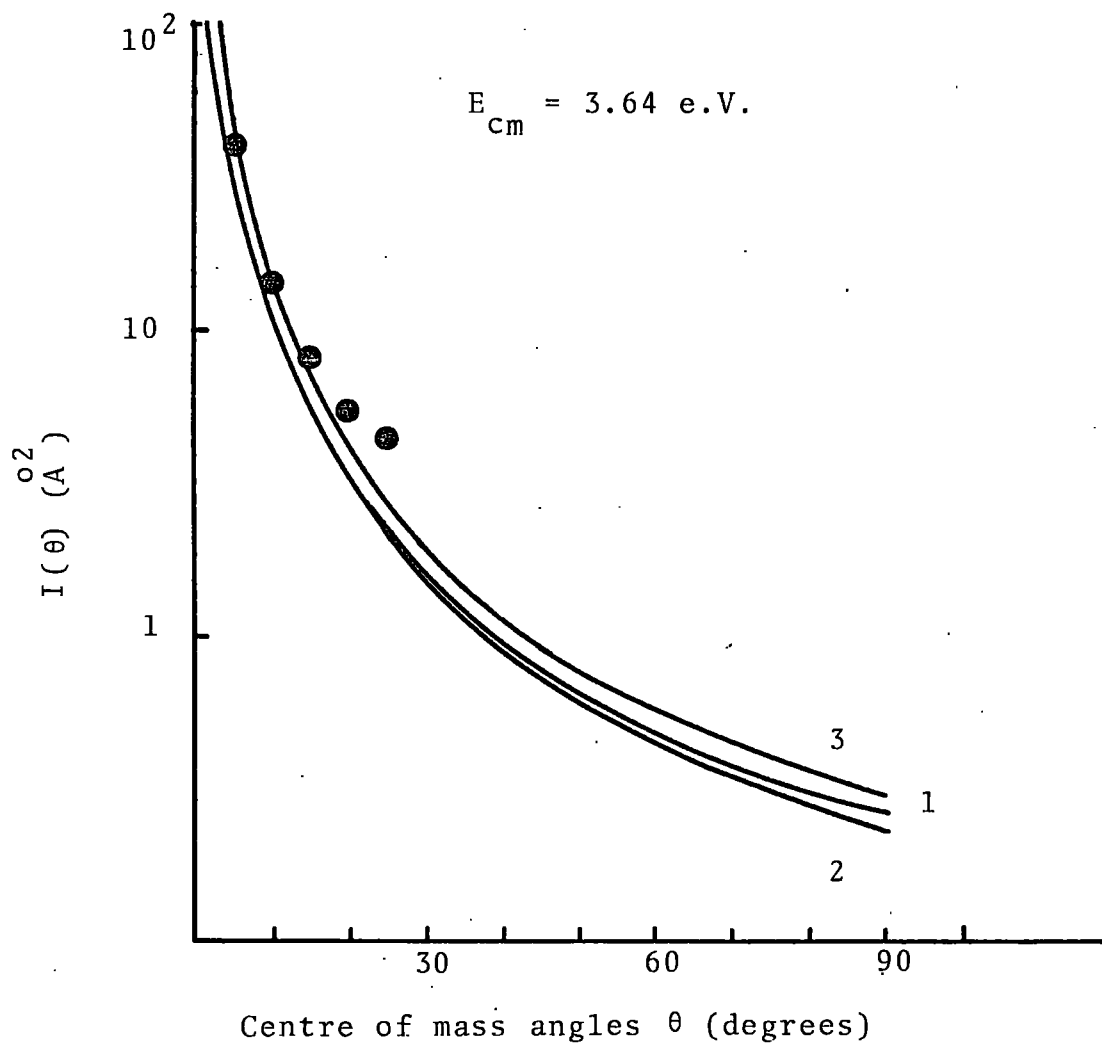
Elastic Differential Cross-Sections

The circles are samples of the experimental points of
Aberth and Lorents (1969). The full curves i = 1,2,3,
are theoretical values calculated semi-classically using
the potentials $V(r)$, $V_2(r)$ and $V_3(r)$ respectively.

FIGURE 2.4b.

$E_{cm} = 36.4$ e.V.

Centre of mass angle θ (degrees)
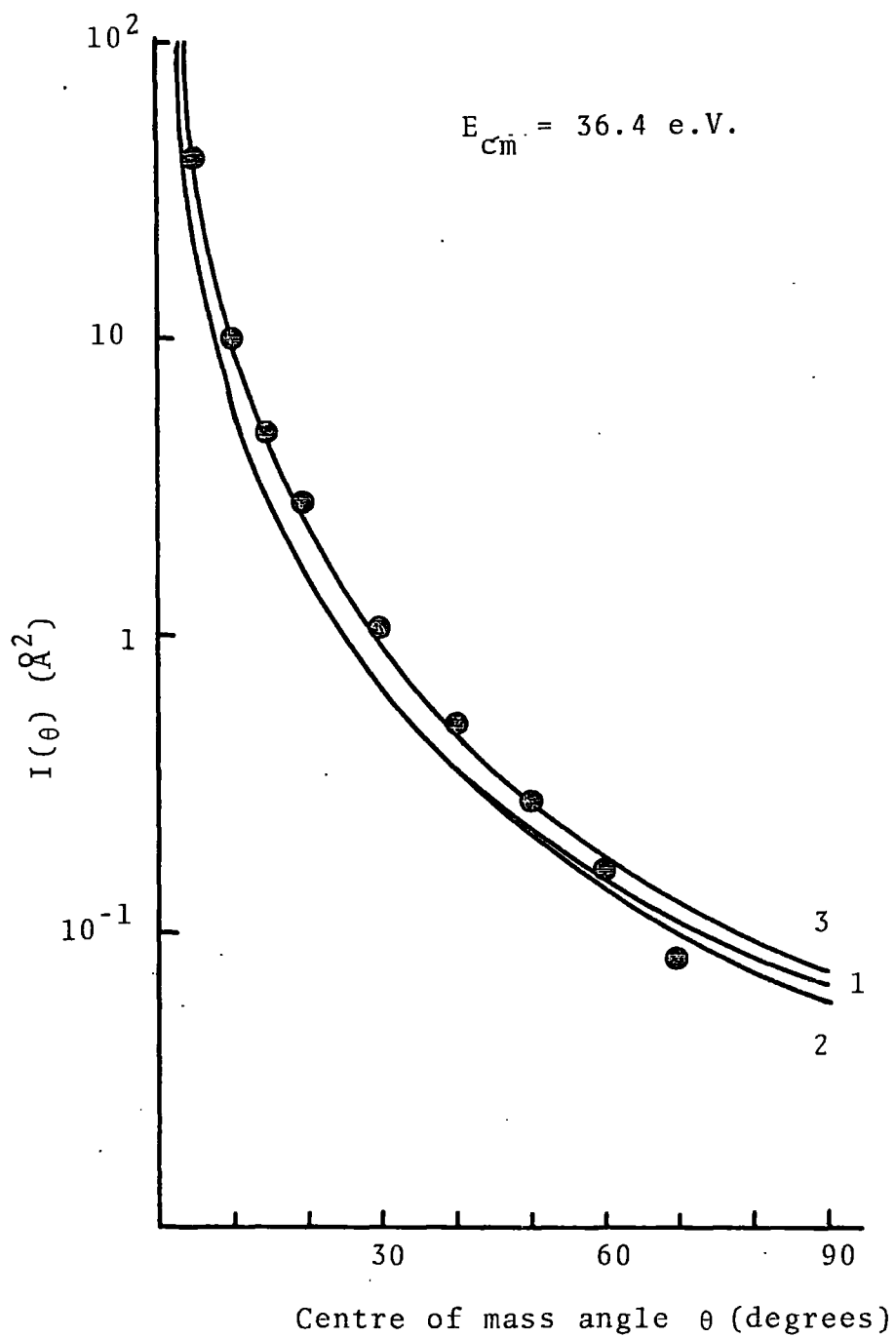
Elastic Differential Cross-Sections.

FIGURE 2.4c

$E_{cm} = 145$ e.V.

Centre of mass angle θ (degrees)

Elastic Differential Cross-Sections
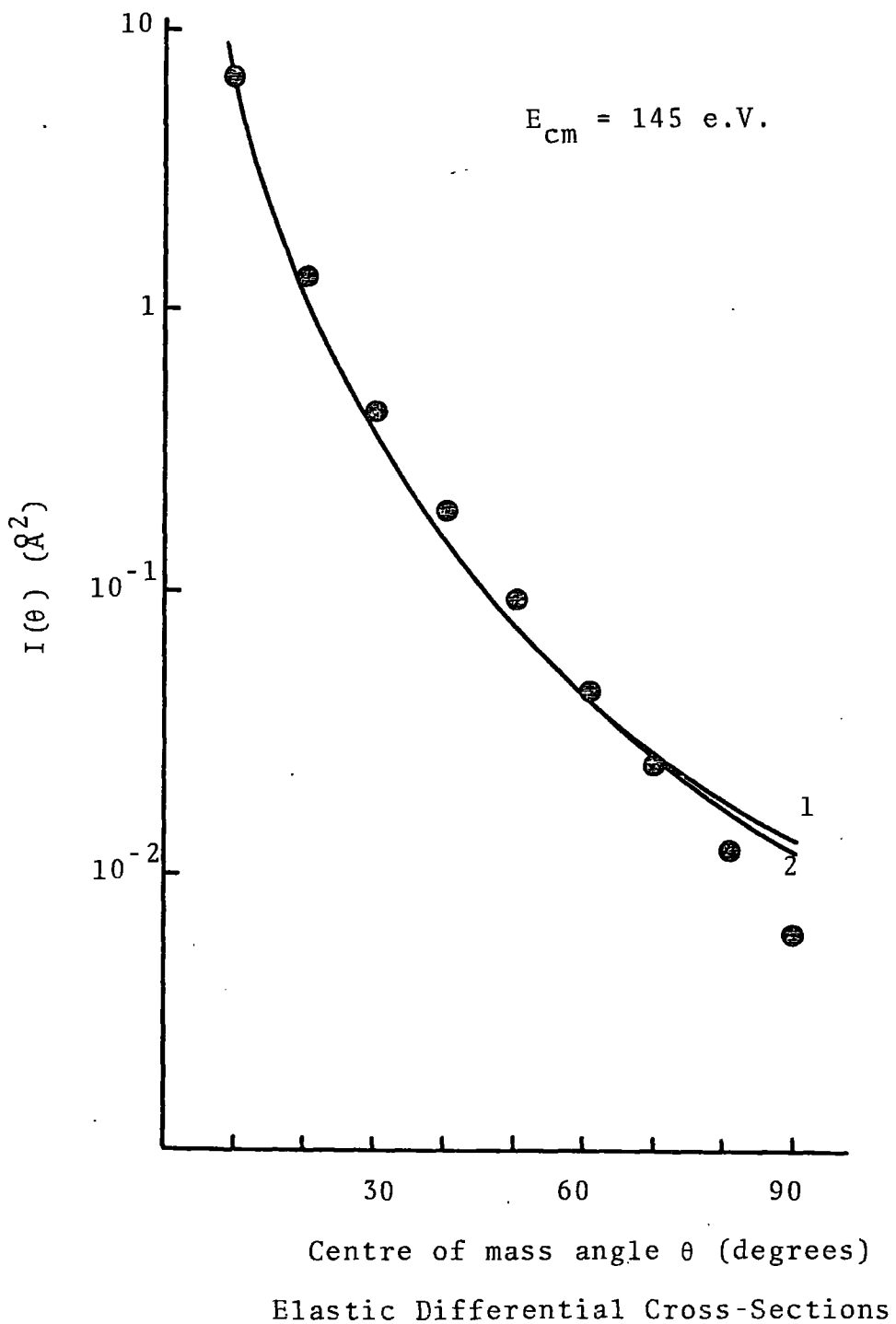
work of Olson et al, is also excellent except at the large

angles for each energy where the calculated cross-sections

are consistently larger. The predicted values of $S(\Theta)$,

discussed in more detail below, also agree well with the ob-

served values of Zehr and Berry (1967). However any rea-

sonable extrapolation to large angles of the Aberth and

Lorents measurements gives values of $S(\Theta)$, $\Theta > 70^{o}$ lying sub-

stantially below the Zehr-Berry data and inconsistent with

them.

At $E_{cm} = 3.64$ e.V. the differential cross-section from

the SCF-MO potential shows some structure although this

cannot be seen in fig. 4a. More detailed results at centre

of mass energies 1.33, 2.65 and 3.64 e.V. are shown in figs.

2.5 for $V(r)$, $V_2(r)$ and $V_4(r)$. Considerable structure is

predicted by the SCF-MO potential and the Junker-Browne po-

tential at centre of mass angles in the range $5^{o} < \Theta < 15^{o}$. The

Zehr-Berry potential, which is purely repulsive, gives a mono-

tonic decreasing differential cross-section and no evidence

of structure. The larger number of phase shifts contributing

to $I(\Theta)$ at small angles $(\Theta < 5^{o})$ lead to convergence diffi-

culties with the code and results in the near forward direc-

tion are not shown.

The structure predicted at $E_{cm} = 3.64$ is not seen in

the published experimental data of Aberth and Lorents (1969).

However the amplitude of the oscillations are of the same

magnitude as the random error associated with the experimental

FIGURE 2.5a.

E_{cm} = 1.33 e.V.

Curve 1 from S.C.F.-M.O potential

2   Junker-Browne

3   Zehr-Berry

Centre of mass angle θ (degrees)

Small Angle Differential Cross-Sections

$I(\theta)$ (Å²)

100

10

1.0

5   10   15   20

FIGURE 2.5b.

E_{cm} = 2.65 e.V.

Curve 1   from S.C.F.-M.O. potential

2   Junker-Browne

3   Zehr-Berry

Centre of mass angle θ (degrees)

Small Angle Differential Cross-Sections

$I(\theta)$ ($\overset{o}{A}{}^2$)

II-28
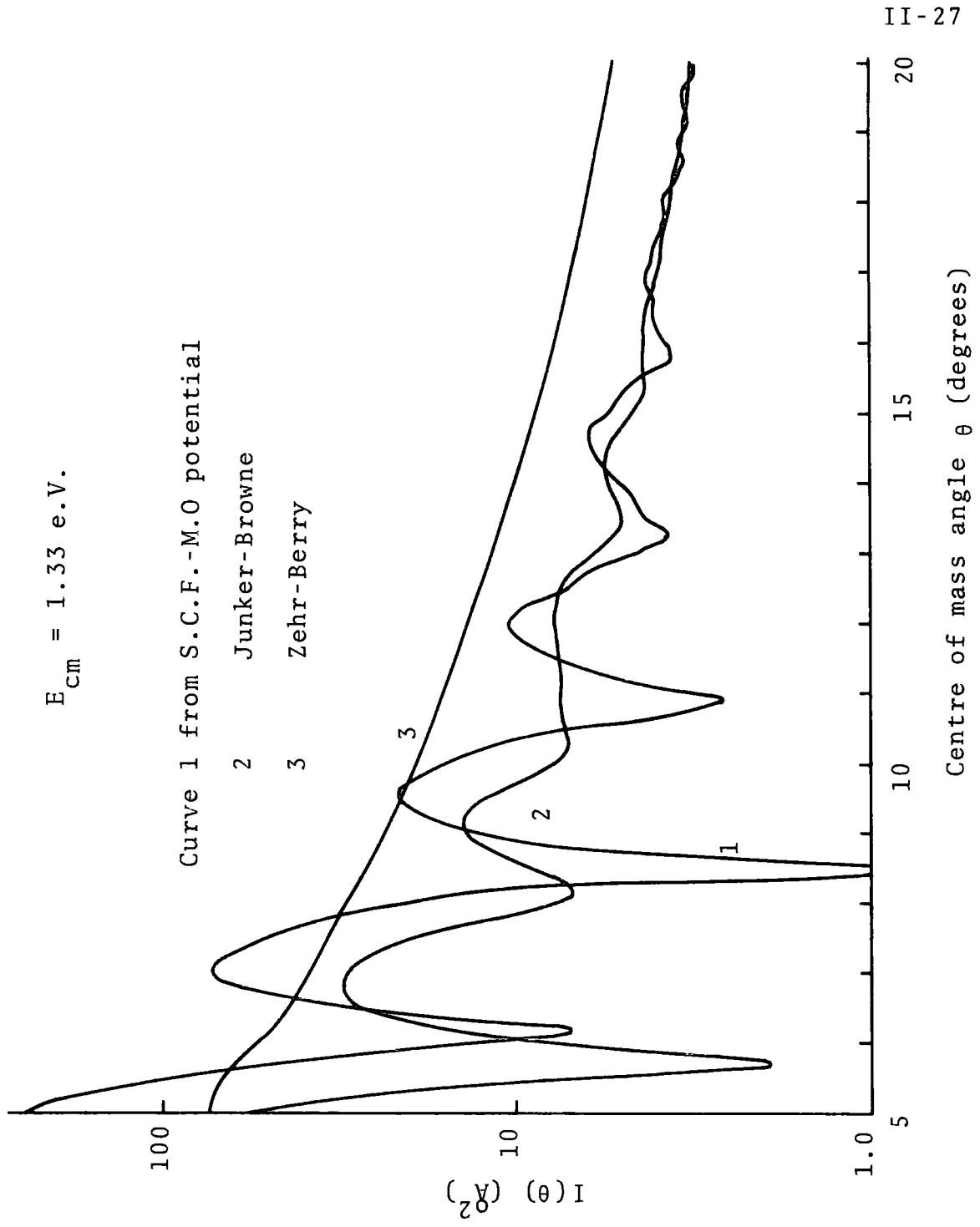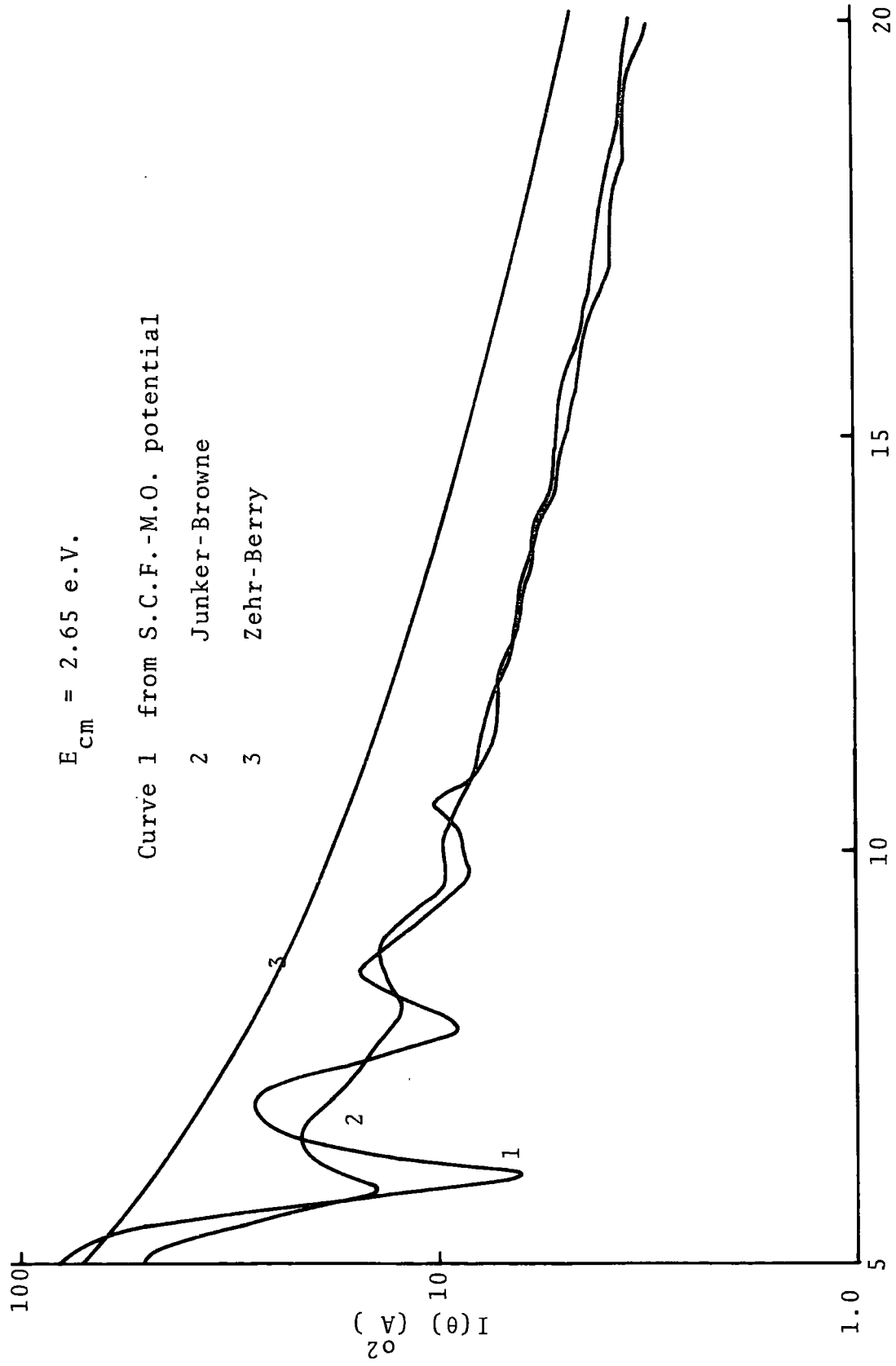
FIGURE 2.5c.

E_{cm} = 3.64 e.V.

Curve 1 from S.C.F.-M.O. potential

2 Junker-Browne

3 Zehr-Berry
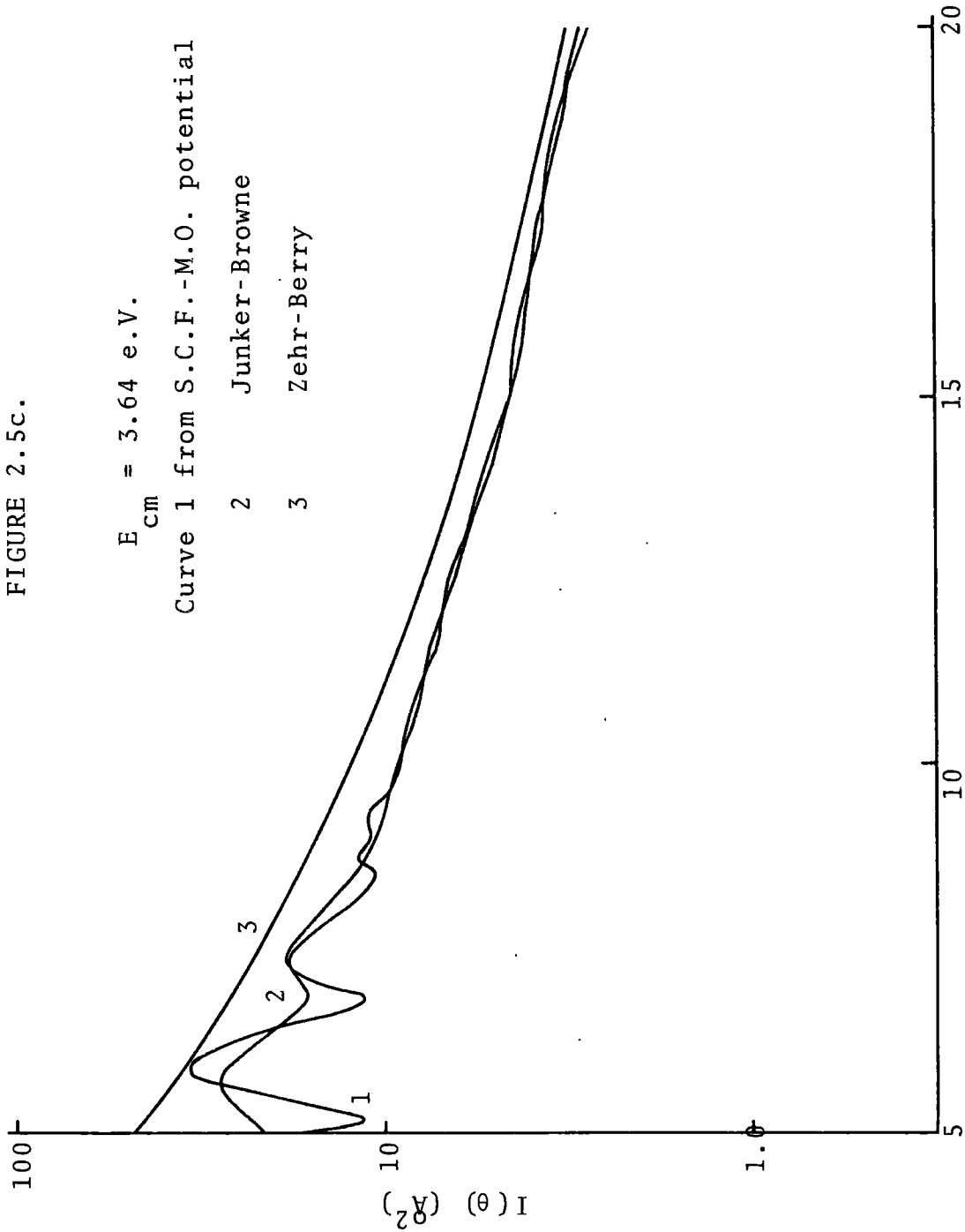
Centre of mass angle θ (degrees)

Small Angle Differential Cross-Sections

work. A more detailed experimental investigation of the energy region below 10e.V. at angles less than 15° would be of interest.

Calculated values of $S(\Theta)$ predicted by the SCF-MO potential and the Zehr-Berry potential are compared at five laboratory energies with the experimental measurements of Zehr and Berry in fig. 2.6. The two sets of results are equally consistent with the data. The slope of the experimental points is less steep than the theoretical curves at small angles and in this region better agreement is obtained with the Zehr-Berry results. At larger angles the SCF-MO potential results are closer to the experimental points.

Total cross-sections $Q_{el}(k^2)$ and diffusion cross-sections $Q_d(k^2)$ are given in detail in the appendix for the SCF-MO and the Junker-Browne potential at energies k=0.02 (0.01) 0.12(0.02)1.0 (0.1) 4.0 (0.5) 20.0 (5.0) 100.0. It is readily seen that for the greater part of the low energy range (E_{cm}<10e.V.) the Junker-Browne cross-sections lie substantially below those predicted by the SCF-MO potential, by as much as a factor of three or four at the lowest energies. This is because the former's potential well is shallower, having only half the depth of the SCF-MO potential well, and at low energies the long range attractive part of the potential dominates the collisions. The discrepancies in the cross-sections increase for the monotonic repulsive potentials. Total cross-section results for the SCF-MO potential and the

FIGURE 2.6

The full curves are calculated using the
S.C.F.-M.O. potential and the dashed curves
using the Zehr-Berry potential at laboratory
energies;

A: E_{lab} = 49 e.V.

B: = 73.7 e.V.

C: = 147.3 e.V.

D: = 397.1 e.V.

E: = 794.6 e.V.

$S(\theta)$ ($\mathring{A}^2$)

20

1.0

0   20   40   60   80   100   120   140   160   180

Angle θ (degrees)
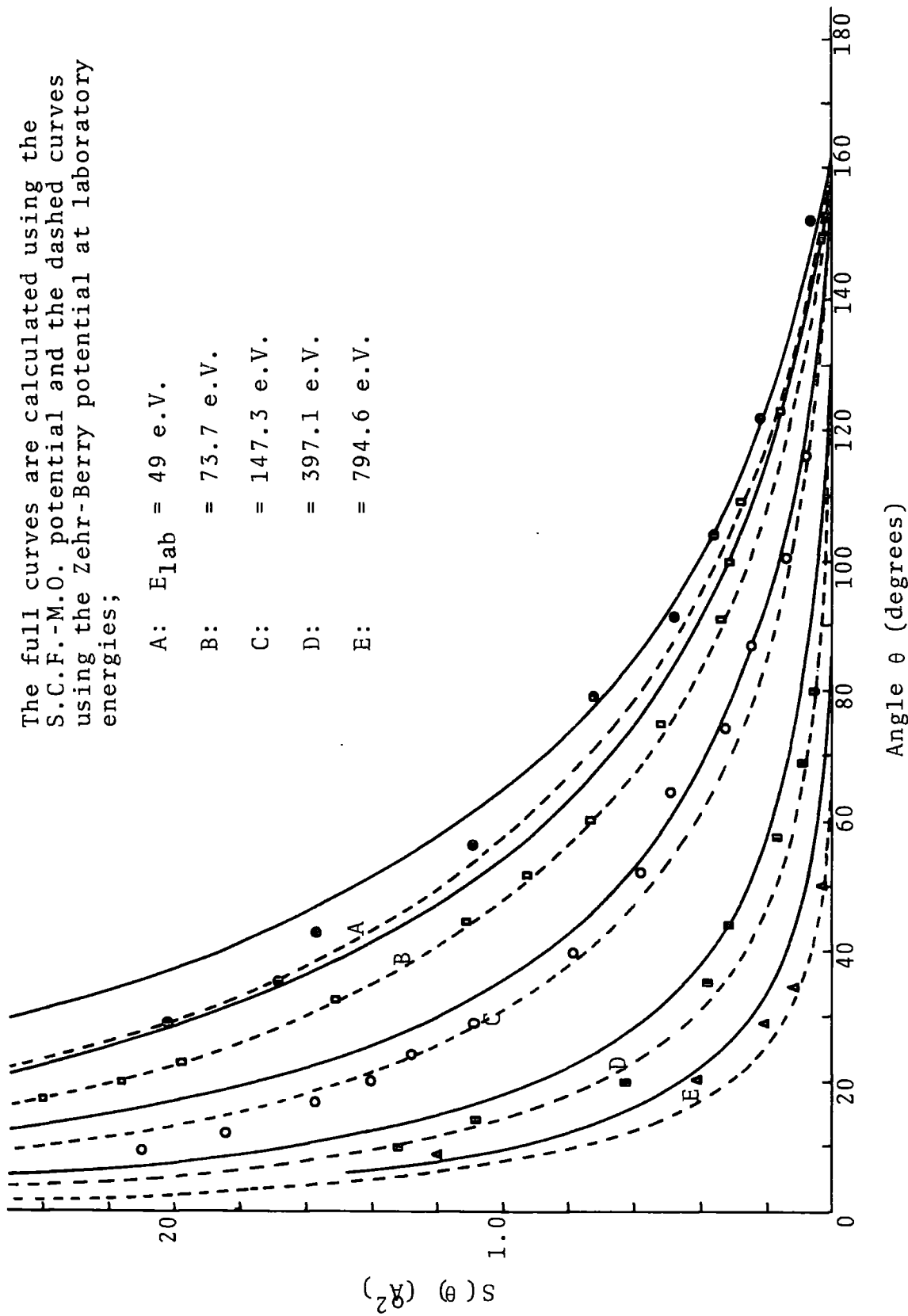
Elastic Scattering Outside Centre of Mass Angle, θ .

monotonic repulsive potentials of Zehr and Berry (V_2) and

Olson et al (V_3) are compared at a few energies in Table 2.6.

It can be seen that energies of the order of 5.10^2 greater

than the well depth (0.05e.v.) are required before the well

becomes negligible.

Bernstein (1962, 1963) has analyzed total cross-

sections and related the number of glory scattering undula-

tions, about the random phase approximation, semiclassically

to the number of bound (vibration-rotation) states that the

potential supports. The SCF-MO total cross-section is com-

pared with the SSL approximation (Bernstein and Kramer, 1963)

in fig. 2.7 and is seen to have nine undulations for k>0.02

a.u. (E_{cm}=1.16 x 10^{-6}e.V.). The two maxima at k=0.03 and

k=0.34 arising from orbiting or rainbow scattering (ℓ=2 and 7

respectively) while the remaining seven correspond well with

the zero energy limit of the s-wave phase-shift which was

found to be 7π. If Levinson's theorem applies, this indicates

the occurrence of seven bound vibrational states. A further

estimation of the number of bound states, n, the SCF-MO poten-

tial could support was given by the JWKB approach in which

$$n+\frac{1}{2} = \frac{1}{\pi} \int_{r_m}^{\infty} (2\mu|V(r)|)^{1/2}dr \qquad (2.23)$$

where r_m is the classical turning point and we assume there are

no bound states at zero energy. A hand computation gives the

rhs of (2.23) to be equal to 7.59, consistent with Levinson's

TABLE 2.6

Comparison of Total Elastic Cross Sections
for the SCF-MO potential and the Monotonic
Repulsive Potentials, V_2 and V_3

k	$E_{c.m.}$ (e.V.)	Q_{el} (k^2)		
		SCF-MO	V_2	V_3
0.21354,2	1.33	103.701	22.246	30.989
0.30178,2	2.65	78.120	20.623	28.707
0.36952,2	3.98	61.846	19.696	27.403
0.47749,2	9.15	44.993	18.541	25.786
0.67527,2	13.31	29.819	17.030	23.668
0.95433,2	26.59	21.036	15.577	21.633
0.11683,3	39.86	17.831	14.736	20.437
0.13478,3	53.03	16.138	14.184	
0.16526,3	79.73	14.309	13.388	

FIGURE 2.7
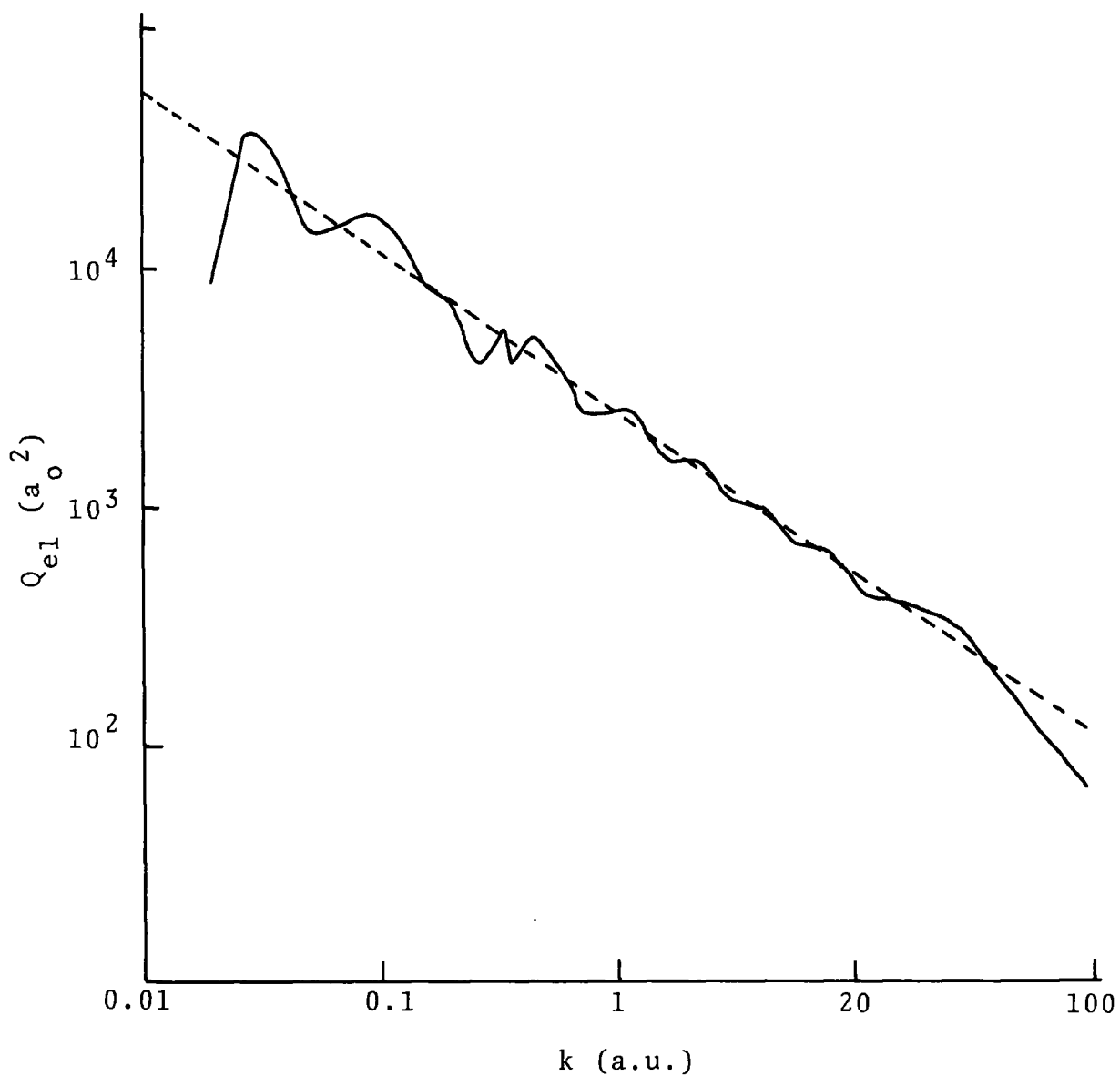
Total Elastic Cross Section.

The full curve is calculated using the S.C.F.-M.O. potential and the dashed curve is the SLL approximation.

theorem prediction and the number of glory undulations in the total cross-section. This confirms in this case Bernstein's (1966) conjecture that "the observation of m maxima in the elastic cross-section implies the existence of at least m vibration states" and Munn et al's (1964) criticism that the undulations due to rainbow scattering must not be counted.

The diffusion cross-section for the SCF-MO potential is shown in fig. 2.8 and compared with the polarization diffusion cross-section. The latter is obtained from the polarization potential (2.3) and the JB approximation. It can be evaluated analytically and is given by

$$Q_{d.pol}(k) = \frac{577.3}{k} a_o^2 \qquad (2.24)$$

The SCF-MO diffusion cross-section has considerable structure which hasn't a simple interpretation. For small k the successive maxima are separated by as little as k=0.16 corresponding to a temperature variation of less than 1^oK. In averaging over Q_d to obtain the mobilities most of the structure is removed.

The reduced mobility, K', as a function of temperature in the range $10^oK < T < 600^oK$ is shown in fig. 2.9 for the SCF-MO potential and the Junker-Browne potential. The results obtained from the former are consistent within the limits of experimental error with the measurements of Hoselitz (1941) over the entire range of temperatures. They do not approach

FIGURE 2.8
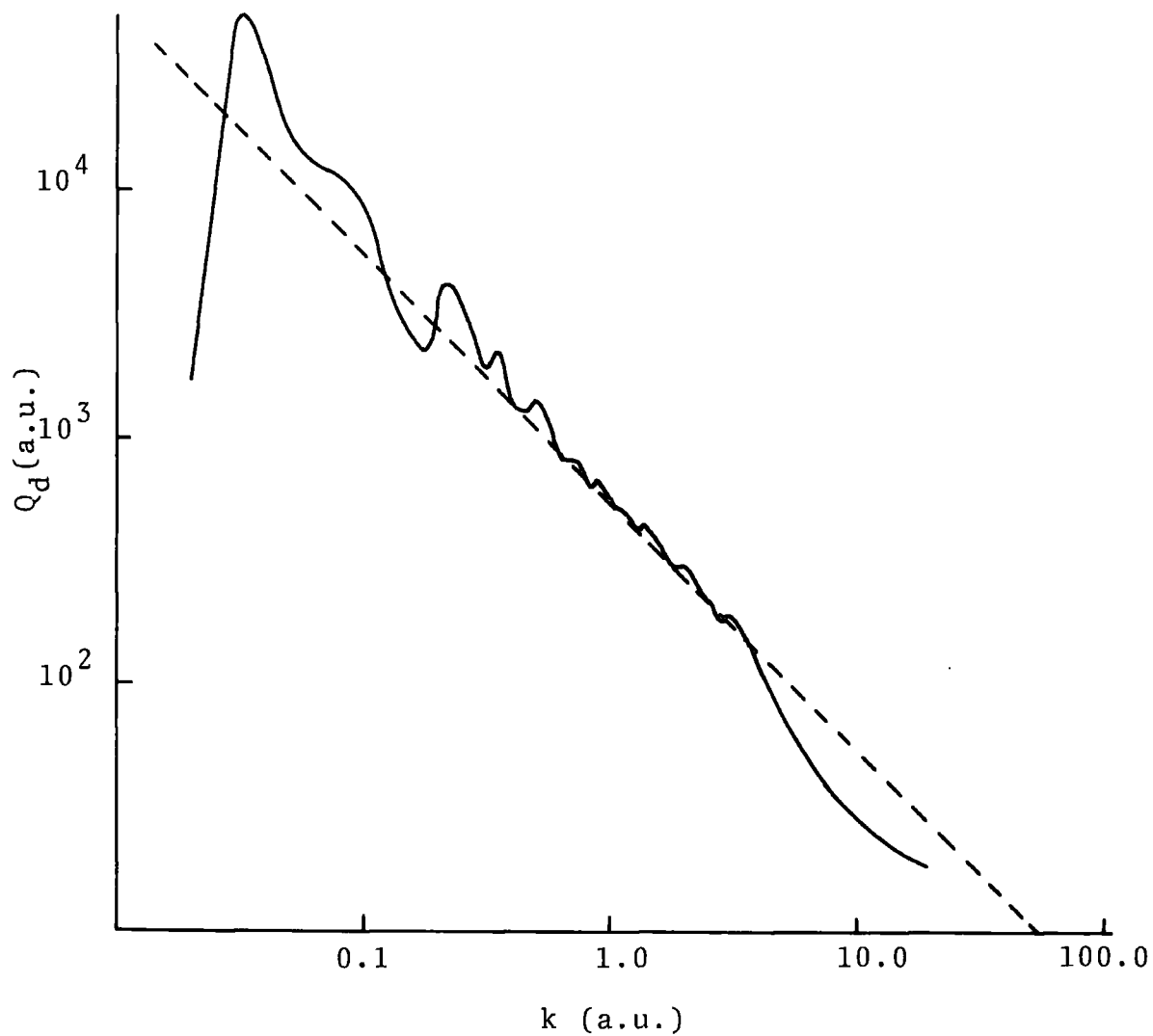
Diffusion Cross Section

The full curve is calculated using the S.C.F.-M.O. potential. The dashed curve is the polarization cross-section.

FIGURE 2.9
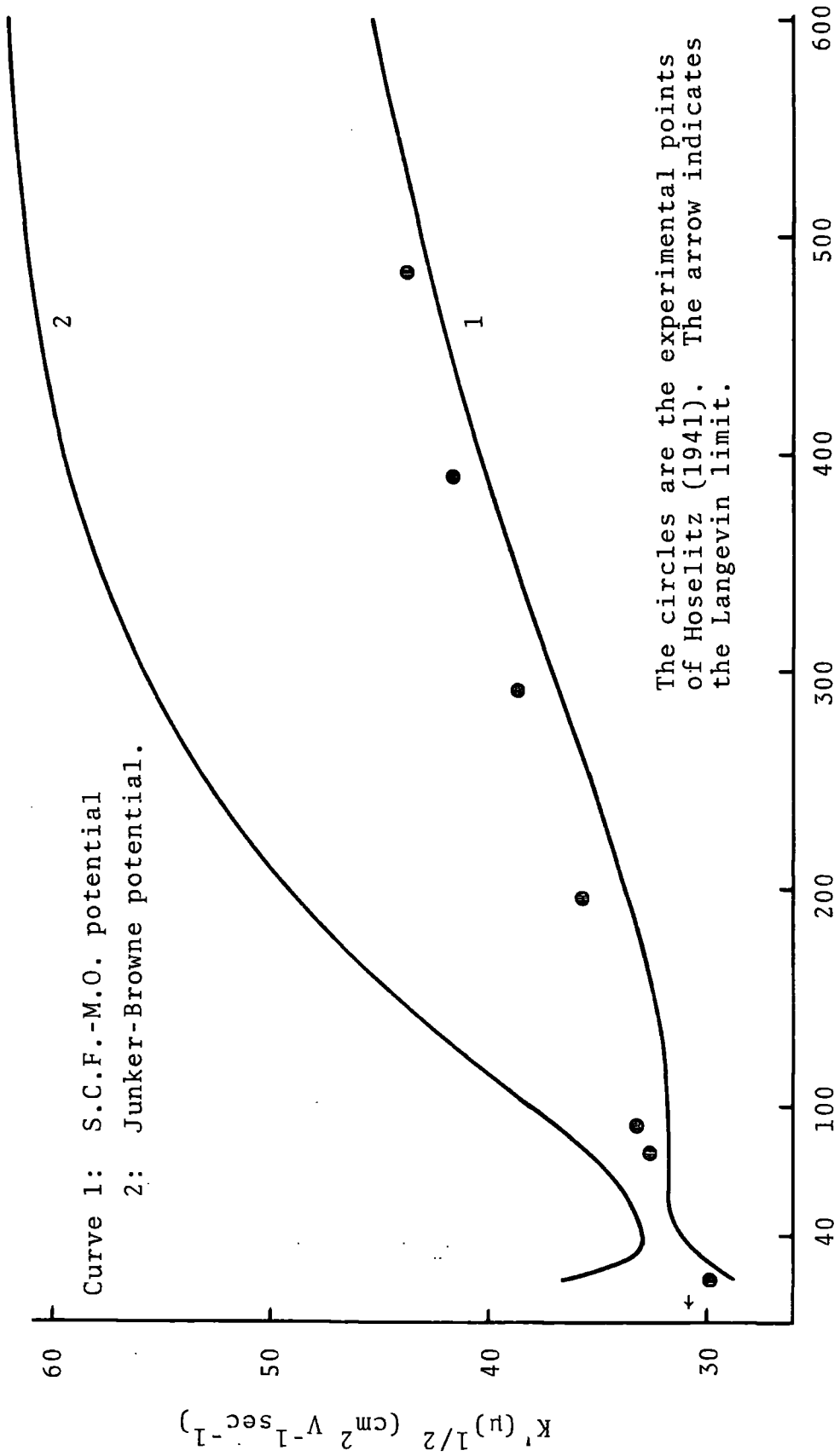
Curve 1: S.C.F.-M.O. potential
2: Junker-Browne potential.

The circles are the experimental points of Hoselitz (1941). The arrow indicates the Langevin limit.

Temperature (°K)

The Mobility of Lithium Ions in Helium

$K'(\mu)^{1/2}$ (cm^2 V^{-1}sec^{-1})

the Langevin limit (Langevin, 1905) (30.6 cm^2 V^{-1} 5^{-1}) as T→o but drop sharply below it due to the mean value of Q_d being larger than $Q_{d.pol}$ in the temperature range of interest (see fig. 2.9). At 20°K the equivalent energy is ∿0.17 x 10^{-2} e.V. and the integral (2.12) has a lower limit corresponding to 1.1 x 10^{-6} e.V.

It was noted earlier (section 4) the excellent agreement between the SCF-MO potential and the potential of Dalgano et al (1958). Dalgano et al derived their potential by trial and error fits to the Hoselitz mobility data using a semiclassical approach for the cross-sections. They reduced the data by a factor of 1/1.08 (which they attributed to a systematic error in Hoselitz's experiment) and ignored the points at T=20°K and 78°K to allow their fitted curve to have the Langevian zero energy limit. In the light of these adjustments, the two calculated mobilities show remarkable agreement considering the diversity of the methods used.

The mobility results predicted by the Junker-Browne potential lie much higher in the temperature range shown.

7. Conclusions

An accurate SCF-MO interaction potential for LiHe$^+$ ($1\sigma^2 2\sigma^2$) over the range $0.1 < r < 8.0$ as is presented and scattering cross-sections of Li$^+$ by He have been calculated and compared with experiment.

Differential cross-sections $I(\Theta)$ agree well with the experimental measurements of Aberth and Lorents (1969) for angles $<70^{\circ}$. For angles greater than 70° the measurements are too low and become inconsistent with the calculated values and the measurements of $S(\Theta)$ by Zehr and Berry (1967). It is of interest to note that analysis of (He^{+}, He) scattering by Boyle (PhD Thesis Queen's University, Belfast, 1969) yields results, from a modified quantal potential, which are inconsistent with the measurements of Lorents, Aberth and Hesterman (unpublished) for $E_{cm}>100$ eV and $\Theta>40^{\circ}$. Using Bernstein's semiclassical relationship, the undulations in the total cross-section for the SCF-MO potential indicate that the potential supports at least seven bound vibrational states. A similar analysis for the Junker-Browne potential shows it supports three such states. It was seen that the potential well depth 0.054 e.V. had a considerable effect on the magnitude of the total cross-section up to energies of the order of 25 e.V.

There are no direct measurements of the diffusion cross-section Q_{d} but the results from the SCF-MO potential correctly reproduce the observed mobility of Li^{+} ions in He both in magnitude and temperature variation. The mobility of the shallower Junker-Browne fails to do this.

These results together with the mobility results point to a well depth of not less than 0.05 e.V. Also it is estimated that for $2.5 < r < 8.0 \, a_{o}$ the SCF-MO potential should

be correct to within 0.05 e.V.

It has been seen that the differential cross-sections above 10 e.V. are comparatively insensitive to the choice of interaction potential; all the potentials considered being equal consistent with the experimental points. The mobility data can be used as a criterion for comparing the relative merits of the long range parts of the potentials. However results of a more detailed experimental investigation, if feasible, of differential cross-sections for energies less than 10 e.V. and at angles less than 15° would provide a stringent test for potentials.

APPENDIX

Total Elastic and Diffusion Cross-Sections for the
SCF-MO and Junker-Browne Potentials.

k	E_{cm}(e.V.)	Q_{el} (a.u.)		Q_d (a.u.)	
		LCAO-SCF	J-B	LCAO-SCF	J-B
0.02	0.11677,-5	8572.983		1689.065	
0.03	0.26273,-5	37759.713		43444.071	
0.04	0.46708,-5	25411.703		37024.733	
0.05	0.72982,-5	14635.127		17361.906	
0.06	0.10509,-4	14456.097		13640.926	
0.07	0.14304,-4	15224.961		12806.702	
0.08	0.18683,-4	16109.800		-11964.664	
0.09	0.23646,-4	17290.532	1211.255	10500.138	1458.234
0.10	0.29193,-4	16668.105	1182.742	8859.688	1395.613
0.11	0.35353,-4	15648.819	1168.507	6507.804	1310.077
0.12	0.42043,-4	14068.394	1160.640	5296.349	1233.204
0.14	0.57218,-4	11760.144	1110.606	3371.540	1067.416
0.16	0.74733,-4	8996.284	1099.588	2516.185	979.787
0.18	0.94584,-4	7772.640	1100.145	2461.331	901.658
0.20	0.11677,-3	7415.217	1102.726	3572.983	833.884
0.22	0.14129,-3	6171.557	1106.976	4327.223	798.737
0.24	0.16815,-3	4722.883	1119.939	3727.801	794.872
0.26	0.19734,-3	4183.848	1174.039	3052.648	886.358
0.28	0.22887,-3	4191.458	1445.958	2577.514	1302.735
0.30	0.26273,-3	4488.247	2310.562	2204.004	1971.063
0.32	0.29893,-3	4985.756	2010.662	1896.055	1253.761
0.34	0.33470,-3	5448.470	1705.918	2043.999	921.279
0.36	0.37834,-3	4134.605	1560.242	2321.905	813.152
0.38	0.42154,-3	4321.499	1472.686	1754.961	778.259
0.40	0.46708,-3	4685.607	1414.509	1464.349	780.512
0.42	0.51496,-3	4941.954	1386.285	1317.902	803.896
0.44	0.56517,-3	5138.954	1403.548	1279.835	828.364
0.46	0.61772,-3	5205.556	1455.831	1316.416	817.105
0.48	0.67260,-3	5082.699	1486.419	1412.950	756.916
0.50	0.72982,-3	4815.250	1452.176	1470.430	676.052
0.52	0.78932,-3	4497.857	1372.05	1445.685	605.279
0.54	0.85126,-3	4221.623	1274.05	1356.462	550.750
0.56	0.91548,-3	4008,026	1178.59	1248.251	506.875
0.58	0.98204,-3	3827.463	1093.56	1145.870	469.859
0.60	0.10509,-2	3661.358		1055.659	
0.62	0.11222,-2	3501.046	1405.38	974.319	908.049
0.64	0.11957,-2	3353.394	968.41	902.572	489.128

0.66	0.12716,-2	3190.993	835.46	851.188	392.437
0.68	0.13499,-2	2931,185	750.39	852.996	355.020
0.70	0.14304,-2	2477.401	676.19	948.455	332.581
0.72	0.15133,-2	2305.658	607.09	939.560	314.489
0.74	0.15986,-2	2397.225	546.60	838.843	304.153
0.76	0.16862,-2	2477.032	497.35	759.169	303.041
0.78	0.17761,-2	2528.723	468.37	704.497	320.582
0.80	0.18683,02	2558.047	479.67	671.608	375.541
0.82	0.19622,-2	2573.195	554.59	654.994	486.078
0.84	0.20598,-2	2585.493	623.48	651.418	573.004
0,86	0.21591,-2	2417.522	581.35	703.753	541.039
0.88	0.22607,-2	2476.936	498.73	692.617	471.608
0.90	0.23646,-2	2464.928	433.99	702.439	419.587
0.92	0.24709,-2	2465.569	395.91	703.402	387.888
0.94	0.25795,-2	2487.037	387.92	692.761	371.387
0.96	0.26904,-2	2524.981	458.28	673.006	397.377
0.98	0.28037,-2	2569.939	623.06	647.757	632.606
1.0	0.29193,-2	2612.981	444.71	620.879	481.914
1.1	0.35323,-2	2612,003	535.36	520.925	375.211
1.2	0.43037,-2	2553.582	801.22	500.835	497.373
1.3	0.49337,-2	2318.837	789.03	440.970	412.188
1.4	0.57218,-2	1993.246	824.79	474.355	293.876
1.5	0.65683,-2	1843.026	978.88	414.496	361.503
1.6	0.74733,-2	1624.061	832.19	378.791	340.897
1.7	0.84367,-2	1564.47	787.33	344.128	363.070
1,8	0.94584,-2	1596.54	781.54	305.438	345.218
1.9	0.10539,-2	1517.66	682.59	301.030	309.635
2.0	0.11677,-1	1581.70	627.45	308.170	299.458
2.1	0.12874,-1	1611.93	590.35	300.075	269.258
2.2	0.14129,-1	1563.82	555.64	282.050	246.355
2.3	0.15443,-1	1614.22	550.19	242.595	225.723
2.4	0.16815,-1	1486.77	544.03	242.808	204.708
2.5	0.18245,-1	1397.91	554.07	225.066	187.070
2.6	0.19734,-1	1335.01	572.38	213.392	171.696
2.7	0.21281,-1	1287.78	590.63	208.124	157.121
2.8	0.22887,-1	1172.69	611.11	187.545	144.917
2.9	0.24551,-1	1129.71	632.28	186.015	133.976
3.0	0.25273,-1	1120.80	648.62	194.582	124.139
3.1	0.28054,-1	1059.87	662.18	181.536	115.693
3.2	0.29893,-1	1043.07	671.90	178.311	108.093
3.3	0.31791,-1	1051.35	676.59	176.465	101.383
3.4	0.33747,-1	1045.85	677.80	170.985	95.395
3.5	0.35761,-1	1044.55	674.96	163.711	90.053
3.6	0.37834,-1	1053.84	668.79	158.109	85.292
3.7	0.39965,-1	1053.37	659.89	150.034	81.014
3.8	0.42154,-1	1054.68	648.79	143.231	77.165
3.9	0.44402,-1	1055.85	636.21	136.886	73.699
4.0	0.46708,-1	1047.06	622.54	130.305	70.571
4.5	0.59115,-1	958.29	556.82	102.076	59.070
5.0	0.72982,-1	835.37	500.93	81.965	51.309

5.5	0.88308,-1	750.95	468.92	67.951	45.960
6.0	0.10509	715.02	456.02	58.035	42.116
6.5	0.12334	708.33	453.86	50.895	39.211
7.0	0.14304	706.16	456.17	45.589	36.929
7.5	0.16421	694.51	458.59	41,553	35.082
8.0	0.18683	671.35	459.42	38.391	33.532
8.5	0.21092	638.58	457.65	35.860	32.208
9.0	0.23646	601.49	453.10	33.786	31.057
9.5	0.26346	564.36	446.40	32.063	30.034
10.0	0.29193	530.19	437.49	30.602	29.134
10.5	0.32185	500.69	427.12	29,344	28.324
11.0	0.35323	476.31	415.73	28.245	27.593
11.5	0.38607	457.09	403.75	27.275	26.913
12.0	0.42037	442.39	391.00	26.409	26.273
12.5	0.45613	431.55	378.37	25.626	25.669
13.0	0.49336	423.77	365.78	24.914	25.095
13.5	0.53204	418.14	353.28	24.261	24.551
14.0	0.57218	414.17	341.00	23,659	24.029
14.5	0.61378	411.22	329.19	23.101	23.534
15.0	0.65683	409.04	317.79	22.581	23,063
15.5	0.70135	407.19	306.79	22,094	22.611
16.0	0.74733	405.41	296.25	21,636	22.174
16.5	0.79477	403.54	286.22	21.204	21.753
17.0	0.84367	401.42	276.59	20.795	21.347
17.5	0.89402	399.06	267.39	20.407	20.957
18.0	0.94584	396.41	258.71	20.037	20.584
18.5	0.97912	393.40	250.54	19.683	20.231
19.0	0.10539,+1	390.06	242.67	19.344	19.895
20.0	0.11677,+1	382.39	228.04	18.708	19.262
25.0	0.18245, 1	332.39			
31.5	0.28966, 1	266.53			
36.5	0.38892, 1	224.12			
41.5	0.50277, 1	191.15			
46.5	0.63122, 1	166.05			
51.5	0.77426, 1	146.40			
56.5	0.93190, 1	130.90			
61.5	0.11041, 2	118.48			
66.5	0.12910, 2	108.31			
71.5	0.14524, 2	99.98			
76.5	0.17084, 2	93.04			
81.5	0.19390, 2	87.21			
86.5	0.21842, 2	82.28			
91.5	0.24441, 2	78.02			
96.5	0.27185, 2	74.41			
101.5	0.30075, 2	71.21			
106.5	0.33111, 2	68.42			
111.5	0.36293, 2	65.98			

The figure after the commas indicate the power of ten by which the entry is multiplied.

REFERENCES

Aberth, W., and Lorents, D.C., 1965, in 4th International
    Conference on the Physics of Electronic and Atomic
    Collisions (Science Bookcrafters, N.Y.).

Aberth, W., and Lorents, D.C., 1969, Phys. Rev., 182 162-7.

Bernstein, R.B., 1962, J. Chem. Phys., 37, 1880-81.

Bernstein, R.B., 1963, J. Chem. Phys., 38, 2599-2609.

Bernstein, R.B., and Kramer, K.H., 1963, J. Chem., Phys., 38,
    2507-11.

Burgess, A., 1963, Proc. Phys. Soc., 82, 442-452.

Catlow, G.W., McDowell, M.R.C., Kaufman, J.J., Sachs, L.M.,
    and Chang, E.S., 1969, to be published.

Dalgano, A., McDowell, M.R.C., and Williams, A., 1968, Phil.
    Trans. Roy. Soc. A., 250, 411-425.

Dickenson, A.S., 1968, J. Phys. B. (Proc. Phys. Soc.), [2],
    1, 387-94.

Fischer, C.R., 1968, J. Chem. Phys., 48, 215-17.

Hobson, E.W., 1931, Spherical and Ellipsoidal Harmonics
    (Camb. Univ. Press N.Y.).

Hoselitz, K., 1941, Proc. Roy. Soc. A, 177, 200-4.

Hoyt, F.C., 1939, Phys. Rev., 55, 664-5.

Junker, B.F., and Browne, J.C., 1969, to be published.

Kennedy, M., and Smith, F.J., 1967, Mol. Phys., 13, 443-48.

Langevin, P., 1905, Ann. Chim. Phys., 245-88.

Moore, C., 1949, Atomic Energy Levels I, (N.B.S. Washington).

Mott, N.F., and Massey, H.S.W., 1965, The Theory of Atomic
    Collisions (Cambridge Univ. Press).

Munn, R.J., Mason, E.A., and Smith, F.J., 1964, J. Chem.
    Phys., 41, 3978-88.

Olson, R.E., Smith, F.T., and Mueller, C.R., 1969, to be published.

Roothaan, C.C.J., 1951, Rev. Mod. Phys., $\underline{23}$, 69-89.

Roothaan, C.C.J., Sachs, L.M., and Weiss, A.W., 1960, Rev. Mod. Phys., $\underline{32}$, 186-94.

Sachs, L.M., and Geller, M., 1967, Int. J. Quantum Chem., $\underline{15}$, 445-55.

Schneiderman, S.B., and Michels, H.H., 1965, J. Chem. Phys., $\underline{42}$, 3706-19.

Seaton, M.J., and Peach, G., 1962, Proc. Phys. Soc., $\underline{79}$ 1296-7.

Smith, F.T., Marchi, R.P., and Dedrick, K.G., 1966, Phys. Rev., $\underline{150}$, 79.

Weber, G.G., and Bernstein, R.B., 1965, J. Chem. Phys., $\underline{42}$ 2166-71.

Zehr, F.J., and Berry, H.W., 1967, Phys. Rev., $\underline{159}$, 13-20.

CHAPTER III

A CLASSICAL MODEL FOR PROTON AND ELECTRON IMPACT IONIZATION

1. Introduction

Although, as discussed in Chapter I, classical models of ionization are in reasonable accord with experiment, they consistently predict cross-sections that are too high at moderate energies and fall off too fast at high energies. In an attempt to partially correct this failing, we will consider a model for ionization of atoms in which the velocity distribution of the atomic electron is given by the analytic Hartree-Fock wave functions of Roothaan and co-workers.

The model is essentially that of Gryzinski (1959). That is to say that the electrons are regarded as indistinguishable and interact separately with the incident particle. Also the binding forces between the bound electrons and target nucleus are switched off during the collision. It is thus a classical binary encounter impulse approximation.

We consider the case of an incident particle of mass m_2 and velocity v_2 impinging on a bound electron with velocity v_1. In the following analysis we shall use atomic units throughout, except for energies which will be expressed in rydbergs. It is convenient to adopt dimensionless variables s, t defined as

$$s^2 = v_2^2/v_o^2 \quad t^2 = v_1^2/v_o^2 = E_1/u \qquad (3.1)$$

where $u = v_o^2$ is the ionization potential in rydbergs. Using these dimensionless variables Stabler's (1964) ionization cross-sections for electron impact (eqn. (1.15)) become

$$u^2 Q(s,t) = \frac{4}{3s^2} \; \frac{2(s^2-1)^{3/2}}{t} \; (\pi a_o^2) \quad 1 \leqslant s^2 \leqslant t^2 + 1$$

$$= \frac{4}{3s^2} \left[2t^2+3 - \frac{3}{s^2-t^2} \right] (\pi a_o^2) \quad s^2 \geqslant t^2 + 1 \qquad (3.2)$$

and from Vriens (1967) for proton impact (eqn. (1.16))

$$u^2 Q(s,t) = \frac{4}{s^2} \left[1 + \frac{2t^2}{3} - \frac{1}{4(s^2-t^2)} \right] (\pi a_o^2) \quad 1 \leqslant 4s(s-t)$$

$$= \frac{2}{s^2 t} \left[\frac{1}{4(s+t)} + t + \frac{2}{3}(2s^3 + t^3 - (1+t^2)^{3/2}) \right] (\pi a_o^2)$$

$$4s(s-t) \leqslant 1 \leqslant 4s(s+t) \qquad (3.3)$$

$$= 0, \text{ otherwise.}$$

$Q(s,t)$ is the ionization cross-section for a projectile of energy $m_2 s^2 u$ rydbergs ($m_2 = 1$ for electron impact) incident on a bound electron (binding energy in rydbergs) of kinetic energy $t^2 u$ rydbergs. Hence the total ionization cross-section for the projectile incident on a target atom is from eqn. (1.17)

$$Q(s) = \sum_{n,\ell} N_{n\ell} \int_0^\infty f_{n\ell}(t) \; Q(s,t) u^{1/2} dt \qquad (3.4)$$

where the summation is over the outer subshells of the target atom, $f_{n\ell}(t)$ is the velocity distribution of one electron in the subshell and $N_{n\ell}$ is the number of bound electrons in the subshell.

2. Velocity Distribution for Atomic Electrons

The velocity distributions are obtained from Fourier transforms of Hartree-Fock wave functions. The wave functions are from Roothaan et al (1960, 1962, 1963) and Bagus (1966) and are of the form

$$\psi_{n\ell m}(\underline{r}) = \left(\sum_i c_i R_{in}(r)\right) Y_{\ell m}(\Theta_r \phi_r) \tag{3.5}$$

where $Y_{\ell m}$ are spherical harmonics, R_{in} are Hartree-Fock radial functions and c_i are normalization constants. In momentum space the wave function is

$$\Psi_{n\ell m}(\underline{p}) = \frac{1}{(2\pi)^{3/2}} \int \psi_{n\ell m}(r \Theta_r \phi_r) e^{i\underline{p}\cdot\underline{r}} d\underline{r} \tag{3.6}$$

where $\underline{p}$ describes the position in momentum space. Now we employ two well known properties of spherical harmonics (Messiah, 1961)

$$\int_0^{2\pi} \int_{-1}^1 Y_{\ell m}^* Y_{\ell'm'} d\phi d(\cos\Theta) = \delta_{mm'}\delta_{\ell\ell'} \tag{3.7}$$

$$e^{i\underline{p}\cdot\underline{r}} = 4\pi \sum_{\ell=0}^{\infty} \sum_{m=-\ell}^{\ell} i^\ell j_\ell(pr) Y_{\ell m}(\Theta_p\phi_p) Y_{\ell m}^*(\Theta_r\phi_r) \tag{3.8}$$

where j_ℓ is the spherical Bessel function and the subscripts
on the angular variables indicate the vector to which they
refer. Hence the momentum space wave function readily re-
duces to

$$\Psi_{n\ell m}(\underline{p}) = \frac{1}{(2\pi)^{3/2}} \int_0^\infty \left[\sum_i c_i R_{in}(r) \right] 4\pi i^\ell j_\ell(pr) Y_{\ell m}(\Theta_p \phi_p) r^2 \ dr$$

$$(3.9)$$

The velocity distribution, which in atomic units is identical
to the momentum distribution for electrons, in the "$n\ell$" sub-
shell of the atom is given as

$$\rho_{n\ell}(\underline{v}_1) = \frac{1}{(2\ell+1)} \sum_{m=-\ell}^{\ell} \Psi^*_{n\ell m} \Psi_{n\ell m}$$

$$(3.10)$$

Using (3.9) in (3.10)

$$\rho_{n\ell}(\underline{v}_1) = \frac{1}{2\pi^2} \left| \int_0^\infty (\sum c_i R_{in}) \ j_\ell(v_1 r) r^2 \ dr \right|^2$$

$$(3.11)$$

Now

$$\rho_{n\ell}(v_1) = \rho_{n\ell}(\underline{v}_1)$$

$$(3.12)$$

and hence the required distribution function for equation (3.4)
is

$$f_{n\ell}(t) = 4\pi t^2 u \rho_{n\ell}(u^{1/2} t)$$

$$(3.13)$$

It is easily seen that the correct normalization of the wave
functions require that

$$\int_0^\infty f_{n\ell}(t) u^{1/2} dt = 1 \qquad (3.14)$$

for all n, ℓ

The wave functions of Roothaan et al and Bagus can be written as in (3.5) with the radial functions of the form

$$R_{in}(r) = (2n!)^{-1/2} (2\zeta_i)^{n+1/2} r^{n-1} e^{-\zeta_i r} \qquad (3.15)$$

and c_i, ζ_i are tabulated constants. The velocity distribution then reduces to a sum of elementary integrals $I_{in\ell}$ of the form

$$I_{in\ell} = c_i (2n!)^{-1/2} (2\zeta_i)^{n+1/2} \int_0^\infty r^{n+1} e^{-\zeta_i r} j_\ell(v_1 r) dr$$

$$(3.16)$$

which can be evaluated in closed form (Dwight 1964)

3. Results & Discussion

Cross-sections for inner and outer shell ionization of He, Li, O, N and Ne by both electron and proton impact are presented and in a few cases and compared with Born calculations of Peach (1968) and experiment.

The integral (3.4) over the velocity distribution of the bound electron was performed numerically by Gauss and Gauss-Laguerre quadratures. The integrand is smoothly varying and convergence is readily attained with a maximum of 24 abscissa. The normalization of the Hartree-Fock wave functions was checked by performing integrations of the form

(3.14). Finally the computer code was checked by reproducing previously published ionization cross-sections for hydrogen (Kingston 1966a, McDowell 1966).

For electron impact, three formulations of ionization cross-sections were calculated and compared. Q_1 was obtained from (3.4) with δ-function velocity distribution. A Hartree-Fock distribution in (3.4) produced a cross-section Q_2, which was subsequently modified, Q_3, by taking

$$f(t) = o \quad t > s$$

That is considering only collisions in which the incident electron is the faster of the two (Kingston 1966). This agrees with the procedure used in a quantal calculation when exchange is neglected (Peterkop 1961). In the case where the ground configuration of the residual ion gives rise to more than one electronic state (eg O^+, N^+), an average ionization potential (Slater 1960) is used. Results at various energies are given for the outer shells of He, Table 3.1 and N, Table 3.2. It is readily seen that in going from Q_1 to Q_3 the maximum value of the cross-section is reduced and its position is moved to higher energies. In fact the maximum of Q_3 is 25% lower than Q_1 in Tables 3.1, 3.2 and this is typical of other cases considered. At high energies Q_2 and Q_3 lie above Q_1. As will be seen below, these features tend to increase the agreement of the calculated cross-section with experiment.

TABLE 3.1

Comparison of Ionization Cross Sections (πa_o^2)
of Helium by Electron Impact

s^2	E_2 (e.V.)	Q_1	Q_2	Q_3
1.2	28.42	0.091	0.121	0.099
1.7	40.60	0.526	0.530	0.455
2.1	50.75	0.868	0.708	0.619
2.5	60.91	0.978	0.788	0.697
2.9	71.06	0.962	0.811	0.727
3.3	81.21	0.911	0.808	0.730
3.7	91.36	0.853	0.789	0.719
4.1	101.51	0.796	0.763	0.699
5.4	131.97	0.653	0.675	0.628
6.6	162.42	0.549	0.593	0.558
8.3	203.03	0.451	0.506	0.481
10.0	243.63	0.382	0.438	0.420
11.6	284.24	0.331	0.386	0.372
14.9	365.45	0.261	0.310	0.301
18.3	446.66	0.216	0.258	0.253

TABLE 3.2

Comparison of Ionization Cross Sections (πa_o^2)
of Nitrogen by Electron Impact*

s^2	E_2(e.V.)	Q_1	Q_2	Q_3
1.1	16.24	0.078	0.066	0.032
1.6	24.36	1.746	1.378	0.854
2.1	32.48	3.778	2.398	1.648
2.6	40.60	3.721	2.981	2.173
3.3	50.76	3.470	3.315	2.536
4.0	60.91	3.119	3.407	2.696
4.6	71.06	2.797	3.374	2.740
5.3	81.21	2.522	3.280	2.719
5.9	91.36	3.291	3.158	2.663
6.6	101.51	2.095	3.024	2.588
8.6	131.97	1.662	2.632	2.328
10.6	162.42	1.375	2.298	2.079
14.5	223.33	1.018	1.806	1.683
21.1	324.84	0.711	1.312	1.256
29.0	446.65	0.522	0.982	0.954

* Only outer shell contribution.

A sample of ionization cross-sections (Q_3 for electron impact, Q_2 for proton impact) are compared with experiment in figures 3.1-3.5.

(Results for helium given previously (Catlow and McDowell 1967) are incorrect). For electron impact on nitrogen, Kieffer & Dunn (1966) think the cross-sections of Peterson (1964) are too large and Smith's (1962) values are to be preferred. If this is the case, the classical results are considerably better than the Born calculations of Peach (1968). In the case of electron ionization of oxygen, although both classical and quantal calculations are in close agreement with the experimental results of Boksenberg (1961) in the energy range shown, the experimental results of Rothe et al (1962) (not shown for the sake of clarity) almost reproduce the points of Fite and Brackmann(1959). This together with the situation for nitrogen would tend to suggest that both the calculations and Boksenberg's results are too high.

The results for neon produce the worst comparison with experiment of the systems considered. This was to be expected as neon is a inert gas with a complete outer shell of six 2p electrons and is not a system to which a binary encounter impulse approximation is really applicable. However these results are approximately 25% lower than those presented by Garcia et al (1968) who used a δ-function velocity distribution for the atomic electrons. It is noticeable that the quantal calculations also fail to an extent for this system.

FIGURE 3.1

Electron Impact Ionization of Helium

— This work

--- Mod. Born (Peach 1965)

● Smith (1930)
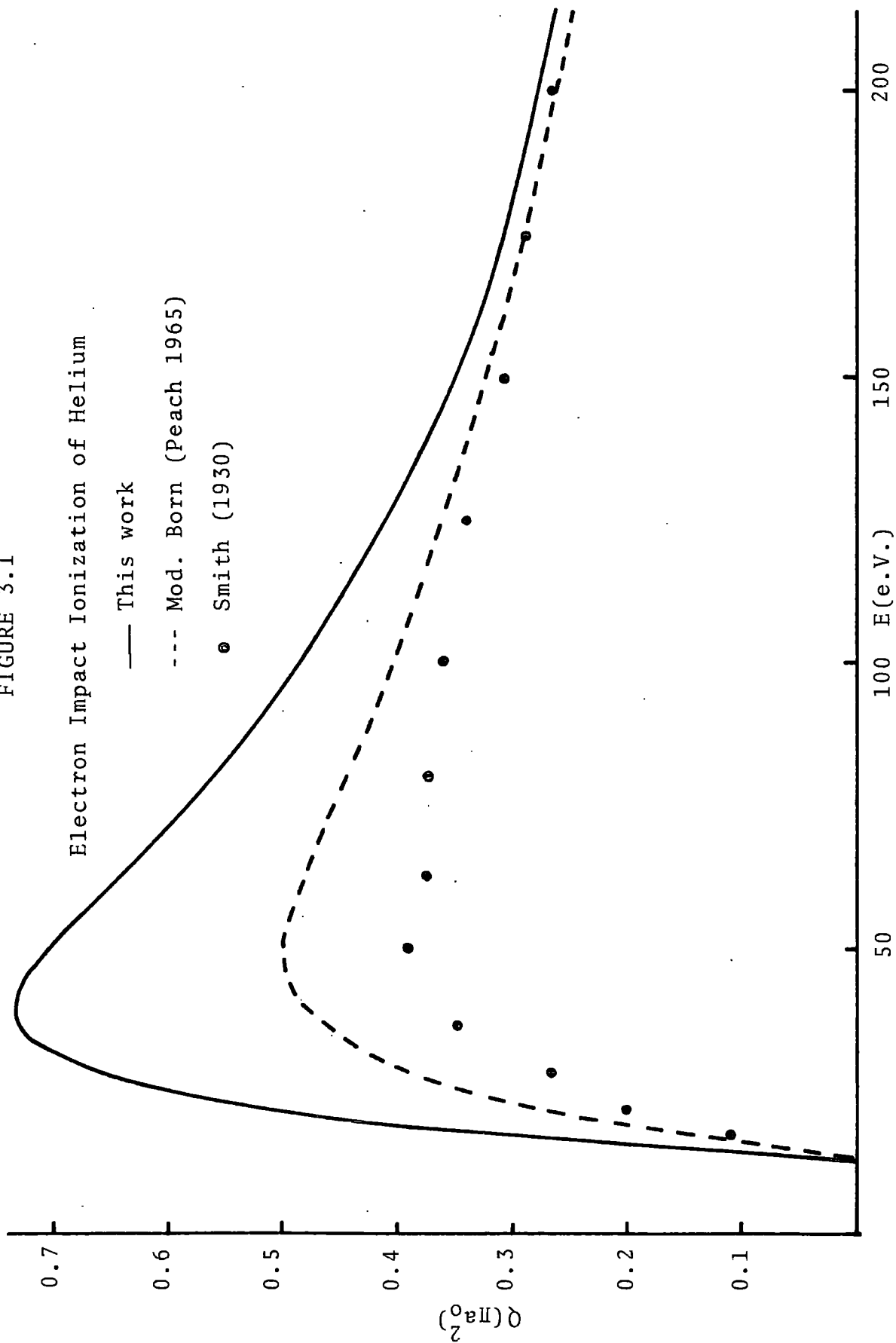
FIGURE 3.2

Electron Impact Ionization of Atomic Nitrogen.

—— This work
-- Peach (1968)
⊕ Peterson (1964)
▲ Smith (1962)

2s+2p

2p

2s+2p

2p

2s

2s

$Q(\Pi a_o^2)$

E(e.V.)

FIGURE 3.3

Electron Impact Ionization of Atomic Oxygen.
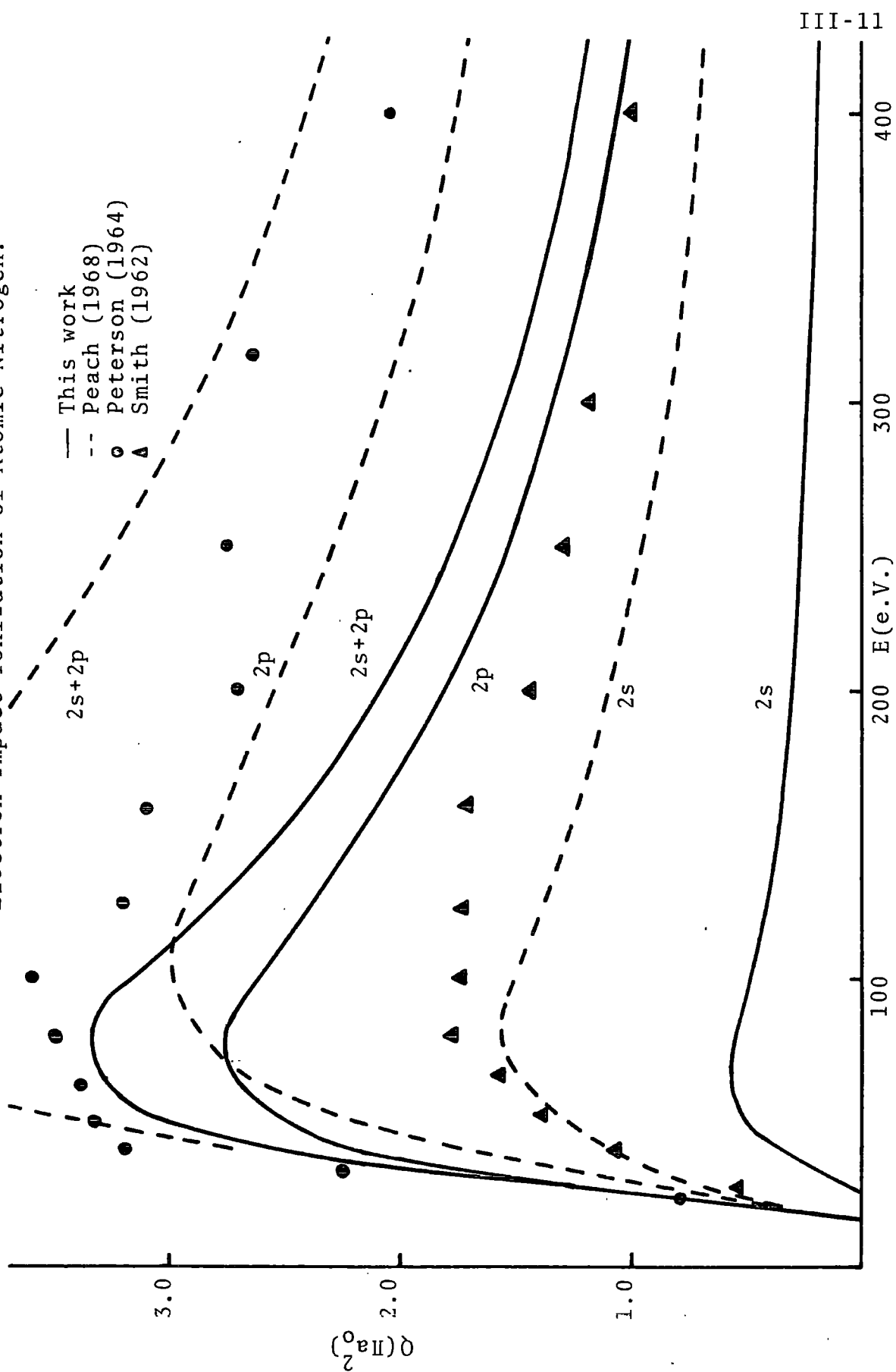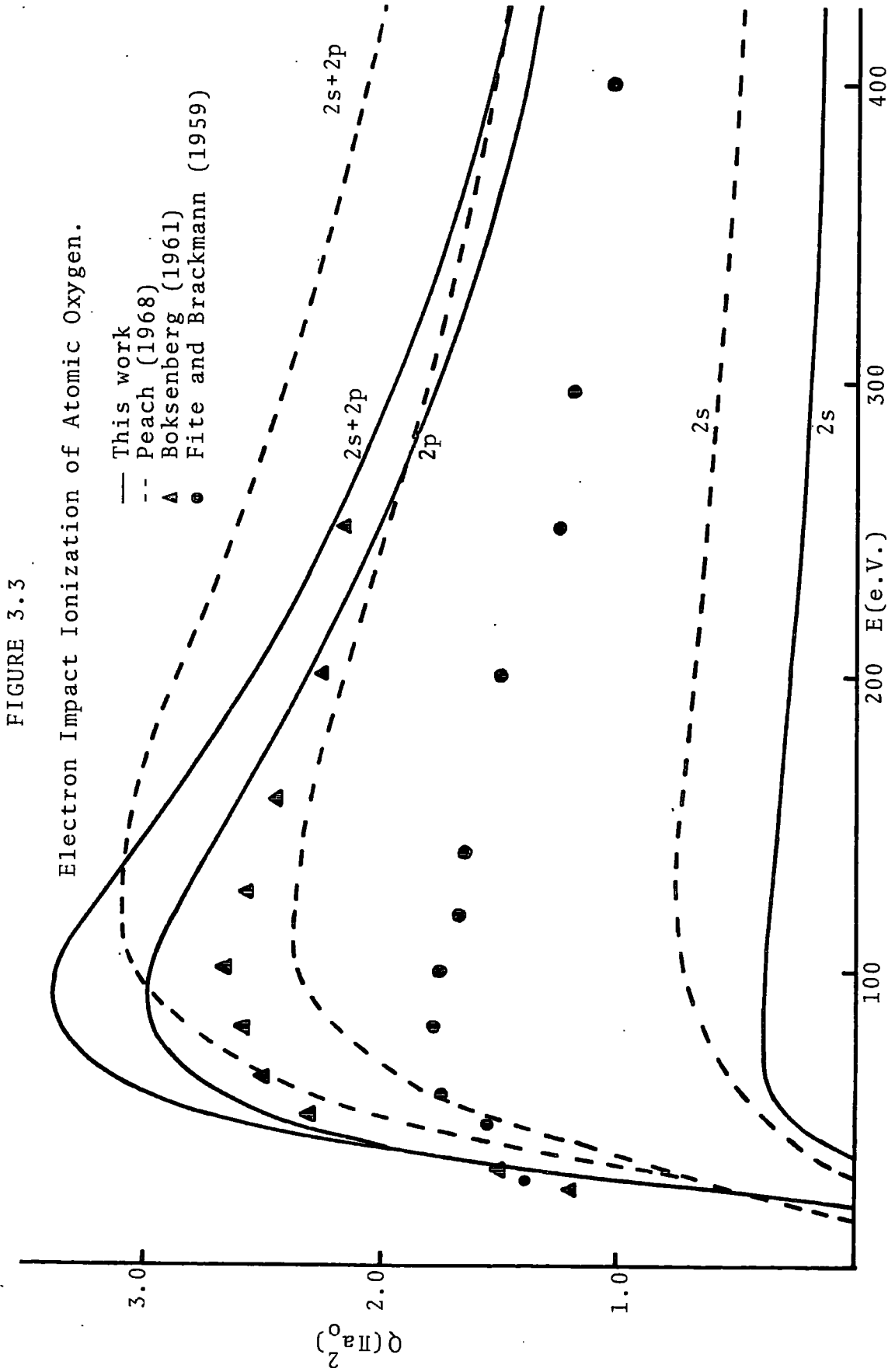
FIGURE 3.4

Proton Impact Ionization of Atomic Helium.

— This work
—‑ Bell and Kingston (1969)
‑‑‑ Peach (1965)
⊕ Solov'ev et al (1962)
▲ de Heer et al (1966)
× McDaniel et al (1962)
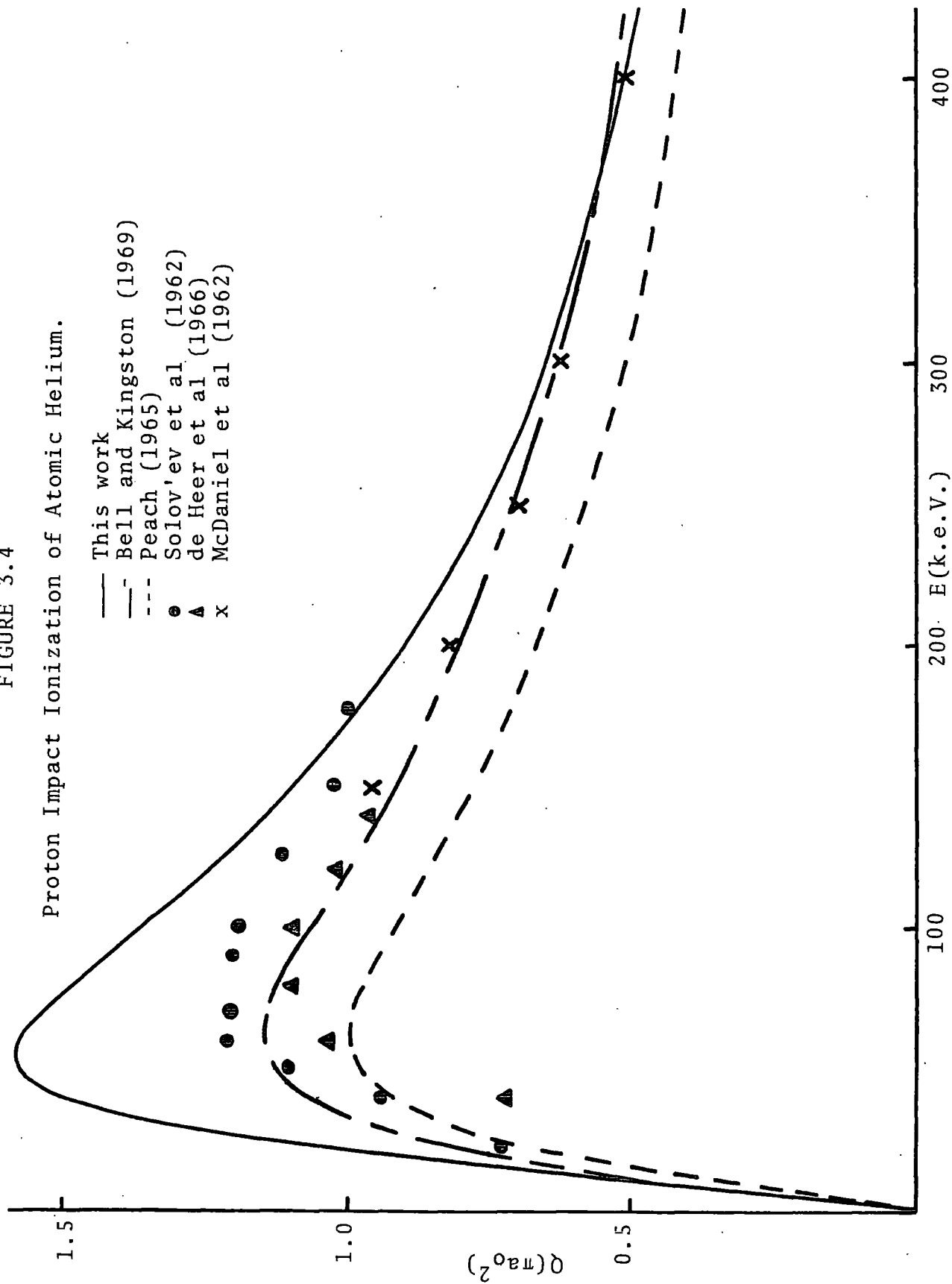
FIGURE 3.5

Proton Impact Ionization of Neon

This work
Peach (1968)
Fedorenko et al (1959)
McDaniel et al (1962)
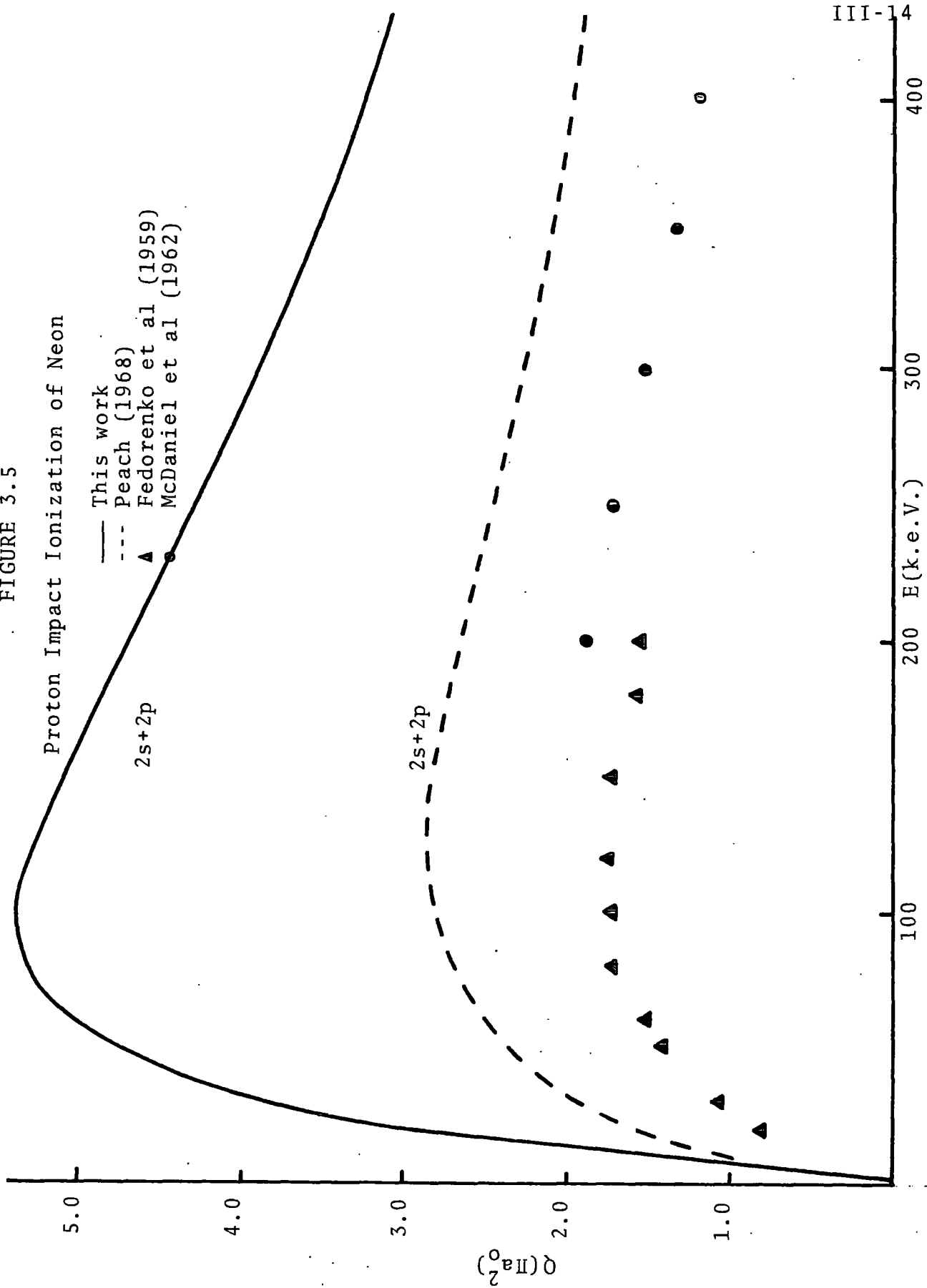
The classical cross-section falls off faster than the quantal cross-section at high energies, although this inherent deficiency in the classical model is not as apparent for electron impact if Q_3 is considered.

Comprehensive tables (3.3-3.7) of cross-sections for inner and outer shell ionization are given below. In the table headings $Q(n,\ell)$ is the ionization cross-section for the loss of an "$n\ell$" electron from the atom. For high energies, proton and electron cross-sections at the same velocity agree closely.

4. Conclusions

Cross-sections for inner and outer shell ionization of He, Li, N, O and Ne by electron and proton impact, as calculated in a classical binary encounter impulse model, have been presented. It was found that cross-sections obtained with a Hartree-Fock velocity distribution for the atomic electrons were as much as 25% lower at their maximum values than corresponding cross-sections using a δ-function distribution, and hence in better agreement with experiment.

Apart from neon, ionization cross-sections for the atoms considered were at most a factor of 2 in disagreement with experiment and for the most part compared favourably with quantal Born calculations. For systems such as neon the model seems unsuitable.

TABLE 3.3

Electron and Proton Impact Ionization of Helium

Electron impact $(\pi a_0{}^2)$		Proton impact $(\pi a_0{}^2)$	
E(e.V.)	Q(1s)	E(KeV)	Q(1s)
		11.2	0.549
		22.3	1.157
		29.8	1.385
		44.7	1.568
28.4	0.099	52.2	1.583
32.5	0.233	59.7	1.572
40.6	0.455	74.6	1.509
50.8	0.619	93.2	1.401
60.9	0.697	111.8	1.291
71.1	0.727	130.5	1.109
91.4	0.719	167.8	1.016
121.8	0.652	223.8	0.827
142.1	0.603	261.0	0.734
182.7	0.517	335.7	0.597
223.3	0.448	410.3	0.501
284.2	0.371	522.2	0.404
365.4	0.301	671.3	0.320
446.6	0.252	820.5	0.265

Ionization potential   1s = 1.808 rydbergs.

TABLE 3.4

Electron and Proton Impact Ionization of Lithium

Electron Impact (πa_o^2)			Proton Impact (πa_o^2)		
E(e.V.)	Q(1s)	Q(2s)	E(K.e.V.)	Q(1s)	Q(2s)
6.1		1.529	11.2	0.014	18.694
10.2		7.061	18.6	0.039	13.695
14.2		7.047	26.1	0.068	10.484
20.3		5.902	37.3	0.109	7.798
28.4		4.734	52.2	0.153	5.899
40.6		3.676	74.6	0.197	4.385
50.8		3.116	93.2	0.217	3.633
71.1	0.008	2.417	130.6	0.231	2.730
91.4	0.045	1.981	167.8	0.228	2.210
121.8	0.082	1.565	223.8	0.212	1.738
142.1	0.096	1.373	261.1	0.199	1.525
162.4	0.103	1.224	298.4	0.187	1.355
182.7	0.107	0.104	335.7	0.176	1.216
223.3	0.107	0.924	410.3	0.155	0.995
263.9	0.103	0.796	484.8	0.139	0.827
324.8	0.095	0.661	596.7	0.119	0.642
365.4	0.089	0.596	671.3	0.108	0.551
446.6	0.079	0.499	820.5	0.092	0.422

Ionization potentials   1s = 4.736 rydbergs

2s = 0.396 rydbergs

TABLE 3.5

Electron and Proton Impact Ionization of Nitrogen

Electron Impact $(\pi a_0{}^2)$			Proton Impact $(\pi a_0{}^2)$		
E(e.V.)	Q(2s)	Q(2p)	E(K.e.V.)	Q(2s)	Q(2p)
			11.2	0.372	2.599
			22.4	0.982	4.097
20.3		0.397	37.3	1.341	5.014
24.3		0.854	44.8	1.381	5.190
32.5	0.125	1.650	59.8	1.337	5.244
40.6	0.351	2.173	74.6	1.233	5.097
50.8	0.502	2.541	93.3	1.092	4.807
60.9	0.555	2.700	111.9	0.967	4.489
71.1	0.560	2.740	130.5	0.862	4.182
91.4	0.543	2.663	167.8	0.706	3.641
121.8	0.430	2.4]1	223.8	0.559	3.013
142.1	0.384	2.242	261.1	0.494	2.692
162.4	0.350	2.081	298.4	0.445	2.428
182.7	0.321	1.933	335.6	0.407	2.209
223.3	0.275	1.683	410.2	0.351	1.866
263.9	0.244	1.484	484.4	0.311	1.613
324.8	0.213	1.261	596.7	0.267	1.336
446.7	0.174	0.954	820.5	0.212	0.991

Ionization potentials   2s = 2.046 rydbergs

2p = 1.136 rydbergs

TABLE 3.6

Electron and Protom Impact Ionization of Oxygen

Electron Impact (πa_o^2)			Proton Impact (πa_o^2)		
E(e.V.)	Q(2s)	Q(2p)	E(K.e.V.)	Q(2s)	Q(2p)
			11.2	0.180	2.577
			22.4	0.549	4.110
20.3		0.214	37.3	0.841	5.193
24.3		0.600	44.8	0.907	5.469
32.5		1.384	59.8	0.944	5.706
40.6	0.112	1.989	74.6	0.915	5.700
50.8	0.262	2.482	93.3	0.845	5.531
60.9	0.346	2.764	111.9	0.770	5.288
71.1	0.384	2.910	130.5	0.699	5.024
91.4	0.391	2.980	167.8	0.583	4.511
121.8	0.347	2.849	223.8	0.463	3.857
142.1	0.315	2.712	261.1	0.409	3.501
162.4	0.286	2.567	298.4	0.367	3.199
182.7	0.261	2.426	335.6	0.334	2.940
223.3	0.224	2.168	410.2	0.287	2.524
263.9	0.197	1.948	484.8	0.253	2.206
324.8	0.169	1.682	596.7	0.218	1.851
446.7	0.138	1.309	820.5	0.175	1.393

Ionization potentials   2s = 2.448 rydbergs

2p = 1.233 rydbergs

TABLE 3.7

Electron and Protom Impact Ionization of Neon

Electron Impact (πa_0^2)			Proton Impact (πa_0^2)		
E(e.V.)	Q(2s)	Q(2p)	E(K.e.V.)	Q(2s)	Q(2p)
			11.2	0.037	1.755
			22.4	0.151	2.895
			37.3	0.289	3.856
24.3		0.072	44.8	0.338	4.180
32.5		0.483	59.8	0.401	4.609
40.6		0.942	74.6	0.429	4.834
50.8	0.003	1.433	93.3	0.435	4.937
60.9	0.060	1.806	111.9	0.424	4.926
71.1	0.108	2.976	130.5	0.405	4.849
91.4	0.165	2.396	167.8	0.360	4.607
121.8	0.188	2.562	223.8	0.300	4.186
142.1	0.184	2.568	261.1	0.267	3.918
162.4	0.176	2.534	298.4	0.241	3.670
182.7	0.166	2.477	335.6	0.219	3.445
223.3	0.145	2.334	410.2	0.186	3.058
263.9	0.128	2.183	484.8	0.163	2.741
324.8	0.108	1.970	596.7	0.138	2.364
446.7	0.085	1.624	820.5	0.110	1.844

Ionization potentials   2s = 3.562 rydbergs

2p = 1.588 rydbergs

REFERENCES

Bagus, P.S., 1966, Phys. Rev., 139, A619-34.

Bell, K.L., and Kingston, A.E., 1969, J. Phys. B (Proc. Phys. Soc.), [2], 2, 653-60.

Boksenberg, A., 1961, Ph.D. Thesis, University of London.

Catlow, G.W., and McDowell, M.R.C., 1967, Proc. Phys. Soc., 92, 875-79.

Dwight, E.B., 1964, Tables of Integrals and other Mathematical Data (MacMillan, N.Y.).

Fedorenko, N.V., Afrosimor, V.V., Il'in, R.N., and Solov'ev, E.S., 1959, in 4th International Conference on Ionization Phenomena in Gases (Amsterdam; North Holland).

Fite, W.L., and Brackmann, R.T., 1959, Phys. Rev., 113, 815-6.

Garcia, J.D., Gerjuoy, E., and Welker, J.E., 1968, Phys. Rev., 165, 66-72.

Gryzinski, M., 1959, Phys. Rev., 115, 374-83.

de Heer, F.J., Schutten, J., and Moustafa, H., 1966, Physica, 32, 1766-92.

Kieffer, L.J., and Dunn, G.M., 1966, Rev. Mod. Phys., 38, 1-35.

Kingston, A.E., 1966, Proc. Phys. Soc., 87, 193-200.

McDowell, M.R.C., 1966, Proc. Phys. Soc., 1966, 89, 23-26.

Messiah, A., 1961, Quantum Mechanics (Amsterdam; North Holland).

Peach, G., 1965, Proc. Phys. Soc., 85, 709-18.

Peterkop, R., 1961, Proc. Phys. Soc., 77, 1220-2.

Peterson, J.R., 1964, Atomic Collision Processes, Ed. M.R.C. McDowell (Amsterdam: North Holland)

Roothaan, C.C.J., Clementi, E., and Yoshimine, M., 1962, Phys. Rev., 127, 1618-20.

Roothaan, C.C.J., and Kelly, P.S., 1963, Phys. Rev., 131, 1177-82.

Roothaan, C.C.J., Sach, L.M., and Weiss, A.W., 1960, Rev. Mod. Phys., 32, 186-94.

Rothe, E.W., Rol, P.K., Neynaber, R.H., Truijillo, S.M., and Marino, L.L., 1962, Phys. Rev., 128, 659-62.

Slater, J.C., 1960, Quantum Theory of Atomic Structure, Vol. I, (London: McGraw-Hill).

Solov'ev, E.S., Il'in, R.N., Oparin, V.A., and Fedorenko, N.V., 1962, Sov. Phys.-JETP, 15, 459-64.

Smith, A.C.H., 1962, Phys. Rev., 127, 1647-9.

Smith, P.T., 1930, Phys. Rev., 36, 1293-302.

Stabler, R., 1964, Phys. Rev., 133, A1268-73.

Vriens, L., 1967, Proc. Phys. Soc., 90, 935-44.

CHAPTER IV

THE CLOSURE APPROXIMATION FOR EXCITATION
OF ATOMIC HYDROGEN BY PROTON IMPACT

1. Introduction

Several attempts have been made in recent years to
include continuum intermediate states in theoretical studies
of ion-atom collisions. In particular the Sturmian expansion
method of Gallaher & Wilets (1967) and the impulse approxima-
tion (Coleman & Trelease (1968) and earlier work referred to
therein) take partial account of the continuum in both direct
and rearrangement processes. The angular momentum expansion
of Cheshire & Sullivan (1967) includes all continuum states
of angular momentum <1 for direct processes.

Cheshire (1965) suggested an alternative treatment
of the continuum, within the impact parameter model, for
proton-hydrogen atom collisions. In this present work we
apply it to the process.

$$H^+ + H(1s) \rightarrow H^+ + H(2s) \qquad (4.1)$$
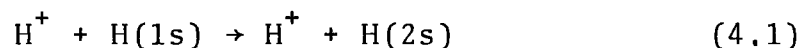
Atomic units will be used throughout.

2. The Closure Approximation

The notation and preliminary results of Chapter I
(section 4) will be used. Within the impact parameter model,
the total electronic wave function is expanded, in turn,

using travelling orbitals about the atomic nucleus, A, and
then similarly about the incident proton B

$$\Psi = \Phi^A A \tag{4.2}$$

$$\Psi = \Phi^B B \ . \tag{4.3}$$

The time variation of the matrices A, B are descri-
bed by the coupled equations (1.43)

$$\frac{dA}{dt} = i(\Phi^A | V_B | \Phi^B) B \tag{4.4}$$

$$\frac{dB}{dt} = i(\Phi^B | V_A | \Phi^A) A \ . \tag{4.5}$$

A truncation of both equations is generally neces-
sary. If however the B coefficients are eliminated between
(4.4) and (4.5) by using closure before truncation, then the
A amplitudes may be calculated with implicit account of the
complete set of rearrangement states. This is the purpose of
the closure approximation.

A detailed derivation of the approximation is given
by Cheshire (1965), and also by Coleman & McDowell (1969),
and will not be reproduced here. The elimination of the B
coefficients from (4.4) and (4.5) gives rise to an infinite
set of second orders coupled differential equations,

$$\frac{d^2 A}{dt^2} - i(\Phi^A | V_B T_B V_B^{-1} | \Phi^A) \frac{dA}{dt} + (\Phi^A | V_B V_A | \Phi^A) A = 0 \tag{4.6}$$

Now

$$V_B T_B V_B^{-1} = -i\frac{d}{dt}\ln V_B + \frac{1}{2}V_B^2 + V_B - V_A \qquad (4.7)$$

(Coleman and McDowell, 1969) so that (4.6) is of the form

$$\ddot{A} + G\dot{A} + HA = 0 \qquad (4.8)$$

with

$$G = -\frac{d}{dt}(\Phi^A|\ln V_B|\Phi^A) -\frac{i}{2}(\Phi^A|V_B^2|\Phi^A) -i(\Phi^A|V_B-V_A|\Phi^A)$$

$$(4.9)$$

$$H = (\Phi^A|V_B V_A|\Phi^A)$$

Equation (4.8) is solved with boundary conditions (1.29),

$$a_n = \delta_{np} \exp\left[-\frac{i}{v}\ln(vR-v^2t)\right] \qquad (4.10)$$

and the transition probability to state q is given by

$$P_{p,q}(\rho,v) = |a_q(+\infty)|^2 \qquad (4.11)$$

where ρ is the impact parameter and v is the velocity of the collision. The required cross-section is

$$Q_{pq}(v) = 2\int_o^\infty \rho\, P_{pq}(\rho v)d\rho \quad (\pi a_o^2) \quad (4.12)$$

3. Analysis

In the present work, the set of equations (4.8) was truncated and only two coefficients corresponding to the 1s and 2s states were retained. Associated variables will be

subscripted by 1 & 2 respectively.

The unitary transformation

$$a_1 = \alpha_1 \, e^{i\eta}$$

$$a_2 = \alpha_2 \, e^{-i\epsilon t + i\eta t} \tag{4.13}$$

is applied to (4.8) where

$$\eta = -\frac{i}{v}\ln(vR - v^2 t) = i \int_{-\infty}^{t} \frac{1}{R} dt$$

and

$$\epsilon = \epsilon_2 - \epsilon_1.$$

This removes the time dependant phase factors from the matrix elements and the logarithmic phase factor from the boundary condition (4.10), so that the equations (4.8) become

$$\ddot{\alpha}_i + \sum_{j=1}^{2} G'_{ij}\dot{\alpha}_j + \sum_{j=1}^{2} H'_{ij}\alpha_j = 0 \tag{4.14}$$

with the boundary conditions

$$\alpha_i(t) \underset{t \to -\infty}{\sim} \delta_{i1} \tag{4.15}$$

Explicit forms of G' and H' are given in the appendix and it can be seen that they involve only the basic matrix elements

$$P_{ij} = (\phi_i | \frac{1}{xs} | \phi_j)$$

$$L_{ij} = (\phi_i | \ln s^{-1} | \phi_j) \tag{4.16}$$

$$Q_{ij} = \frac{1}{2} (\phi_i | \frac{1}{s^2} | \phi_j) + (\phi_i | \frac{1}{s} - \frac{1}{x} | \phi_j)$$

where

$$Z_{ij} = \int \phi_i^*(x) \ Z(x,s) \ \phi_j(x) d\underline{\tau}$$

$$= \int \phi_i(x) \ Z(x,s) \ \phi_j(x) d\underline{x} \qquad (4.17)$$

and ϕ_i is the hydrogenic eigenfunction. Now

$$\phi_{n\ell m} = R_{n\ell}(x) \ Y_{\ell m}(\hat{x}) \qquad (4.18)$$

where the $Y_{\ell m}$ are spherical harmonics and

$$R_1 = R_{1s} = 2e^{-x}$$

$$R_2 = R_{2s} = 2^{-1/2}(1-x/2)e^{-x/2} .$$

Sack (1964) has expanded some functions of "s" in terms of Legendre polynomials,

$$Z(x,s) = \sum_{\ell=0}^{\infty} \gamma_\ell(x,R) \ P_\ell(\cos\Theta) \qquad (4.19)$$

where Θ is the angle between $\underline{R}$ and $\underline{x}$. For s-states the angular integrations of (4.17) are trivial and the integral reduces to

$$Z_{ij} = \int_0^\infty R_1 R_2 \gamma_0 x^2 dx \qquad (4.20)$$

From Sack the expansion functions γ_0 for $\ln s$ and s^{-2} are

$$\gamma_{0,\ln s} = \ln|x-R| + \frac{(x+R)^2}{4xR} \ln\frac{x-R}{|x-R|} - \frac{1}{2} \qquad (4.21)$$

$$\gamma_{0,s-2} = \frac{1}{2xR} \ln \left| \frac{x+R}{x-R} \right| \tag{4.22}$$

and the integrals (4.20) are reducible to linear combinations of the exponential integrals. Explicit forms of equations (4.16) are given in the appendix.

Unlike the usual procedure of imposing the boundary conditions (4.15) at a large but finite internuclear separation (although see Bell (1967)), the initial solutions are obtained by solving the equation (4.14) using asymptotic expansions for the matrix elements and the solutions which are valid for large negative values of the time, t. Let $\underline{\alpha}$ denote the column vector $(\alpha_i, i=1,2)$ then for large R, write the asymptotic expansions as

$$\underline{\alpha} = \sum_{n=1}^{\infty} \frac{\underline{\alpha}^{(n)}}{R^{n-1}} \qquad\qquad \underline{G}' = \sum_{n=1}^{\infty} \frac{\underline{g}^{(n)}}{R^{n-1}}$$

$$\underline{\dot{\alpha}} = \sum_{n=2}^{\infty} \frac{\underline{\beta}^{(n)}}{R^{n}} \qquad\qquad \underline{H}' = \sum_{n=1}^{\infty} \frac{\underline{h}^{(n)}}{R^{n-1}} \tag{4.23}$$

$$\underline{\ddot{\alpha}} = \sum_{n=3}^{\infty} \frac{\underline{\gamma}^{(n)}}{R^{n}}$$

where $\underline{g}^{(n)}, \underline{h}^{(n)}$ are square matrices. Hence from (4.14) in the asymptotic region

$$\sum_{n=3}^{\infty} \frac{\underline{\gamma}^{(n)}}{R^{n}} + \sum_{\substack{n=1 \\ m=1}}^{\infty} \frac{\underline{g}^{(n)} \underline{\beta}^{(m+1)}}{R^{n+m}} + \sum_{\substack{n=1 \\ m=1}}^{\infty} \frac{\underline{h}^{(n)} \underline{\alpha}^{(m)}}{R^{n+m-2}} = 0 \tag{4.24}$$

Writing

$$\dot{R} = v\left(1-\frac{\rho^2}{R^2}\right)^{1/2} = \sum_{n=1}^{\infty} \frac{z^{(n)}}{R^{n-1}}$$

we obtain the relations

$$\underline{\beta}^{(n)} = -\sum_{m=1}^{n-1} (n-m) \, z^{(m)} \, \underline{\alpha}^{(n+1-m)} \qquad (4.25)$$

$$\underline{\gamma}^{(n)} = -\sum_{m=1}^{n-1} (n-m) \, z^{(m)} \, \underline{\beta}^{(n-m)} \qquad (4.26)$$

The $\underline{g}^{(n)}$ and $\underline{h}^{(n)}$ matrices can be obtained in closed form for any n, and hence from (4.24), (4.25) and (4.26), the $\underline{\alpha}^{(n)}$ vectors are found. This procedure was carried out for n=1..8 and the solutions and their derivatives were approximated by

$$\underline{\alpha} = \sum_{n=1}^{8} \frac{\alpha^{(n)}}{R^{n-1}} \qquad \underline{\dot{\alpha}} = \sum_{n=2}^{7} \frac{\underline{\beta}^{(n)}}{R^{n}} \qquad \underline{\ddot{\alpha}} = \sum_{n=3}^{7} \frac{\underline{\gamma}^{(n)}}{R^{n}} \qquad (4.27)$$

for large R.

4. Numerical Methods

In the above analysis the amplitude and matrices were complex variables and it was convenient to separate equations (4.14) into real and imaginary parts and solve four coupled differential equations.

The starting solution for these equations at large R ($R = R_o, t = t_o$) is given by (4.27). The solution of equations

(4.22) is non-trivial especially when considering the coefficients of the higher order powers of $\frac{1}{R}$. A procedure was coded so the higher order coefficients and their derivatives could be derived on the computer using values already evaluated for $\underline{\alpha}^{(1)}, \underline{\alpha}^{(2)}$ and $\underline{\alpha}^{(3)}$. The approximate solution (4.27) was tested by checking it satisfied equation (4.14) to a pre-set precision. For example at $R=R_o=50$ (t<o) we find agreement to one part in 10^{11}.

This expansion of the solution is a strict asymptotic expansion and is not valid for small R. The range of validity was tested by comparing various solutions at t=-10 arising from different starting positions, R_o, and performing the time integration. On starting the time integration, it was checked that the solution ran smoothly from the asymtotic region (i.e. continuous solutions and continuous first and second derivatives). Results for three solutions with different values of R_o are given in Table 4.1. It can be seen that the solutions $|\alpha_1|^2$, $|\alpha_2|^2$ are stable to one part in 10^6 at t=-10. For $R_o<12$ the asymptotic solution did not yield useful starting values.

The time integration of (4.14) was performed using a Runge-Kutta method for second order equations (Abramowitz and Stegun, 1964). In addition (4.14) were transformed into eight first order differential equations by writing

TABLE 4.1

Dependence of Solutions on Starting Positions, R_o.

Collision parameters; $\rho=1$, $v=1$.

Time	$|\alpha_1|^2$	$|\alpha_2|^2$	Real α_2	Imag. α_2
$R_o = 50$				
- 49.98	0.99998784	0.97989113,-11	0.31193772,-5	-0.26152912,-6
- 20.88	0.99984385	0.22126650,-8	0.46890133,-4	-0.37390392,-5
- 10.88	0.99900836	0.12427820,-6	0.35222953,-3	0.14579361,-4
49.11	0.88781744	0.157411811	0.24392790	0.31291739
$R_o = 25$				
- 20.88	0.99984373	0.22602608,-8	0.474997843,-4	-0.20530875,-5
- 10.88	0.99900595	0.12347384,-6	0.35113730,-3	0.13282997,-4
49.12	0.88781947	0.157411293	0.24507163	0.31201414
$R_o = 15$				
- 10.88	0.99900715	0.13914885,-6	0.36021724,-3	0.96914314,-4
49.13	0,88778569	0.157466697	0.24659974	0.31089474

(The figure following the comma indicates the
power of 10 by which the entry is to be multiplied)

$$\dot{\alpha}_i = \sum_{j=1}^{2} G'_{ij}\alpha_j + \delta_i$$

$$\dot{\delta}_i = -\sum_{j=1}^{2} \dot{G}'_{ij}\alpha_j - \sum_{j=1}^{2} H'_{ij}\alpha_j \qquad (4.28)$$

and separating into real and imaginary parts. These equations were solved with the additional boundary condition.

$$\delta_i \underset{t\to\infty}{\sim} 0 \qquad \text{for all } i \qquad (4.29)$$

using either a first order Runge-Kutta or Adams-Bashforth predictor-corrector method. A sample of results for all methods are compared in Table 4.2. No attempt was made to deduce the relative merits of the integration procedures from the solutions. All that was required was that the results predicted by the various procedures for the same collision parameters, were consistant with each other. It can be seen that agreement was attained to 1%.

TABLE 4.2

Comparison of Solutions Predicted by Various
Integration Procedures

Collision parameters: $v=1$, $\rho=1$, $R_o=50$

Integration procedures	$|\alpha_1(t=50)|^2$	$|\alpha_2(t=50)|^2$
First order methods		
Runge-Kutta	0.8889	0.1599
Adams-Bashforth		
predictor	0.8886	0.1589
corrector	0.8889	0.1589
Second order method		
Runge-Kutta	0.8878	0.1575

The derivative of the asymptotic solution, $\underline{\alpha}$, was found to be of order $\frac{1}{R^3}$ for large R. However in the first in the first order equation (4.28), the additional derivatives, $\dot{\delta}_i$, are of order $\frac{1}{R^2}$ for large R. This means that to obtain the same degree of stability in the solution at large R, the step length in the integration procedures for the first order equations (4.28) must be considerably smaller than that required for the second order equations (4.12). So, in the main, calculations were performed using the second order equations.

The matrix elements of $\underline{G}'$ and $\underline{H}'$ were coded as linear combinations of exponential integrals; all possible concellation of terms having been performed in the analysis (see appendix). This ensured minimum round-off error in their computation. The exponential integrals were evaluated to an accuracy of sixteen significant figures. It was checked that the asymptotic forms and the exact values of the matrix elements were in agreement for large R. For R>40 where the routines for the exponential integrals were inadequate, the exact matrix elements in $\underline{G}'$ & $\underline{H}'$ were replaced by their asymptotic forms including terms up to $1/R^7$. This proved useful in allowing the time integration to be continued to large positive times.

The matrix elements varied smoothly with time throughout the collision and their time derivatives could be obtained from a standard five-point formulae.

The computer code was written so that the equations and solutions could be transformed at $R=R_1$ say, to reintroduce the logarithmic phase factors into the solution and remove the corresponding $\frac{1}{R}$ terms from the matrix elements, thus avoiding rapid changes in the latter near $R=0$. It was found that there was no detectable change in eight significant figures in the calculated amplitudes when this transformation was made.

The step length $h=\Delta R$ ($\Delta t=\Delta R/v$) could be changed at six values of R throughout the run. In Table 4.3 solutions $|\alpha_1|^2$, $|\alpha_2|^2$ obtained from integration procedures with different mesh sizes are compared. Results predicted by the procedure using the larger mesh are in agreement to one part in 10^7 with those obtained with the finer mesh. This might be considered sufficient accuracy but for small velocities ($v<0.5$) and certain impact parameters, the excitation probability to the 2s-state is of order 10^{-7} or smaller (see fig. 4.2 below) and the crude mesh would produce an error in the probability of a comparable magnitude to the probability itself. For moderate velocities the transition probabilities are larger and an integration mesh

$$h = 0.1 \quad R > 2$$
$$h = 0.01 \quad R < 2$$

was sufficient.

TABLE 4.3

Dependence of Probabilities on the Integration Mesh Size

Time	h	$|\alpha_1|^2$	$|\alpha_2|^2$	h	$|\alpha_1|^2$	$|\alpha_2|^2$
-44	1.0,-1	0.99815660	0.24985511,-6	1.0,-2	0.99815657	0.23575761,-6
-24		0.99150985	0.73694941,-5		0.99150959	0.72923905,-5
-4	5.0,-2	0.91576561	0.38875522,-2	1.0,-4	0.91475387	0.38835527,-2
25	1.0,-1	0.99222133	0.51793319,-5	1.0,-2	0.99214422	0.52841291,-5
40		0.99769416	0.12500684,-5		0.99764625	0.12724146,-5
60		0.99929327	0.44719360,-6		0.99923140	0.46748650,-6
80		0.99971834	0.64772880,-6		0.99966104	0.62665581,-6

(The figure after the comma indicates the power of 10 by which the entry is to be multiplied).

For t>0, the amplitudes $\left|\alpha_1\right|^2$, $\left|\alpha_2\right|^2$ exhibited an oscillatory behavior and this is illustrated in fig. 4.1. This behaviour hinders the task of obtaining an accurate asymptotic value of the excitation probability $\left|\alpha_2\right|^2$. Asymptotic expansions of the real and imaginary parts of the solution α_2, of the type

$$\begin{matrix} \text{Real} \\ \text{Imag} \end{matrix} \; \alpha_2 = (a_o + \frac{a_1}{R} + \frac{a_2}{R^2}..) \; \begin{matrix} \sin(f(t)) \\ \cos(g(t)) \end{matrix} \qquad (4.28)$$

where $f(t) \underset{t \to \infty}{\sim} k(t)$, $g(t) \underset{t \to \infty}{\sim} k(t)$, and use of an asymptotic procedure similar to that used for large negative time, were considered as a method of obtaining the exact asymtolic amplitude a_o. Unfortunately, although there is an overall damping of the solutions as t→∞, the amplitude of the real and imaginary parts is not in practice a monotonic decreasing function and cannot be fitted with the asymptotic solutions (4.28).

It was decided that the most expedient method to obtain an accurate asymptotic value for the amplitude was by close scrutiny of the maxima and minima of the real and imaginary parts of the solution. The modulus of the maxima and minima considered as a function of time is also a damped oscillatory function but its behaviour is such that an accurate estimate of it's limit for large t can be obtained. The square of this limit was taken to be the excitation probability to the 2s-state. A few sample solutions were integrated out to R=500 and the above procedure gave a consistant result

FIGURE 4.1
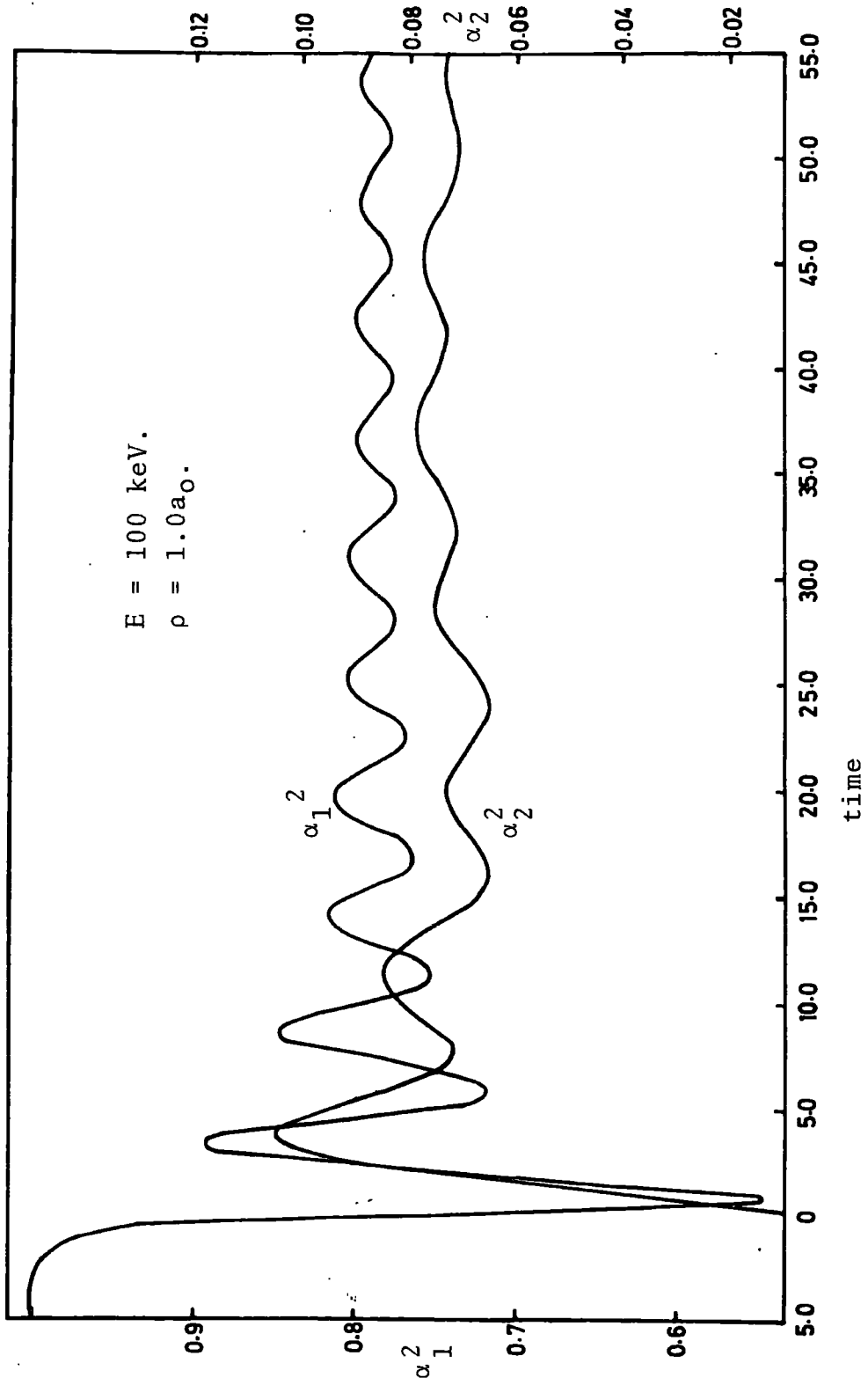
Variation of Solutions with Time

(to 3 decimal places) for the excitation probability with that obtained from far fewer maxima and minima.

5. Results and Discussion

The calculations were carried out on the NUMAC IBM 360/67. The time taken for one computer run for one velocity and one impact parameter was, of course, mainly depended on the integration mesh size and also how far the solution was integrated out for positive time. In the main, the average time was 3 minutes but with the fine mesh used for the low velocities, the run time might be extended to anything up to 30 minutes. Since care was taken to ensure minimum cancellation in the matrix elements, computer round-off error was negligible. Results were obtained in the energy range 1 k.e.V→625 k.e.V from impact parameters $0<\rho<3$ a_o.

The transition probability as a function of impact parameter exhibited similar oscillatory behaviour at low energies as observed by Wilets and Gallaher (1966). Figure 4.2 shows the transition probability for E=1 k.e.V. However the final amplitudes for the 1s-state do not oscillate appreciably with impact parameter and furthermore in this model $|\alpha_2|^2>0.985$ for all impact parameters, E<10k.e.V. This in disagreement with the experiments of Helbig and Everhart (1965) and of other theoretical calculations which include Φ_{1s}^B explicitly (Wilets and Gallaher (1966), Cheshire (1968))

Green (1965) has shown that for first order expansion methods, the sum of the probabilities is conserved throughout

FIGURE 4.2
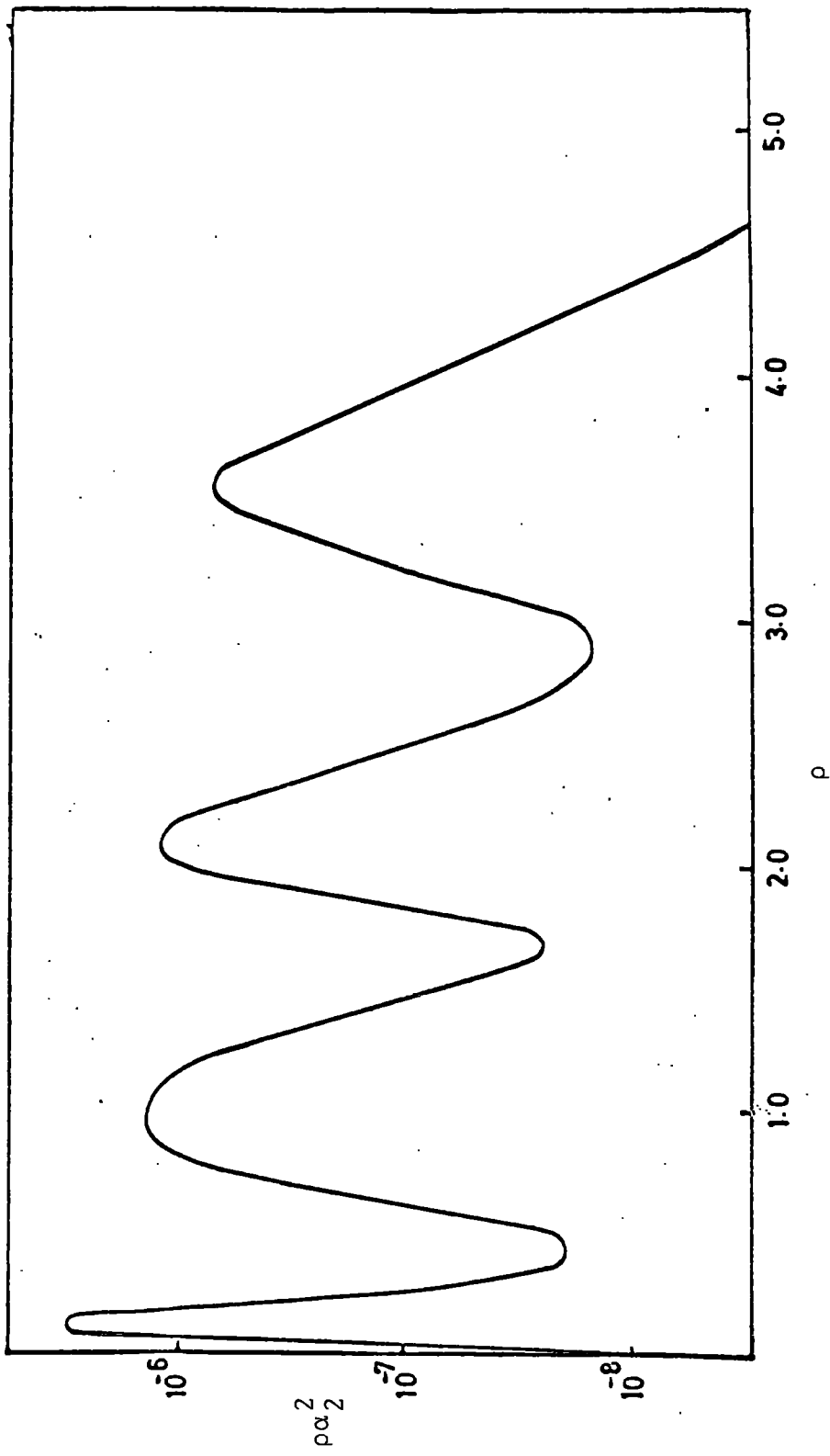
Transition Probability at E=1 keV.

the collision. Unfortunately this does not apply to the closure approximation and for energies less than 50 k.e.V. and small impact parameters ($\rho<1$), unitarity is violated. At $v=1$, $\rho=0.25$ the sum of the probabilities reaches its over-all maximum value of 1.31. Computed values of $|\alpha_1|^2$ and $|\alpha_2|^2$ for $v=1$, 2 are given in Table 4.4.

To calculate the excitation cross-section to the 2s-state, the probabilities are replaced when necessary by

$$|\bar{\alpha}_2|^2 = |\alpha_2|^2 \, / \, (|\alpha_1|^2 + |\alpha_2|^2)$$

and are given for a range of energies and impact parameters in Table 4.5. A sample of these transition probabilities are shown in fig. 4.3 as a function of impact parameter.

Excitation cross-sections were obtained by a Simpson's integration and are given in Table 4.6 and compared with other theoretical calculations in figure 4.4.

At low energies (E<20 k.e.V.) the present results lie between those of the two state calculation of Lovell and McElroy (1965) and the impulse approximation results of Coleman (1968). At intermediate energies (25<E<100 k.e.V) the results are in general agreement with the two centre hydrogenic expansion calculations of Wilets and Gallaher (1965). Gallaher and Wilets (1968) give 6-state Sturmian expansion results at two energies in this range and we also show these values.

Above 100 k.e.V., the present results lie above

TABLE 4.4

Probabilities $|\alpha_1|^2$, $|\alpha_2|^2$

v = 1   E = 25 k.e.V.

ρ	$|\alpha_1|^2$	$|\alpha_2|^2$	$\sum |\alpha_i|^2$
0.25	0.8920	0.4185	1.3105
0.5	0.8722	0.3513	1.2235
0.75	0.8760	0.2608	1.1368
1.0	0.8973	0.1671	1.0644
1.25	0.9256	0.0949	1.0199
1.5	0.9496	0.0485	0.9981
2.0	0.9813	0.0098	0.9911
3.0	0.9985	0.0000_5	0.9985

v = 2   E = 100 k.e.V.

ρ	$|\alpha_1|^2$	$|\alpha_2|^2$	$\sum |\alpha_i|^2$
0.25	0.5847	0.3136	0.9983
0.5	0.6428	0.2223	0.8651
0.75	0.7172	0.1357	0.8529
1.00	0.7899	0.0739	0.8638
1.25	0.8506	0.0365	0.8871
1.50	0.8971	0.0164	0.9135
2.0	0.9522	0.0026	0.9548
3.0	0.9886	0.0003	0.9890

TABLE 4.5

Probabilities, $\rho|\bar{\alpha}_2|^2$

Impact parameters ρ

E(k.e.V.)	0.25	0.5	0.75	1.0	1.25	1.5	2.0	3.0
6.25	1.3 , -3	1.0 , -6	4.2 , -3	1.72, -2	2.78, -2	3.16, -2	1.70, -2	1.8 , -3
9.0	2.7 , -3	1.58, -2	4.03, -2	6.07, -2	6.77, -2	7.15, -2	2.64, -2	1.8 , -3
25.0	7.98, -2	1.43, -1	1.72, -1	1.57, -1	1.16, -1	7.27, -2	1.86, -2	1.0 , -4
57.5	9.1 , -2	1.45, -1	1.64, -1	1.42, -1		5.19, -2	1.12, -2	8.0 , -4
50.0	1.08, -1	1.59, -1	1.54, -1	1.22, -1	7.67, -2	4.24, -2	9.0 , -3	3.0 , -4
75.0	9.37, -2	1.35, -1	1.25, -1	9.14, -2	5.64, -2	3.01, -2	6.0 , -3	1.0 , -3
100.0	7.84, -2	1.11, -1	1.04, -1	7.38, -2	4.56, -2	2.46, -2	5.2 , -3	1.0 , -3
225.0	4.11, -2	5.76, -2	5.26, -2	3.93, -2	2.56, -2	1.51, -2	4.8 , -3	1.3 , -3
400.0	2.34, -2	3.25, -2	3.04, -2	2.35, -2	1.60, -2	1.02, -2	4.0 , -3	1.2 , -3
625.0	1.41, -2	2.02, -2	1.92, -2	1.54, -2	1.10, -2	7.4 , -3	3.4 , -3	1.2 , -3

(The figure following the comma indicates the power of 10 by which the entry is to be multiplied)

FIGURE 4.3

Curve 1 , E = 75 k.e.V.
      2 , E = 25 k.e.V.
      3 , E = 12.5 k.e.V.
      4 , E = 9 k.e.V.
      5 , E = 6.25 k.e.V.
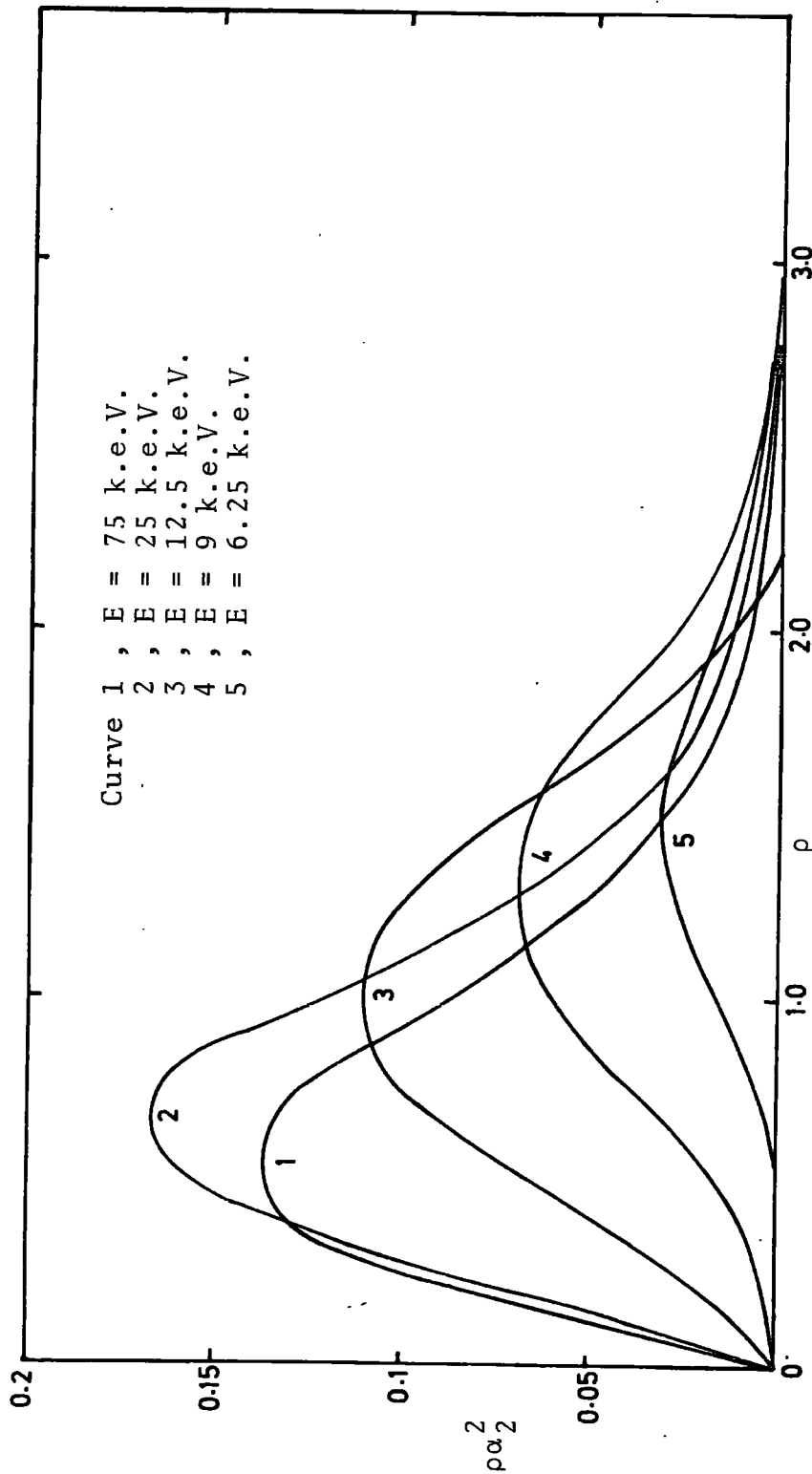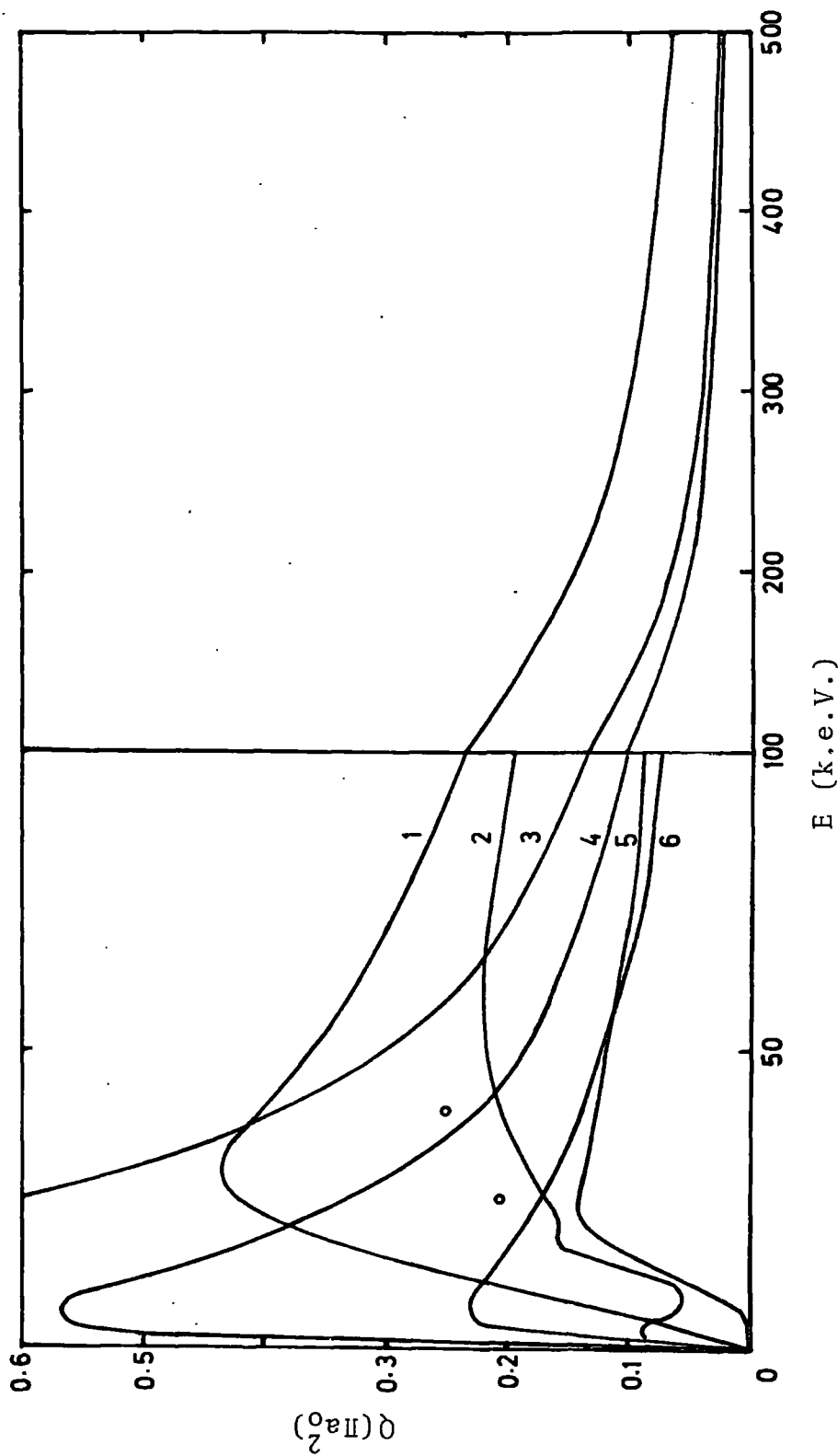
Comparison of Transition Probabilities

TABLE 4.6

Excitation Cross-Sections $H^+ + H(1s)$ $H^+ + H(2s)$

Energy (K.e.V.)	$Q(\pi a_0^2)$
6.25	0.08
9.0	0.19
12.5	0.24
25.0	0.42
37.5	0.40
50.0	0.36
75.0	0.29
100.0	0.24
225.0	0.13
400.0	0.08
625.0	0.05

FIGURE 4.4

Comparison of Excitation Cross-Section: $H^+ + H(1s) \rightarrow H^+ + H(2s)$

Curve 1, Closure approximation: curve 2, Wilets and Gallaher, 4-state hydrogenic:
Curve 3, Cheshire and Sullivan "all s+p" calculation: curve 4, 1st Born:
Curve 5, Lovell and McElroy 1sA/1sB calculation: curve 6, Impulse approximation
of Coleman: The circles are 6-state Sturmian results of Gallaher and Wilets.

those of Cheshire and Sullivan (1967) and the second Born approximation calculation of Holt and Moiseiwitch (1968). The latter are indentical with the former and are not shown in fig. 4.4.

It is noticeable that in calculations which include the 1sA/1sB channel implicitly or explicitly (this includes a psuedo-state expansion calculation of Cheshire,Gallaher and Taylor (1969) which is not shown), the cross-sections peak at higher energies than for the single centre expansions. This is because the 1sA/1sB channel dominates the collision at low energies.

6. Conclusions

Direct excitation cross-sections into the 2s-state have been calculated using the closure approximation, retaining only the first two states in the expansion of the electronic wave function. An accurate asymtotic solution for large negative t allowed the time integration of the coupled equations to start at $R_o=15$. The time integration for the second order equations was performed by a Runge-Kutta method with an error term of order h^5. The 2s-state amplitude, α_2, was extracted for large positive t with an accuracy of three decimal figures.

The results are in reasonable accord with those of other theoretical calculations but in the absence of experimental information no conclusions can be drawn as to which method is to be preferred.

APPENDIX

The (2x2) square matrices of the second order coupled
equations (4.12)

$$\ddot{\alpha}_i + \sum_{j=1}^{2} G'_{ij}\dot{\alpha}_j + \sum_{j=1}^{2} H'_{ij}\alpha_j = 0 \qquad i=1,2$$

are given by

$$G'_{ij} = -\dot{L}_{ij} - iQ_{ij} + i \begin{vmatrix} \dfrac{2}{R} & \varepsilon L_{12} \\ \\ -\varepsilon L_{21} & 2(\varepsilon + \dfrac{1}{R}) \end{vmatrix}$$

$$H'_{ij} = P_{ij} + \dfrac{Q}{R}_{ij} - \dfrac{i\dot{L}}{R}_{ij} + \begin{vmatrix} -\dfrac{1}{R^2} & \varepsilon Q_{12} - \varepsilon L_{12}(\varepsilon + \dfrac{1}{R}) \\ \\ \dfrac{\varepsilon L}{R}_{21} & \varepsilon Q_{22} - (\varepsilon + \dfrac{1}{R})^2 \end{vmatrix}$$

$$+ i \begin{vmatrix} -\dfrac{\dot{R}}{R^2} & -\varepsilon\dot{L}_{12} \\ \\ 0 & -\varepsilon\dot{L}_{22} - \dfrac{\dot{R}}{R^2} \end{vmatrix}$$

where

$$P_{ij} = (\phi_i | \frac{1}{xs} | \phi_j)$$

$$L_{ij} = (\phi_i | \ln s^{-1} | \phi_j)$$

$$Q_{ij} = \frac{1}{2}(\phi_i | \frac{1}{s^2} | \phi_j) + (\phi_i | \frac{1}{s} - \frac{1}{x} | \phi_j).$$

The exponential integrals are defined as

$$E_1(x) = \int_x^\infty \frac{e^{-t}}{t} dt$$

$$E_i(x) = -\oint_{-x}^\infty \frac{e^{-t}}{t} dt .$$

Let

$$\bar{E}_1 = \bar{E}_1(\lambda R) = e^{\lambda R} E_1$$

$$\bar{E}_i = \bar{E}_k(\lambda R) = e^{-\lambda R} E_i$$

then

$$P_{11} = \frac{1}{R}\left(1 - e^{-\lambda R}\right)$$

$$-L_{11} = \ln R + \frac{1}{4}\left[\bar{E}_1(\frac{3}{\lambda R} - 1) + \bar{E}_i(\frac{3}{\lambda R} + 1)\right]$$

$$\lambda = 2$$

$$Q_{11} = \frac{\bar{E}_1}{2}\left(\frac{1}{\lambda R}-1\right) + \frac{\bar{E}_i}{2}\left(\frac{1}{\lambda R}+1\right) + \frac{1}{R}\left(1-e^{-\lambda R}\right) - e^{-\lambda R} - 1$$

$$\lambda = 2$$

$$P_{12} = P_{21} = \frac{1}{2^{1/2}\lambda^2}\left[\frac{1}{\lambda R}(1-e^{\lambda R}) + e^{-\lambda R}\right]$$

$$-L_{12} = -L_{21} = \frac{1}{2^{1/2}\lambda^3}\left[\frac{1}{\lambda} - \bar{E}_1(\frac{\lambda R}{3}-1+\frac{1}{\lambda R}) - \bar{E}_i(\frac{\lambda R}{3}+1+\frac{1}{\lambda R})\right]$$

$$Q_{12} = Q_{21} = \frac{2^{1/2}}{8\lambda^3 R}\left[\bar{E}_1(1-\lambda R-\lambda^2 R^2) + \bar{E}_i(1+\lambda R-\lambda^2 R^2) + 2\lambda R\right]$$

$$+ \frac{1}{2^{1/2}\lambda^3}e^{-\lambda R}(\lambda R+1) - \frac{1}{2^{1/2}\lambda^3}$$

$$\lambda = 3/2$$

$$P_{22} = \frac{1}{8}\left[\frac{2}{R}-\frac{2}{R}e^{-\lambda R}-Re^{-\lambda R}\right]$$

$$-L_{22} = \ln R + \frac{1}{8}\left[-6 + \bar{E}_1(\frac{12}{R}-8+\frac{5}{2}R-\frac{1}{2}R^2) + \bar{E}_i(\frac{12}{R}+8+\frac{5}{2}R+\frac{R^2}{2})\right]$$

$$Q_{22} = \frac{1}{32R}\left[\bar{E}_1(2-2R-R^2-R^3) + \bar{E}_i(2+2R-R^2+R^3)\right]$$

$$+ \frac{1}{8}\left[\frac{8}{R} - e^{-\lambda R}(\frac{8}{R}+6+2R+R^2)\right] - \frac{1}{4}$$

$$\lambda = 1$$

REFERENCES

Abramowitz, M., and Stegun, I.A., 1964, Handbook of Mathematical Functions. (N.B.S. Washington).

Bell, R.J., 1961, Proc. Phys. Soc., 78, 903-11.

Cheshire, I.M., 1965, Phys. Rev., 138, A992-98.

Cheshire, I.M., 1968, J. Phys. B (Proc. Phys. Soc.), [2], 1, 428-37.

Cheshire, I.M., Gallaher, D.F., and Taylor, A.J., private communication.

Cheshire, I.M., and Sullivan, E., 1967, Phys. Rev., 160, 4-8.

Coleman, J.P., 1968, J. Phys. B (Proc. Phys. Soc.), [2], 1, 567-74.

Coleman, J.P., and McDowell, M.R.C., Introduction to the theory of Ion-Atom Collisions (Amsterdam: North Holland).

Coleman, J.P., and Trelease, S., 1968, J. Phys. B (Proc. Phys. Soc.), [2], 1, 172-80.

Gallaher, D.F., and Wilets, L., 1968, Phys. Rev., 169, 139-49.

Green, T.A., 1965, Proc. Phys. Soc., 86, 1017-29.

Helbig, H.F. and Everhart, E., 1965, Phys. Rev., 136, A674-79.

Holt, A.R., and Moiseiwitch, B.L., 1968, J. Phys. B (Proc. Phys. Soc.), [2], 1, 36-47.

Lovell, S.E., and McElroy, M.B., 1965, Proc. Roy. Soc. A, 283, 100-14.

Sack, R.A., 1964, J. of Math. Phys. 5, 245-51.

Wilets, L., and Gallaher, D.F., 1966, Phys. Rev., 147, 13-20.

PUBLICATIONS

G. W. Catlow and M.R.C. McDowell, 1967,

Proc. Phys. Soc., 92, 875-79.

"A classical model for electron and proton

impact ionization."

M.R.C. McDowell, I.M. Cheshire, and G.W. Catlow, 1968,

Proceedings of Conference on Atomic Collisions
of Heavy Particles (Belfast) pp. 57-63.

"Proton impact excitation of H(2s)".

A classical model for electron and proton impact ionization

G. W. CATLOW and M. R. C. McDOWELL

Mathematics Department, University of Durham

MS. received 12th June 1967

Abstract. Ionization cross sections of He, Li, O and N by electrons and protons are calculated in a classical model, and compared, where possible, with quantal calculations and experiment.

1. Introduction

Recently, classical calculations of electron and proton impact ionization of atomic hydrogen by Kingston (1966), McDowell (1966), Percival and Valentine (1966) and Vriens (1967) have shown that such models can predict accurate values of the cross section for such processes at low and moderate energies (up to proton energies of say 200 kev).

It is of interest to extend the calculations to other atomic species. The model adopted is essentially that of Gryzinski (1965), as modified by Stabler (1964) and Vriens (1967). That is to say, the atomic electrons are regarded as distinguishable, and interact separately with the incident particle, the binding potentials being neglected during the collision. It is thus a binary encounter classical impulse approximation.

In this paper the atomic electrons are taken to have a momentum distribution given by the Fourier transform of the Hartree–Fock density distribution.

The analysis is outlined in § 2, and the calculations described and compared with other estimates and the available experimental data in § 3.

2. Theory

Following McDowell (1966) if V_1, V_2 are the velocities in atomic units of the bound electron and the incident particle, and $u = V_0{}^2$ is the ionization potential in rydbergs, then introducing dimensionless variables s, t

$$s^2 = V_2{}^2/V_0{}^2, \qquad t^2 = V_1{}^2/V_0{}^2 \tag{1}$$

the ionization cross section for an incident particle of energy $m_2 s^2 u$ rydbergs (where m_2 is the mass of the incident particle in electron units) is

$$Q(s) = N \int_0^\infty f(t) Q(s, t) u^{1/2} \, dt \text{ (in units of } \pi a_0{}^2) \tag{2}$$

(including only the contribution of the N electrons in the outermost shell). Here $f(t)$ is the momentum distribution of a single electron in this shell, and $Q(s, t)$ is the cross section for ionization of a bound electron of energy $t^2 u$.

For electron impact (Stabler 1964, McDowell 1966)

$$u^2 Q(s, t) = \frac{4}{3s^2} \frac{2(s^2 - 1)^{3/2}}{t} \qquad 1 \leqslant s^2 \leqslant t^2 + 1$$

$$= \frac{4}{3s^2} \left\{ (2t^2 + 3) - \frac{3}{s^2 - t^2} \right\} \qquad s^2 \geqslant t^2 + 1 \tag{3}$$

and for proton impact it follows readily from Vriens (1967) that

$$u^2 Q(s, t) = \frac{4}{s^2} \left\{ 1 + \frac{2t^2}{3} - \frac{1}{4(s^2 - t^2)} \right\} \qquad 1 \leqslant 4s(s - t)$$

$$= \frac{2}{s^2 t} \left[\frac{1}{4(s + t)} + t + \frac{2}{3} \{ 2s^3 + t^3 - (1 + t^2)^{3/2} \} \right] \qquad 4s(s - t) \leqslant 1 \leqslant 4s(s + t)$$

$$= 0 \qquad 1 \geqslant 4s(s + t) \tag{4}$$

for all atomic systems. The momentum distribution $f(t)$ is given by

$$f(t) = 4\pi t^2 u p_{nl}(tu^{1/2}) \tag{5}$$

where $p_{nl}(x)$ is defined by

$$p_{nl}(x) = p_{nl}(\mathbf{x}) = \frac{1}{2l+1} \sum_{m=-l}^{+l} |\Psi_{nlm}(\mathbf{x})|^2. \tag{6}$$

Here

$$\Psi_{nlm}(\mathbf{x}) = \frac{1}{(2\pi)^{3/2}} \int \Phi_{nlm}(\mathbf{r}) \, e^{i\mathbf{x}\cdot\mathbf{r}} \, d\mathbf{r} \tag{7}$$

in which $\Phi_{nlm}(\mathbf{r})$ is a one-electron orbital.

The normalization is

$$\int p_{nl}(\mathbf{x}) \, d\mathbf{x} = 1. \tag{8}$$

The $\Phi_{nlm}(\mathbf{r})$ were taken to be of the form

$$\Phi_{nlm}(\mathbf{r}) = N_{nl} R_{nl}(\mathbf{r}) Y_{lm}(\Omega)$$

where N_{nl} is a normalization constant and $R_{nl}(\mathbf{r})$ are Hartree–Fock radial functions (Roothaan, Sachs and Weiss 1960, Roothaan, Clementi and Yoshimine 1962, Roothaan and Kelly 1963).

3. Results and discussion

Ionization cross sections have been calculated for H, He, Li, O and N. The results for hydrogen are in agreement with earlier work.

For electron impact two alternative sets of results are presented: the initial calculations were used in (2) above to give a value Q_1 and were subsequently modified (Q_2) by taking

$$f(t) = 0, \qquad t > s \tag{9}$$

(see Kingston 1966), that is collisions in which the incident electron is the slower of the two are neglected. This agrees with the procedure used in a quantal calculation when exchange is neglected (Peterkop 1961). The experimental results for electron impact ionization are taken from the critical review by Kieffer and Dunn (1966) and from McFarland (1967).

In cases where the ground configuration of the residual ion gives rise to more than one electronic state (e.g. O^+, N^+) an average ionization potential (Slater 1960) is used. The results for electron impact are presented in figures 1 (a), (b), (c) and (d). In general Q_1 is too large, though the situation for atomic nitrogen is not clear, as Peterson's (1964) experimental values may be preferable, although much larger than the generally accepted values (Smith 1962). If Boksenberg's (1961) results for atomic oxygen are too high, our calculations would lend support to the view that the Smith values are to be preferred for nitrogen.

Our results for Q_2 at energies up to 250 ev are always within a factor or two of experiment, and are in general much closer to experiment than this, particularly for Li and He. The agreement in Li may not be relevant, in view of the uncertainty attaching to the experimental values until the discrepancy at high energies between these and the Born calculations is resolved.

Only Q_1 is relevant for proton impact. The results are shown in figures 2 (a), (b), (c) and (d). The only comparison with experiment that is possible is excellent below 200 kev. At high velocities ($s^2 > 20$) the proton and electron cross sections agree closely. Both fall off as s^{-2} as $s \to \infty$.

When $u^2 Q(s)/N$ is considered as a function of s, it is found that in this model curves for H and Li, and for N and O are quite similar (in each pair), but there does not appear to be any universal curve which will fit all the calculations to better than $\pm 30\%$.

As the number of electrons in the outer shell increases the error in the prediction of the model appears to increase proportionately.
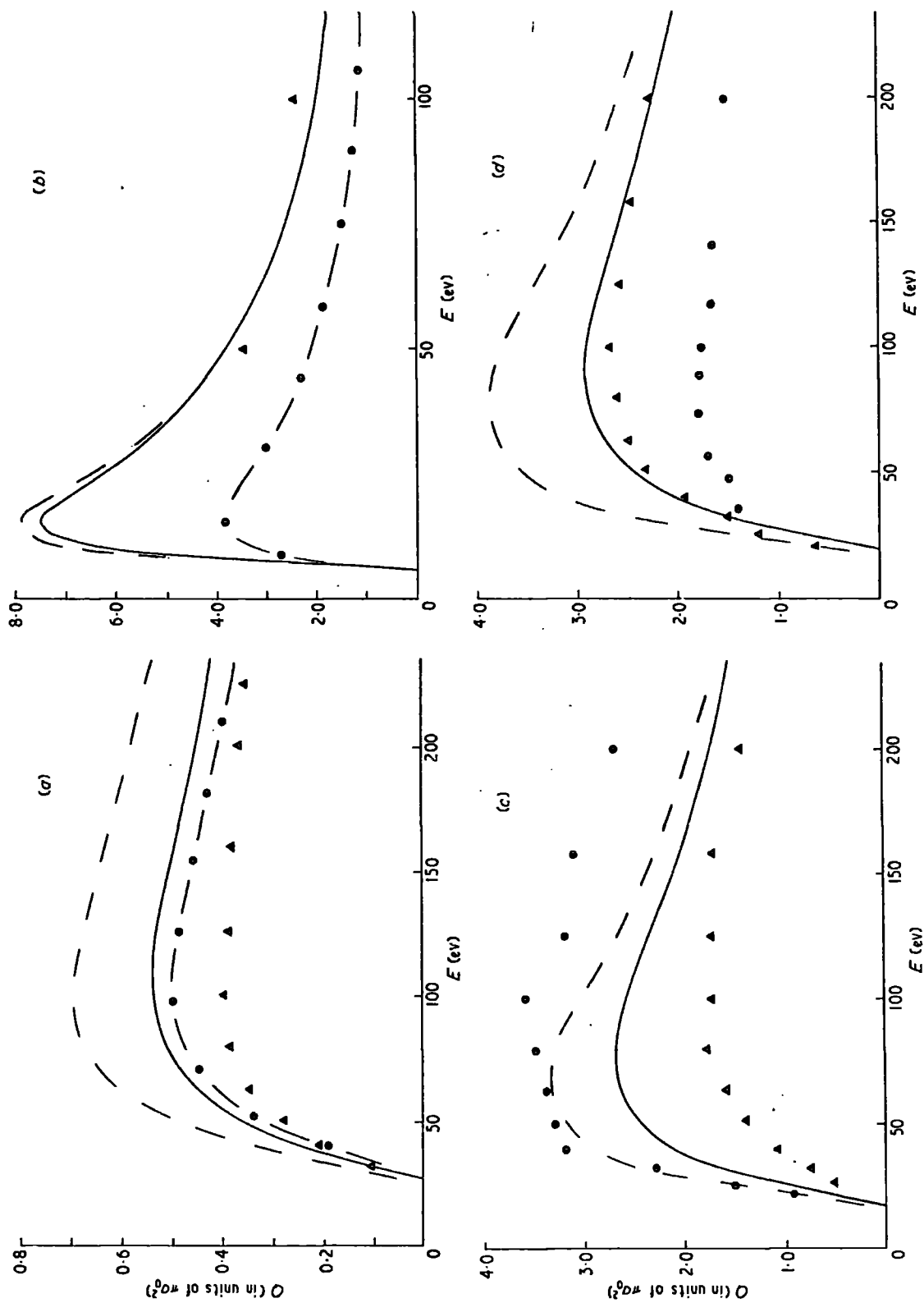
Figure 1. Cross sections for electron impact ionization of (a) He, (b) Li, (c) N, (d) O: - - - Q_1 calculated in this paper; ——— Q_2 calculated in this paper; —●—●— modified Born cross section (Peach 1965). Experimental values: He ▲ Smith 1930; Li ▲ McFarland 1967; N ● Peterson 1963; N ▲ Smith 1962; O ● Fite and Brackmann 1959; O ▲ Boksenberg 1961.
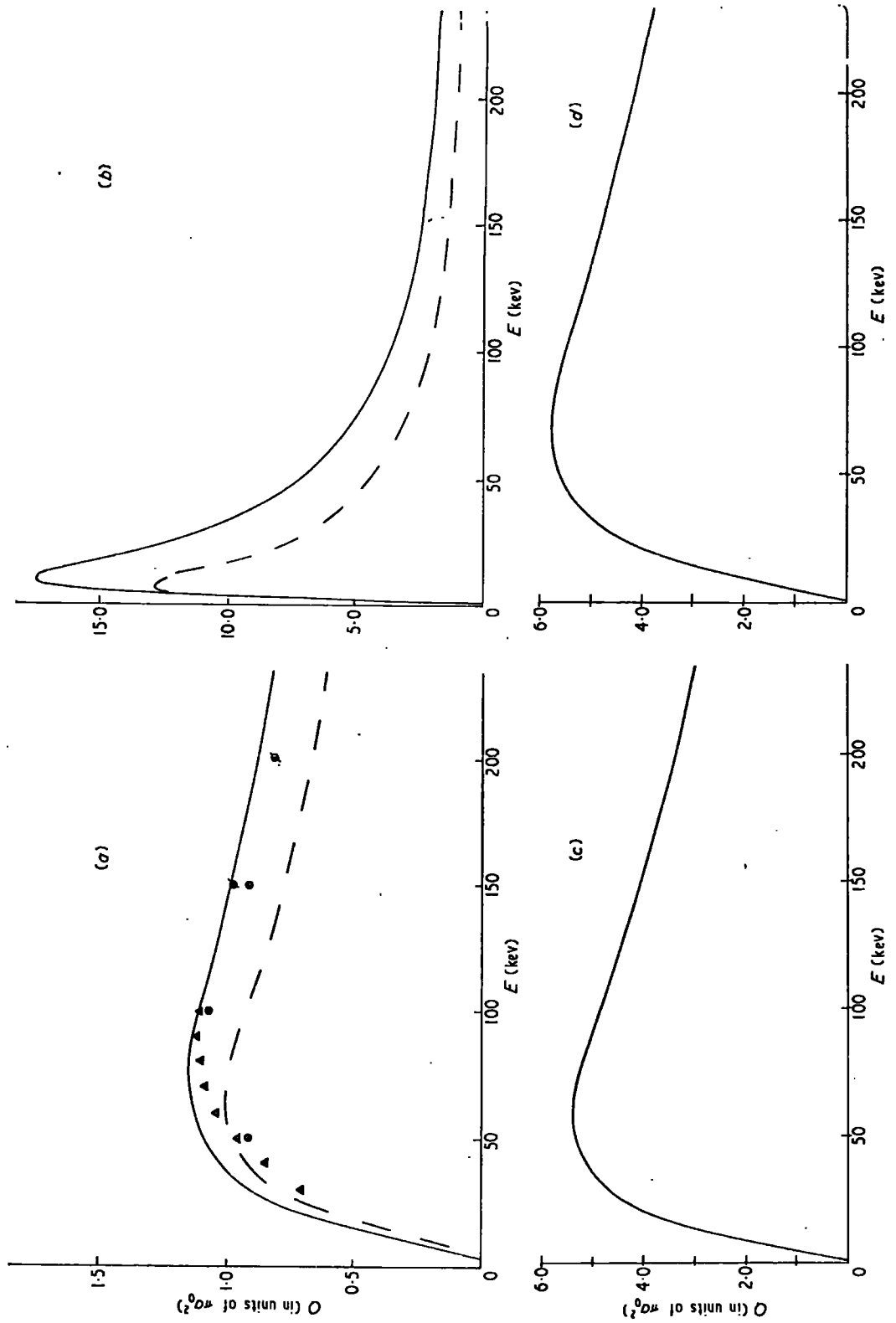
Figure 2. Cross sections for proton impact ionization of (a) He, (b) Li, (c) N, (d) O: —— Q_1, this paper; — — — Born cross section (Peach 1965). Experimental values (He only): ● Rudd and Jorgensen 1963; ▲ de Heer *et al.* 1966; ◉ McDaniel *et al.* 1961.

Acknowledgments

One of us (G.W.C.) is indebted to the Science Research Council for a Research Studentship.

References

BOKSENBERG, A., 1961, *Ph.D. Thesis*, University of London.
FITE, W. L., and BRACKMANN, R. T., 1959, *Phys. Rev.*, **113**, 815–6.
GRYZINSKI, M., 1965, *Phys. Rev.*, **138**, A305–21.
DE HEER, F. J., SCHUTTEN, J., and MOUSTAFA, H., 1966, *Physica*, **32**, 1766–92.
KIEFFER, L. S., and DUNN, G. H., 1966, *Rev. Mod. Phys.*, **38**, 1–35.
KINGSTON, A. E., 1966, *Proc. Phys. Soc.*, **87**, 193–200.
MCDANIEL, E. W., HOOPER, J. W., MARTIN, D. W., and HARMER, D. S., 1961, *Proc. 5th Int. Conf. on Ionization Phenomena in Gases, Munich*, 1961, Vol. I (Amsterdam: North-Holland), pp. 60–8.
MCDOWELL, M. R. C., 1966, *Proc. Phys. Soc.*, **89**, 23–6.
MCFARLAND, R. H., 1967, *U.C.R.L.* 70248 *Preprint*.
PEACH, G., 1965, *Proc. Phys. Soc.*, **85**, 709–18.
PERCIVAL, I. C., and VALENTINE, N. A., 1966, *Proc. Phys. Soc.*, **88**, 885–92.
PETERKOP, R., 1961, *Proc. Phys. Soc.*, **77**, 1220–2.
PETERSON, J. R., 1964, *Atomic Collision Processes*, Ed. M. R. C. McDowell (Amsterdam: North-Holland), pp. 465–73.
ROOTHAAN, C. C. J., CLEMENTI, E., and YOSHIMINE, M., 1962, *Phys. Rev.*, **127**, 1618–20.
ROOTHAAN, C. C. J., and KELLY, P. S., 1963, *Phys. Rev.*, **131**, 1177–82.
ROOTHAAN, C. C. J., SACHS, L. M., and WEISS, A. W., 1960, *Rev. Mod. Phys.*, **32**, 186–94.
RUDD, M. E., and JORGENSEN, T., 1963, *Phys. Rev.*, **131**, 666–75.
SLATER, J. C., 1960, *Quantum Theory of Atomic Structure*, Vol. I (London: McGraw–Hill), pp. 364–8.
SMITH, A. C. H., 1962, *Phys. Rev.*, **127**, 1647–9.
SMITH, P. T., 1930, *Phys. Rev.*, **36**, 1293–302.
STABLER, R., 1964, *Phys. Rev.*, **133**, A1268–73.
VRIENS, L., 1967, *Proc. Phys. Soc.*, **90**, 935–44.

z

PROTON IMPACT EXCITATION OF H(2s)

M. R. C. McDowell*†

I. P. Cheshire
A.E.R.E., Harwell, Berks.

G. W. Catlow
Mathematics Department, University of Durham

Laboratory for Theoretical Studies
NASA-Goddard Space Flight Center
Greenbelt, Maryland

Various methods have been proposed for including continuum contributions in eigenfunction expansions for the proton-hydrogen atom problem. Calculations for the process

$$H^+ + H(1s) \rightarrow H^+ + H(2s)$$
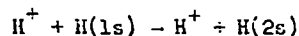
discussed in this paper have been reported in the impulse approximation (Coleman 1967), a Sturmian expansion (Gallaher and Wilets 1967) and in an angular momentum expansion (Cheshire and Sullivan 1967), all of which include some continuum contributions.

We report briefly on results obtained using a closure approximation due to Cheshire (1965)* . Adopting the notation of that paper, and working in an impact parameter formulation, the time dependent Schrodinger equation for the electronic wave function becomes

$$(T_A + V_B)\Psi = (T_B + V_A)\Psi = 0 \tag{1}$$

where

$$T_A = \frac{1}{2}\nabla_r^2 + \frac{1}{s} + i\frac{\partial}{\partial t} , \quad V_B = \frac{1}{x}$$

$$T_B = \frac{1}{2}\nabla_r^2 + \frac{1}{x} + i\frac{\partial}{\partial t} , \quad V_A = \frac{1}{s} \tag{2}$$

---

*The numerical results given in that paper should be disregarded.

.*National Academy of Sciences - National Research Council Resident Research Fellow.

†On leave of absence, 1967-8, from University of Durham.

If $\phi_n(\underline{s})$ is a hydrogen atom eigenfunction, the electron being on **proton A**, then

$$|A>_n = \phi_n(\underline{s}) \exp\{-i(\tfrac{1}{2}\underline{v}\cdot\underline{r} + \tfrac{1}{8}v^2 t + \epsilon_n t)\} \qquad (3)$$

satisfies

$$T_A|A>_n = 0. \qquad (4)$$

Defining the parallel set of states $|B>_m$ on B and expanding Ψ alternatively as

$$\Psi = \sum_k \alpha_k |A>_k = \sum_j \beta_j |B>_j \qquad (5)$$

yields first order coupled equations

$$\dot{\alpha}_k = i <A|V_B|B> \beta_j \qquad (a$$

$$\qquad\qquad\qquad\qquad\qquad\qquad (6)$$

$$\dot{\beta}_k = i <B|V_A|A> \alpha_j. \qquad (b$$

Now differentiate (6a) with respect to time and eliminate the $\dot{\beta}_k$ using (6b) and closure

$$\sum_k |B_k> <B_k| = 1 \qquad (7)$$

to obtain

$$\ddot{\alpha}_k - i < A|V_B \, T_B \, V_B^{-1}|A> \dot{\alpha}_j - < A|V_B \, V_A|A> \dot{\alpha}_j = 0 \tag{8}$$

subject to the boundary conditions

$$\alpha_{k1} \quad t \underset{-\infty}{\sim} \delta_{k1} \, e^{-i \int_{-\infty}^{t} \frac{1}{R} dt'} \tag{9}$$

We have solved (8) in a two-state approximation retaining the 1s and 2s states of A explicitly. A four state (1sA, 2sA, $2p_0A$, 2p-A) calculation is in hand.

Noting that

$$< A|V_B \, T_B \, V_B^{-1}|A > = < A|V_B(T_A + V_B - V_A) \, V_B^{-1}|A >$$

and that

$$< A|V_B \, T_A \, V_B^{-1}|A > = -i \frac{d}{dt} < A|\ln V_B|A > + < A(\frac{1}{2} V_B^2) \, A >$$

(8) becomes

$$\ddot{\alpha}_k + \gamma \dot{\alpha}_k + H \, \alpha_k = 0 \tag{8'}$$

where

$$\gamma = -\frac{d}{dt} < A|\ln V_B|A > + \frac{1}{2} < A|V_B^2|A > + < A|V_B - V_A|A >$$

$$H = < A|V_B \, V_A|A >.$$

It is convenient to rewrite (8^1) in Hamiltonian form as

$$\dot{\underline{\alpha}} = \gamma \underline{\alpha} + \underline{\xi} \tag{10}$$

$$\dot{\underline{\xi}} = (\dot\gamma - \Xi)\underline{\alpha}$$

with the boundary conditions $\xi_{n \, t} \simeq_\infty 0$ (all n). Introducing the real and imaginary parts of $\underline{\alpha}$, $\underline{\xi}$ and retaining n states (9) becomes

$$\dot{\mathcal{A}} = G \, \mathcal{A} \tag{11}$$

where $\mathcal{A}$ is a 4 x n dimensional column vector.

In solving (11) we first obtain asymptotic series $(t \to -\infty)$ for the α_k (k = 1,2) after removing the logarithmic phase factors. Reintroducing these phase factors (so that all the elements of G are regular near R = 0) (11) is solved either by Runge-Kutta-Gill or Adams-Bashforth techniques. The solutions at large positive time behave as

$$\begin{matrix} Re \\ Im \end{matrix} (\alpha_{2s}) = (A_{2s} + \frac{a_0}{t} + \frac{a_1}{t^2} + \cdot) \begin{matrix} \cos \\ \sin \end{matrix} (\epsilon t + b_0 + \frac{b_1}{t} + \cdots)$$

and $A_{2s}^2(+\infty)$ may be extracted without difficulty.

In general the computed values of A_{1s}^2, A_{2s}^2 do not satisfy unitarity, their sum being as large as 1.12 for small velocities and small impact parameters, and are replaced by

$$\bar{A}_{2s}^2 = A_{2s}^2 / (A_{1s}^2 + A_{2s}^2).$$

This is expected, as the expansion includes the 1sA and 2sA states both explicitly and in the closure.

Calculations were carried out in the energy range $6.25 \le E_i \le 100$ keV, for impact parameters in the range $0 < \rho \le 3.0 \, a_0$. The asymptotic

solutions were interval and integration method dependendent to 1% accuracy, the forward integrations being stopped at t = + 70 in general. Transition probabilities for four energies as a function of impact parameter are shown in Fig. 1. The values of A_{2s}^2 obtained nowhere exceed 0.5. For E_i= 6.25 keV a double peak is obtained as in Lovell and McElroy's work.

In Fig. 2 we compare our values of the calculated cross section

$$Q_{1s \to 2s} = 2 \int_0^\infty \rho \, A_{2s}^2 \, (\rho,V) \, (\pi \, a_0^2)$$

with those obtained in other models. At low energies our results lie between those of the 1s-2s (without closure, McElroy and Lovell 1965) and impulse (continuum only, Coleman 1967) calculations. At higher energies (> 40 keV) our results are larger than those obtained in other models (with the possible exception of the 12-state Sturmian expansion, Wilets and Gallaher 1967). In comparing with Cheshire and Sullivan's "all s + all p" non-adiabatic calculation it should be noted that the present model, but not theirs, implicitly allows for the 1sA/1sB rearrangement which should reduce the value of A_{2s}^2 at low energies (< 40 keV) where that channel dominates. At higher energies the present model, which makes some allowance for d and higher states and implicitly contains part of all of them lies, not unreasonably, above the "all s" and "all s + all p" sequence.

We have shown the 12-state Sturmian result from 20 to 45 keV only, as Gallaher and Wilets compute results at 25 and 40 keV only. Their approach is rather similar to ours, but includes rearrangements explicitly. The general trend compares well with our results. Both

our results and those of Gallaher and Wilets are in strong disagreement with the impulse approximation prediction. It would appear that this is due to including bound intermediate in addition to continuum intermediate states. Perhaps experiment may resolve the ambiguities.

ACKNOWLEDGEMENTS

G.W. Catlow wishes to thank the Science Research Council for a Studentship.

REFERENCES

Cheshire, I.P., 1965, Phys. Rev. 138, A 992

Cheshire, I.P. and Sullivan, E., 1967, Phys. Rev. 160, 4.

Coleman, J.P., 1967 Leningrad Conf., p.76, and private communication.

Gallaher, D.F. and Wilets, L., 1967 Leningrad Conf., p.65.

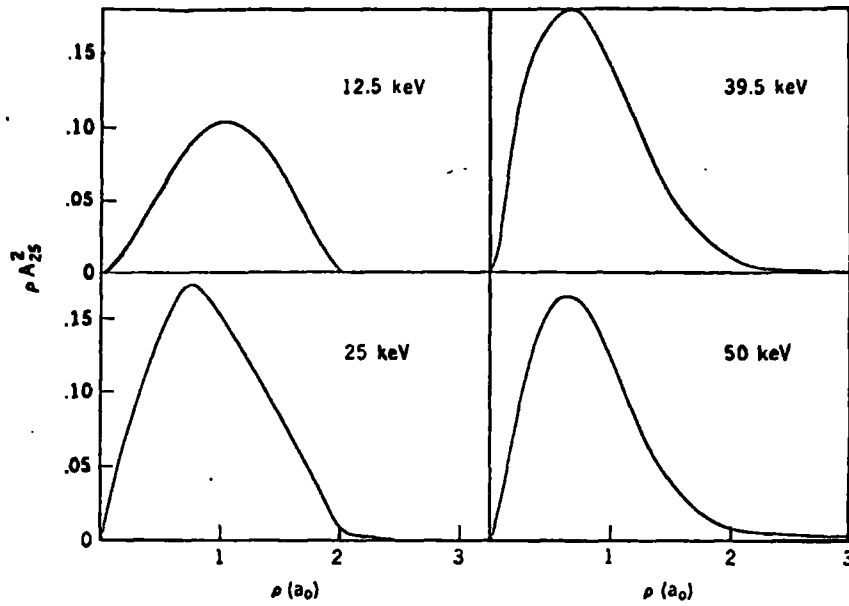Lovell, S.E. and McElroy, M.B., 1965, Proc. Roy. Soc. A. 283, 100.

Fig· 1   Computed (unitarized) values of the weighted transition
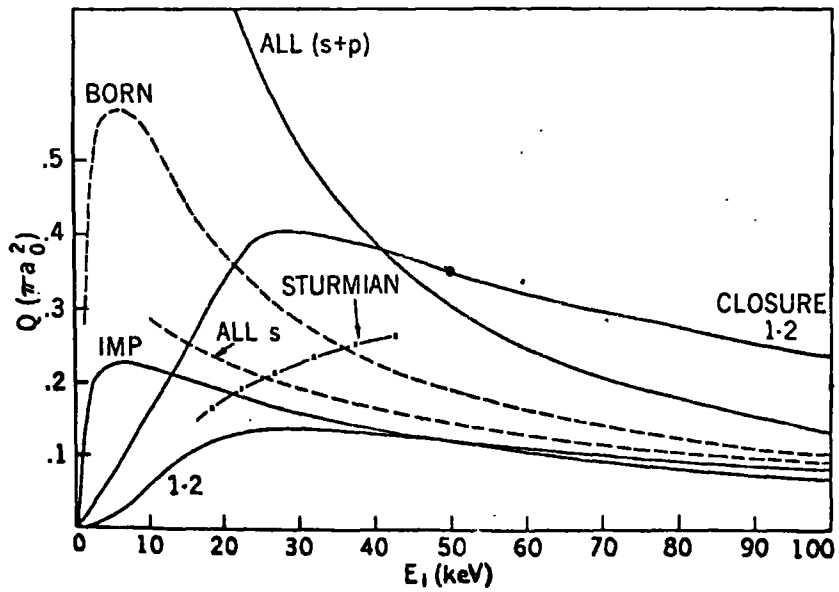probability $\rho A_{2s}^2 (\rho)$ at $E_i = 12.5$, 25.0, $\overline{37.5}$ and $50 keV$

Fig· 2   Calculated values of the $1s \rightarrow 2s$ cross section :
the various curves are labelled by the name of the
corresponding approximation